Lehrstuhl für
THERMODYNAMIK

SEMESTER THESIS

Design of a low-tech water wheel for the electrical power supply in Nepal

Author:
Lukas Geß

Student number:
3616025

Supervisor:
Prof. Dr.-Ing. Thomas Sattelmayer
Dr.-Ing. Markus Spinnler
Dipl.-Phys. Stephan Baur

July 31, 2017

Statutory declaration

I declare that I have authored this thesis independently, that I have not used others than the declared sources / resources, and that I have explicitly marked all material which has been quoted either literally or by content from the used sources.

_____

Place, Date

_____

Lukas Geß

Abstract

Nepal still faces a great lack of electrical energy. That also leads to many hours of load shedding during the day. Rural areas are affected in particular, because some of them do not even have a proper connection to the electrical grid. With respect to the large hydro potential of Nepal the idea is powering rural households or small neighbourhoods independently using overshot water wheels. The costs and the feasibility of the production are the challenges that have to be taken care of.

In the present work, a simple but at the same time effective design concept is created. Therefore, the basic demand, the general usage of overshot water wheels for electricity supply and the limitations due to material and machinery are addressed. Based on that, a modular water wheel concept that allows constructing water wheels with varying diameters and width is developed. Sheet metal is identified as the perfect material for the water wheel rim construction in Nepal. In addition, a dimensioning-tool is developed in Matlab which allows an optimization of the concept for different operating sites and computes the expected behaviour of the power output.

Finally, the generated design concept and the Matlab-tool are adapted to design a prototype. Afterwards, this prototype is constructed to check the manufacturability with respect to the circumstances in Nepal. The results demonstrate that the designed concept is convertible and that a production in Nepal should be easily possible. Furthermore, the provided cost and time estimations show that the modular design is a cheap possibility to construct overshot water wheels in little time.

To finally verify the developed concept, the prototype should be operated in test mode to examine, if the prediction on the behaviour of the power output is reliable.

Key words: overshot water wheel, modular water wheel concept, dimensioning, rural electrification, small scale power supply

Table of Contents

List of Figures

List of Tables

Abbreviations

Abbreviation	Meaning
CAD	Computer Added Design
pcs	piece
PD	person-day
pkg	package
NEA	Nepal Energy Agency
Pb-acid	lead-acid

Notation

Latin letters

Symbol	Unit	Meaning
$\overrightarrow{v_{bottom\ top}}$	[m]	Vector between two points (bottom, top)
$B_{WW,opt}$	[m]	Optimum total width of the water wheel
B_{WW}	[m]	Total width of the water wheel
D_{PxPy}	[m]	Distance of the points x and y
D_{Pxlyz}	[m]	Distance of point x to line yz
$D_{active\ in}$	[m]	Active inner diameter of the water wheel
$D_{active\ out\ opt}$	[m]	Optimum active outer diameter depending on the number of modules
$D_{active\ out}(k)$	[m]	Active outer diameter depending on the number of modules
D_{open}	[m]	Clear opening of the chamber
$D_{total\ opt}$	[m]	Optimum total diameter depending on the number of modules
$D_{total}(k)$	[m]	Total diameter depending on the number of modules
H_{max}	[m]	Maximum height of fall in chamber size 1
M_{max}	[Nm]	Maximum torque
P_{Dim}	[W]	Dimensioning power
P_{el}	[W]	Electrical power output of the water wheel
P_{max}	[W]	Maximum power output
P_{mech}	[W]	Mechanical power output of the water wheel
P_{pot}	[W]	Gravitational power of water
$V_{chamber\ max}(i)$	[m³]	Holding capacity of a chamber depending on the chamber position
$V_{chamber\ max\ tot}$	[m³]	Maximum holding capacity of a chamber

Symbol	Unit	Meaning
$a_{mean}(H_{min,section})$	[m]	Mean value of the rim width within a concept design section
a_{real}	[m]	Real rim width of the water wheel
a_{secure}	[m]	Extended length for splash water protection
a_{th}	[m]	Theoretical rim width of the water wheel
$b_{ch,opt}$	[m]	Optimum total width of the channel
b_{ch}	[m]	Total width of the channel
b_1	[m]	Width of the first module variation
b_2	[m]	Width of the second module variation
d_o	[m]	Outer diameter
e_{max}	[m]	upper limit for e
e_{min}	[m]	Lower limit for e
h_{secure}	[m]	Clearance beneath the water wheel and the ground
k_{opt}	[-]	Optimum number of modules
$l_{ip,st}$	[m]	Straight length of the impact paddle
l_{lp}	[m]	Length of the lock paddle
n_{cutout}	[1/min]	Idling speed of the water wheel
t_i	[m]	Inner partition of the water wheel
t_o	[m]	Outer partition of the water wheel
$v_{ch,opt,mean}$		Mean value of the optimum flow velocity in the channel for several cases
$v_{ch,opt}$	[m/s]	Optimum flow velocity in the channel
$v_{ch}(o)$	[m/s]	Flow velocity in the channel depending on the total channel width
v_t	[m/s]	Tangential flow velocity at the entry point with respect to the water wheel
$x_{rel,opt}$	[m]	Relative horizontal position of the channel end towards the upper vertex of the water wheel

Symbol	Unit	Meaning
$xw_{rad}(o,e)$	[rad]	Gradient angle between the water flow line and the horizon
y_{secure}	[m]	Clearance above the water wheel
z_{max}	[-]	Maximum number of modules within a concept size
z_{min}	[-]	Minimum number of modules within a concept size
α_0	[rad9	Angle between vertical line and connection of the water wheel centre with the entry point
ρ_W	[kg/m³]	Density of water
A_pxyz	[m²]	Area of a triangle spanned by the points x,y and z
$BX(o,e)$	[-]	Matrix for optimization of entry point and water wheel width
H	[m]	Free available height of fall
M	[Nm]	Mechanical torque
O	[-]	Number of permissible variations in the total width of the water wheel and the channel
Q	[m³/s]	Volume flow rate of water
Y	[-]	Number of water interacting chambers
Z	[-]	Step range from z_{min} to z_{max}
a	[m]	Rim width of a water wheel
b	[m]	Inner width of the modules
$combi_{opt}$	[-]	Optimum combination of the various module types
$combi$	[-]	Variable for the possible combinations of the module variations
d	[m]	Thickness of the chamber material
e	[m]	Control variable of the vertical position of the entry point
g	[m/s²]	Gravitational constant
k	[-]	Number of modules
n	[1/min]	Number of revolutions
o	[-]	Control variable of the total width of the water wheel and the channel

Symbol	Unit	Meaning
s	[m]	Free radius around bores for good accessibility
$wd_{orth}(o,e)$	[m]	Thickness of the water flow orthogonal to the flow direction depending on the total channel width
$wd_{v,opt}$	[m]	Optimum water depth in the channel
$wd_v(o)$	[m]	Water depth in the channel depending on the total channel width
$xw(o,e)$	[m]	Bottom stream line depending on the total channel width
z	[m]	Length of the unfolded paddle

Greek letters

Symbol	Unit	Meaning
η_{WW}	[-]	Efficiency of the water wheel - isolated
η_{gen}	[-]	Efficiency of an induction generator
η_{tot}	[-]	Efficiency of the entire installation
ε_{min}	[°]	Minimum value of ε
ε_{real}	[rad]	Real angle between outer section of the impact paddle and the tangent on the water wheel depending on the number of modules
ξ_{opt}	rad	Optimal segment angle
ρ_W	[kg/m³]	Density of water
$\Psi(i)$	[rad]	Angle between chamber entry and water level in a chamber depending on the chamber position
β	rad	Angle between t_i and the vertical edge of the module
δ	[°]	Angle between the two impact paddle segments
ε	[°]	Angle between outer section of the impact paddle and the tangent on the water wheel
ξ	[rad]	Segment angle
$\xi(k)$	rad	Segment angle depending on the number of modules
ω	[°]	Angle for entry tolerance of the water flow

1 Introduction

1.1 Motivation

Nepal is a country with great resources of hydro power provided by many big rivers and thousands of small streams. Although there is such a great renewable energy potential, a lot of Nepali still have no proper access to electrical energy. This state is caused by two main reasons.

On the one hand, there still exist rural areas without access to the electrical grid. On the other hand, the requested demand can neither be covered by the electricity supply of the Nepalese power plants nor through the import from neighbouring countries India and China. That leads to long periods of load shedding during the day all around the country. Figure 1-1 shows this effect impressively.

The graph displays the load curve of the 9th of November in 2015 and points out which sources provided the necessary capacity at that day. In red is the produced capacity of the power plants owned by the Nepal Energy Agency (NEA). Blue is the production of power plants operated by private investors. Yellow marks the amount of imports of electrical energy form other countries and green the capacity hedged by NEA energy storages. During the maximum peak load from 17:00h to 21:00h a little part of the required capacity is covered by diesel power plants (blue line). Finally, the purple part of the graph represents the capacity that could not be covered by production or import and had to be compensated by load shedding. Figure 1-1 illustrates that the electrical power producers in Nepal cannot deliver the required capacity to cover the energy demand at any time of the day. At the peak load, there is a lack of capacity of roughly 535 MW. The constant necessity of energy imports during the entire day furthermore show a lack of a base load production capacity of about 100 MW.
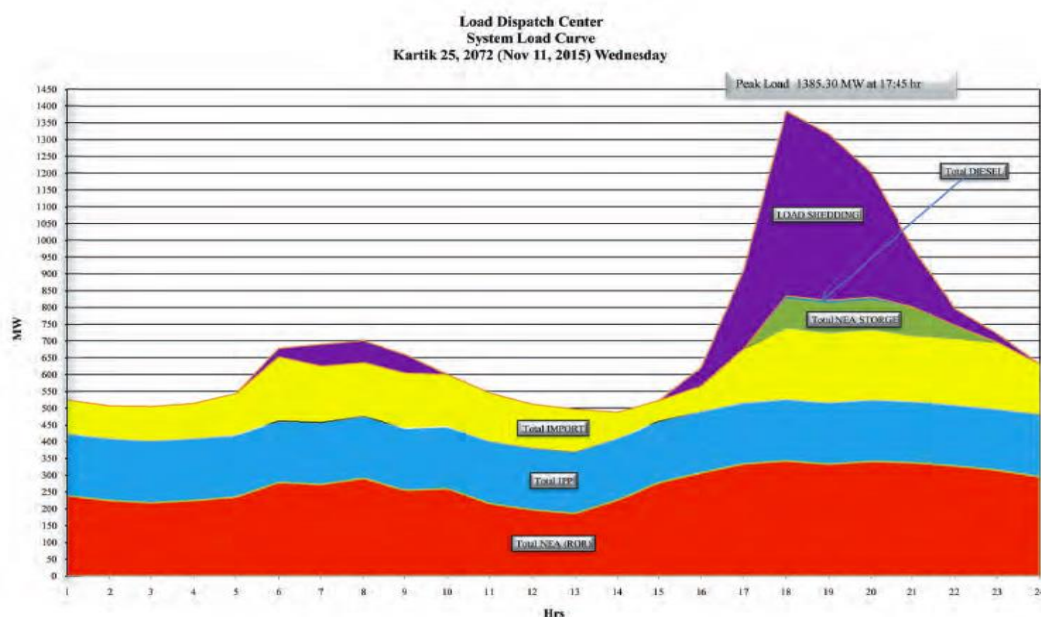
Figure 1-1: Load curve of Nepal – 9th of November 2015 [1]

Besides this lack of capacity in the electricity production nowadays, an increasing demand of electrical power has to be covered in the next years (see Figure 1-2). This distinct increase refers to a rising number of private and industrial customers on the one hand and an increasing request of energy of each user on the other hand.
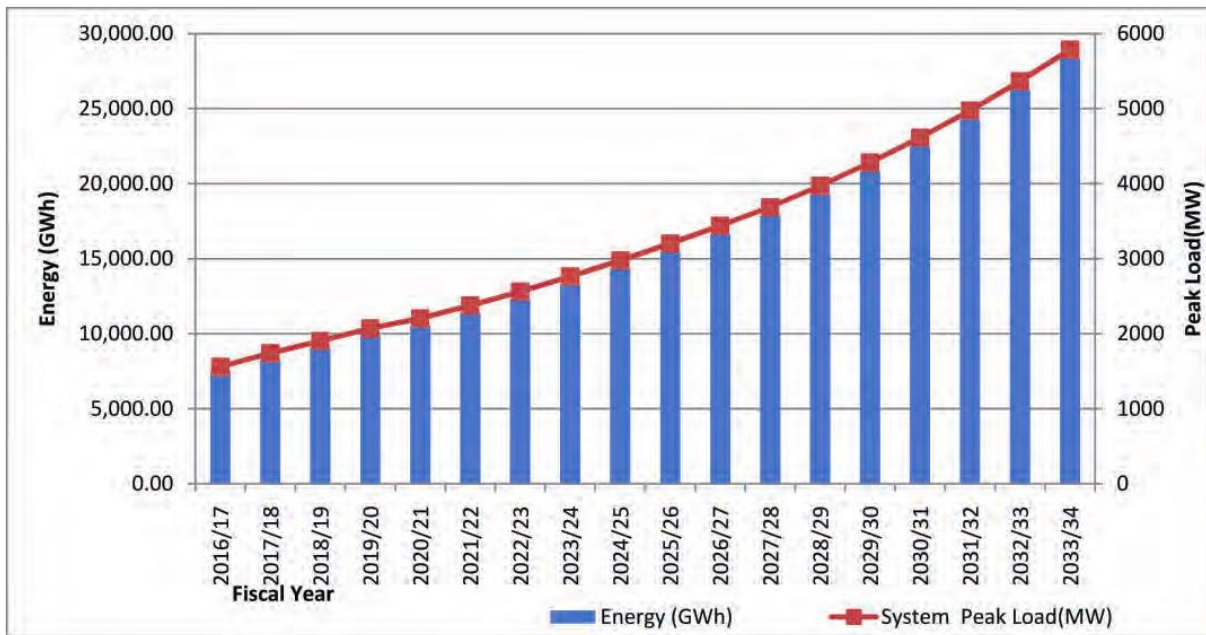
Figure 1-2: forecast on development of Nepalese energy demand [1]

To satisfy the demand of electrical energy, Nepal already puts great effort into the development of micro-hydro power plants to harvest the enormous hydro potential given in the Himalayan Mountains. Besides the project on improved water mills, all concepts are quite expensive and require special knowledge to install and run these micro-hydro power plants [2].

The use of overshot water wheels can be a new, in Nepal unknown option technology [3], to produce hydro electric energy. The advantage of the water wheel is a technically very easy concept that requires no specific knowledge to enable operation. That creates the opportunity to open the hydroelectric resource to a wider range of people, especially in rural areas.

1.2 Task

Based on the previously mentioned hydro potential and the enormous lack of electrical energy production, the distribution of overshot water wheels for small scale electrical power production is targeted in Nepal.

The task of this thesis is to develop a design concept for overshot water wheels that takes the limitations of the manufacturing process in Nepal in to account. The focus should be set on the hydro-mechanic acting part – the water wheel rim. Thus, the concept shall be easily reproducible with equipment available in Nepal. The goal is to combine the expertise of good water wheel technology with a very easy way of manufacturing.

Available materials and their prices, as well as possible manufacturing processes, should be identified. Also, fluid-mechanic considerations should be taken into account in the paddle design. On this base, a water wheel concept should be developed and a prototype for a head of about $1,5\ m$ and water volume flow rate of $20\ l/s$ has to be constructed and a cost estimation compiled.

In addition, a dimensioning tool should be developed that optimizes the water wheel design for certain operating site and gives information on the numbers of rotation as well as the behaviour of power and torque for given heights of fall and water volume flow rates.

1.3 Outline

At the beginning in chapter 2 the fundamentals are described, analysing the small scale power demand in the rural regions in Nepal, regarding the use of overshot water wheel as electrical power source in Nepal and showing the limitations in materials and machinery.

Chapter 3 considers the water wheel concept and design. Therefore, at first the general idea and the related requirements are introduced. Second, the theoretical basis including design criteria and limitations is approached. The concept is afterwards transferred into a CAD-Modell. Finally, the entire water wheel concept is presented and the chapter concludes with an evaluation of the water wheel concept and design.

Based on the created concept a dimensioning-tool is designed using Matlab. Thus, in chapter 4 the developed Matlab-tool is presented. First of all, the required input parameters are identified. Then the two-part structure and the strategies are described. The first part addresses the optimization of the concept and the second the behaviour of the power output. At the end follows an evaluation of the Matlab-tool.

The following chapter 5 "Results and practice" presents the results of the previously generated concepts and models specifically computed for a certain prototype. After the optimization of the prototype is completed and all required parameters are determined, the prototype is constructed using basic technologies to get an impression on the manufacturability of the design. Also, time and cost estimations are part of this chapter. The lessons learnt from realizing the prototype are presented in the conclusion.

2 Fundamentals

This chapter addresses the technical basis of this work. First of all, the small scale energy demand of a Nepali household is approached to identify a required range for the power supply. After that, the use of overshot water wheels to supply electrical energy in Nepal is discussed. Finally, available materials and machinery are presented as basis for the later development of the design concept.

2.1 Power output for small scale energy demand in Nepal

As basis for the estimation of the rural small scale electrical energy demand in Nepal the Semester Thesis "Analysis of the Energy Demand for Designing Off-Grid Energy Systems for Developing Countries Based on the Example of Nepal" by Johannes Eisner [4] is used.

He performed measurements on the electricity consumption of rural households, lodges and schools in Nepal. The results for the occurring peak and mean load of the examined cases are summarized in Table 2-1.

Table 2-1: Energy demand in rural areas in Nepal [4, pp. 34-67]

Location	Mean load	Peak load
Household-1	26,4 W	65,8 W
Household-2	42 W	1740 W
Lodge-1	123,7 W	424 W
Lodge-2	454 W	1893 W
Lodge-3	128,4 W	875,9 W
School-1	179,8 W	1636,5 W
School-2	13,8 W	79,2 W

It is clearly recognizable that a high peak power does not necessarily imply a high mean load. Thus, the challenge is to find a good range for the required electrical power output of the water wheel system to meet the need as good as possible and balance effort and benefit.

Since low tech water wheels are not operated load-controlled but run constantly, they perform like baseload generators. Preventing to install a way over dimensioned water wheel-generator-system, it is better to adapt the system to the required mean load instead of the peak load. Differences in production and demand can be compensated using simple energy storages like Pb-acid automotive batteries. This concept further more supports the grid stability and reduces the waste of energy to the dump load. [5, p. 45]

The average of the mean loads of the above presented cases adds up to 138,3 W. This could probably form a limit for the minimum power output, but neglects that for many households already less power supply is sufficient. Preventing very small inefficient systems the minimum

power supply respected in this work is 100 W which corresponds with the recommendation of [6] and at least allows the support of electrical light in a household.

The upper limit for small scale demand is stated to 700 W which is, according to Professor Maskey of Kathmandu University, the target value for a household to allow using basic electrical cooking appliances [4, p. 97].

With this borders for the power output a basic supply as well as a coverage of a better equipped household is provided. Also, the supply of a rural neighbourhood, a Lodge or school is possible.

2.2 Overshot waterwheels for electricity supply in Nepal

Of all hydraulic machines water wheels have the longest history. They have been utilized from ancient times till the beginning of the industrial revolution when they were more and more suppressed by steam engines and later combustion motors. Finally, most of the remaining water wheels were substituted by modern water turbines. [7]

Due to this development, all resent publications connected to water wheel design refer to the experts that addressed design and construction of water wheels at the beginning of the 20th century like Bach [8], Müller [9] or Henne [10]. The book "Wasseräder mit Freihang – Entwurfs- und Berechnungsgrundlagen" by Nuernbergk from 2007 [11] joins their knowledge on overshot water wheels. Thus, it is used as fundamental source of the work at hand.

Although water wheels nowadays play a minor part in energy production the interest in using this simple and robust technology for electrical power supply is rising again. According to [12, p. 629] especially for very small power ranges they are a practical completion to turbines.

Since the electricity demand in the rural areas in Nepal is quite small, it fits perfectly to the operating range of water wheels. For Nepal, the focus is set on overshot water wheels, because "*among the different kinds of water wheels, the overshot ones exploit the lowest flowrates with the highest efficiency*" [13] and the landscape with terraced fields offer the required head differences of one to three meters [6].

The advantages are an easy maintenance, a high robustness in operation and low investment costs due to the simple design [12, p. 629]. Moreover, "*since the efficiency of overshot wheels remains high for a wide range of flowrates, they become suitable also in sites where the water resource is variable in time or lacking*" [13]. These facts are essential requirements for a successful transfer of the technology to developing countries like Nepal.

A water wheel system to produce electrical energy consists of three major parts. They are the channel guiding the water to the water wheel, the water wheel itself and the generator set including the gearbox etc. to transform the mechanical power of the wheel into usable electrical power. This thesis focuses on the design of the hydro-mechanical part of the water wheel, the water wheel rim, as presented in detail in the following chapters.

Nevertheless, designing the hydraulic machine some information about the guiding channel are required. In respect to [11] four designs for the channel and the entry are possible. These are: feeding using a weir, feeding through a link, and feeding using an open channel with or without a slope. To keep the design as facile as possible and maximizing the geometric head in order to maximise the efficiency [13], an open channel without a slope is the best design for Nepal. Therefore, the entire design of the water wheel in the study assumes the use of an open channel without a slope as presented in Figure 2-1.
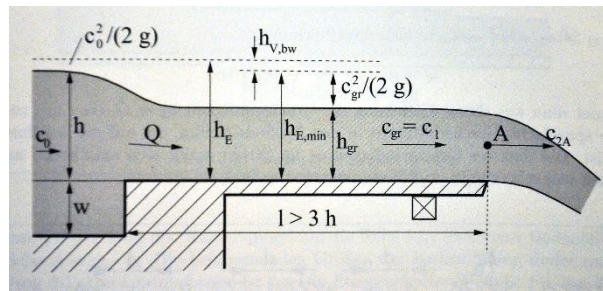
Figure 2-1: Open channel without a slope [11, p. 24]

2.3 Available materials and machinery in Nepal

Nepal is one of the 20 poorest countries in the world [14] thus also the availability of materials and the machinery infrastructure is limited.

2.3.1 Materials

On the one hand, wood is the classical material to build water wheels in the past centuries in Europe because it is very easy to handle and available all over. Generally, wood is also available in Nepal, but experiences in the construction of a wooden water wheel prototype in Nepal showed that wood in a sufficient quality and durability is very expensive and difficult to get in Nepal [6]. In the rural areas wood is furthermore used as crucial heat energy source and thus already is a scarce good.

Moreover, the acceptance of technical products based on wood is very little [6]. This is an important fact because installing technical equipment that is not accepted by the population derelicts fast. That leads to non-working systems and emphasis the dislike of the people against the matter even more.

Additionally, wooden water wheels are less efficient compared to sheet metal water wheels due to higher discharge losses and the diminished holding capacity of the chambers. Thus, nowadays sheet metal should be preferred towards wood as constructing material for water wheels. [11, p. 49]

Sheet metal, on the other hand, is a very common material in Nepal, it is used for example in the construction of roofs etc. (compare Figure 2-2). Thus, sheet metal in various styles is available all over the country and many small workshops are used to handle it. The two most common types are galvanized and colour coated sheet metal plates in thicknesses from $0{,}12 - 1{,}20 \ mm$ (see appendix A)).

Figure 2-2: Sheet metal store in Nepal [Stephan Baur]

Besides the good availability of sheet metal, the Nepali also trust more in products made of that material as it appears more modern to them.

Attending the described merits the work at hand focuses on the use of sheet metal material to construct the rim of the water wheel.

Additionally, required materials as screws etc. are imported from India and represent standard products in Nepal [6].

2.3.2 Machinery

The availability of machinery to treat sheet metal is comparably good in Nepal, too. All basic processes like drilling, cutting, bending, and riveting are possible in the machine shops all around Nepal. However, big machines like an engine lathe or a vertical drilling machine are not accessible to the majority [6].

Thereby, the work stages must be reduced to the use of simple hand devices or mechanical tools, like a hand drill, mechanic metal plate shear, mechanic sheet metal bender etc. Using these tools, the Nepali have developed great skills in processing sheet metal. (Compare Figure 2-3)

Furthermore, simple welding processes but not spot welding is feasible in Nepali workshops.

For the development of the water wheel concept with sheet metal these limitations are taken into account to guarantee the practicability of the idea in Nepal.

Figure 2-3 gives an impression of the working conditions and skills in Nepali workshops.

Figure 2-3: Impressions of a Nepal sheet metal workshop [Stephan Baur, 2017]

3 Water wheel concept and design

Since the technical basis and the requirements on the energy supply are clarified in chapter 2, the current chapter presents the development of the design of the water wheel rim.

The focus is set on a simple manufacturability of the water wheel rim using sheet metal so that a reproducibility is guaranteed in developing countries like Nepal. Thus, the limitations due to the available machinery and tools are taken into account.

3.1 General concept of water wheel rim

Following the concept idea and the derived requirements are presented.

3.1.1 Idea

The aim of the project is to find an easy concept to construct a water wheel rim. To be able to open the water wheel implementation to the majority of the Nepali, the costs have to be low, the design must by robust against tolerances in production and mistreatment, the maintenance in case of damage should be easily manageable and it should not be required to have a special knowledge or high-tech machines to convert the concept into reality. Additionally, it would be an advantage, if transport and assembly can be keep simple so that the water wheel can be installed in remote areas even without road connection or special equipment. All the mentioned needs occur due to the circumstances that exist in Nepal.

To meet these challenges, the idea is to realize a modular design. Meaning, the rim of the water wheel should be assembled from many similar parts (cells, modules, segments). Such a modular concept also has been realized in a high-tech version by [15].

By varying the number of cells used for one water wheel, it should be possible to optimize the water wheels for different heights of fall and volume flowrates of water without redesigning the parts every time. Hereby, a modular concept allows that the single parts can be produced in an easy way and the manufacturer can use the learnt skills more often what accelerates the total production process.

The water wheel assembly based on single modules enables a very easy transportation to the site and submits a preparation of the segments in a workshop such that only little work has to be done to finalize the water wheel on site. It gets clear that the modular design is a key to meet all the occurring needs for water wheel construction in Nepal.

3.1.2 Related requirements

The above introduced idea of a modular concept implicates some requirements that have to be taken care of while developing the specific design.

First of all, has to be noticed that by using varying numbers of segments in the water wheel the relative position of each module to the neighbouring module is changing. Therefore, the possibility to rotate the segments relative to each other has to be enabled whereas the solidity of the system still has to be guaranteed.

The second main issue is to identify a design for the segments that allows the use of equal modules for different water wheel diameters without reducing the efficiency too much. Only then, it is possible effectively harvest the advantages of a modular concept towards a specific design for every single site. Thus, a range of validity for a certain concept that fulfils this terms has to be detected.

These two main thoughts have to be kept in mind during the following development of the design concept.

3.2 Theoretical module design

3.2.1 Validity

First of all, after estimating the principle idea of the modular concept, we check which ranges of heights of fall and volume flow rates are possibly sufficient to cover the basic electrical demand of a Nepali household. It is very important to clarify these parameters early because they are the main input variables and influence the design of the single modules.

To do so, a simple estimation of the given gravitational power of the water and the achievable electrical power output is executed.

The gravitational power P_{pot} is roughly calculated like follows in formula (3-1) depending on the density of water ρ_W, the gravitational constant g, and the existing volume flow rate Q and height of fall H.

$$P_{pot} = \rho_W * g * Q * H \qquad\qquad (3\text{-}1)$$

Proceeding from the gravitational power, the potential electrical power output of the whole system can be calculated. The efficiency of small scale water wheels is assumed to 50 % [16] and the efficiency of and induction generator to 60 % [17]. The assumptions from [16] and [17] are sufficient to give a first impression of the potential energy output.

The results of the calculations for a range of heights of fall $H \in [1,0\ m; 2,3\ m]$ and volume flow rate $Q \in [0,02\ m^3/s; 0,1\ m^3/s]$ are presented in Table 3-1. The first line shows the corresponding gravitational power potential for each volume flow rate Q and a height of fall H and the second line the resulting electrical power output based on the before introduced values for the efficiencies. Moreover, the calculated electrical power output is highlighted in different colours. Red signifies an electrical power output below $100\ W$ or above $700\ W$ which are the borders of the basic energy demand of a rural household in Nepal (compare chapter 2.1). Green shows an electrical power output between $100\ W$ and $700\ W$.

The analysis of the table clarifies that for little volume flow rates, up to $Q = 0,03\ m^3/s$ and small heights of fall, close to $H = 1,0\ m$ the possible power output is not sufficient to supply a rural household in Nepal. However, neither the low heights of fall nor the small flow rates should be neglected because higher flow rates with small heights of fall or greater heights of fall with low flow rates still offer potential in fulfilling the basic demand. Shifting the lower limits for H and Q to smaller values than the minima considered in Table 3-1 is not useful.

Furthermore, as expected Table 3-1 shows that greater heights of fall and volume flow rates lead to an increasing power output. Nevertheless, under the present range with the estimated efficiencies, the upper limit of the required electrical power of $700\ W$ (paragraph 2.1) is just not reached.

A concept starting with low heights of fall of $H = 1,0\ m$ enables the use of the little gravitational power potential that is available at many sites in Nepal (compare paragraph 2.2).

Table 3-1: Estimation of the potential power output

power output P [W]		height of fall H [m]													
		1,0	**1,1**	**1,2**	**1,3**	**1,4**	**1,5**	**1,6**	**1,7**	**1,8**	**1,9**	**2,0**	**2,1**	**2,2**	**2,3**
volume flow rate Q [m³/s]	**0,02**	196	216	235	255	275	294	314	334	353	373	392	412	432	451
		59	65	71	77	82	88	94	100	106	112	118	124	129	135
	0,03	294	324	353	383	412	441	471	500	530	559	589	618	647	677
		88	97	106	115	124	132	141	150	159	168	177	185	194	203
	0,04	392	432	471	510	549	589	628	667	706	746	785	824	863	903
		118	129	141	153	165	177	188	200	212	224	235	247	259	271
	0,05	491	540	589	638	687	736	785	834	883	932	981	1030	1079	1128
		147	162	177	191	206	221	235	250	265	280	294	309	324	338
	0,06	589	647	706	765	824	883	942	1001	1059	1118	1177	1236	1295	1354
		177	194	212	230	247	265	283	300	318	336	353	371	388	406
	0,07	687	755	824	893	961	1030	1099	1167	1236	1305	1373	1442	1511	1579
		206	227	247	268	288	309	330	350	371	391	412	433	453	474
	0,08	785	863	942	1020	1099	1177	1256	1334	1413	1491	1570	1648	1727	1805
		235	259	283	306	330	353	377	400	424	447	471	494	518	542
	0,09	883	971	1059	1148	1236	1324	1413	1501	1589	1678	1766	1854	1942	2031
		265	291	318	344	371	397	424	450	477	503	530	556	583	609
	0,10	981	1079	1177	1275	1373	1472	1570	1668	1766	1864	1962	2060	2158	2256
		294	324	353	383	412	441	471	500	530	559	589	618	647	677

3.2.2 Basic module design

After verifying a valid start point for the range of the height of fall and the volume flow rate, the module design has to be developed. This includes two main tasks. First, a design for the modules must be created that allows an efficient utilization for different heights of fall and varying volume rates, whereas normally a water wheel is designed for each site separately. The second task is to enable the modularity, means the single segments have to be conceptualised such that assembly of the cells themselves and among themselves is possible.

To set the first framework conditions, the knowledge gained in the design of overshot water wheels during the last centuries in Europe is used as a basis. Two important relations are taken from two experts on the design of water wheels, who researched the topic at the end of the 19th and the beginning of the 20th century, namely Bach [8] and Henne [10].

The first relation describes the dependency of the rim width a of the water wheel of the available height of fall H. (Equation (3-2))

$$a = \frac{1}{6} * (H)^{1/3} \ ... \ \frac{1}{4} * (H)^{1/3} \quad [8] \tag{3-2}$$

The dimension of the rim width of the water wheel is very important, because together with the total width of the water wheel it decides how much water can be absorbed into the water wheel.

Smaller rim widths lead to smaller absorbable amounts of water but create a longer lever arm for the gravitational force and thereby gain better efficiencies.

The second important value is the outer partition t_o of the water wheel. It defines the number of chambers in the water wheel and influences the clearance of the entry which confines the permissible thickness of the water jet. According to Grashof referred to by [10] the partition is directly related to the rim width by following formula (3-3).

$$t_o = 0{,}75 * a + 0{,}1\, m \quad [10] \tag{3-3}$$
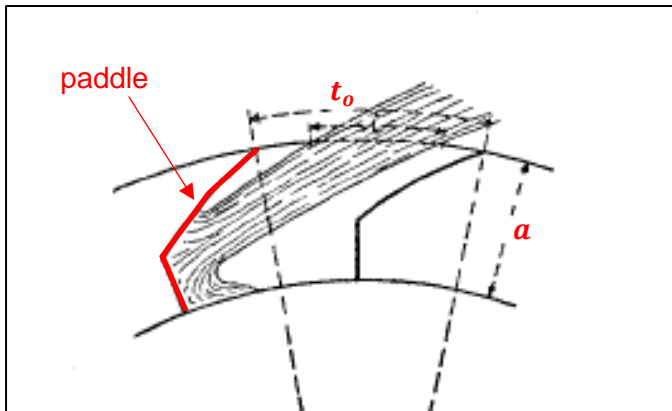
Figure 3-1: rim width and partition of a water wheel [10] (adapted by Lukas Geß in 2017)

For a better understanding, these two main parameters are illustrated in Figure 3-1.

The rim width can be described as the difference between the outer and the inner radius of the water wheel rim.

The outer partition is defined as the distance between two chambers segments at the outer diameter of the rim.

Furthermore, the reddish highlighted barrier separating the chambers is referred to as "paddle" in this paper.

The size of the modules is reduced to the dimension of one chamber in the water wheel. In other words, the number of modules to build a water wheel is equal to the number of chambers in the water wheel. Using the above presented equations, it is possible to set the framework for the module design. To do so, a consideration of the parameters in respect to different heights of fall is realize and illustrated in the following diagram (Figure 3-2). As the outer partition t_o depends directly on the rim width a it is sufficient analysing only the rim width as a function of the height of fall.

The graph shows the minimum and maximum rim width as a function of height of fall according to equation (3-2). The task is selecting a proper value for a which is valid for a defined range of heights of fall. As the volume flow rate is generally kept low with a maximum of $Q = 0{,}1\, m^3/s$, the single chambers do not need to absorb a big amount of water. Thus, the rim width can be kept small and, thereby, hold the water further away from the axis to create a greater lever arm. For that reason, the idea is to select a rim width that ranges between the allowed mean value and the minimum for all valid diameters. The mean value of the rim width is plotted in Figure 3-2, too.

Using the describe restriction, the hole graph can be divided in separate sections. Each one of them represents the range of validity for a module that uses the mean value of the lower limit of the interval. In other words, the mean value of the rim width of the smallest height of fall in the section is equal to the minimum rim width of the greatest height of fall of the section. Therefore, the rim width of an entire section is defined as $a = a_{mean}(H_{min,section})$. Doing this, all the heights of fall $H \in [1{,}0\, m; 8{,}0 m]$ are covered with three different module sizes. The table with the underlying values for Figure 3-2 is deposited in appendix B).
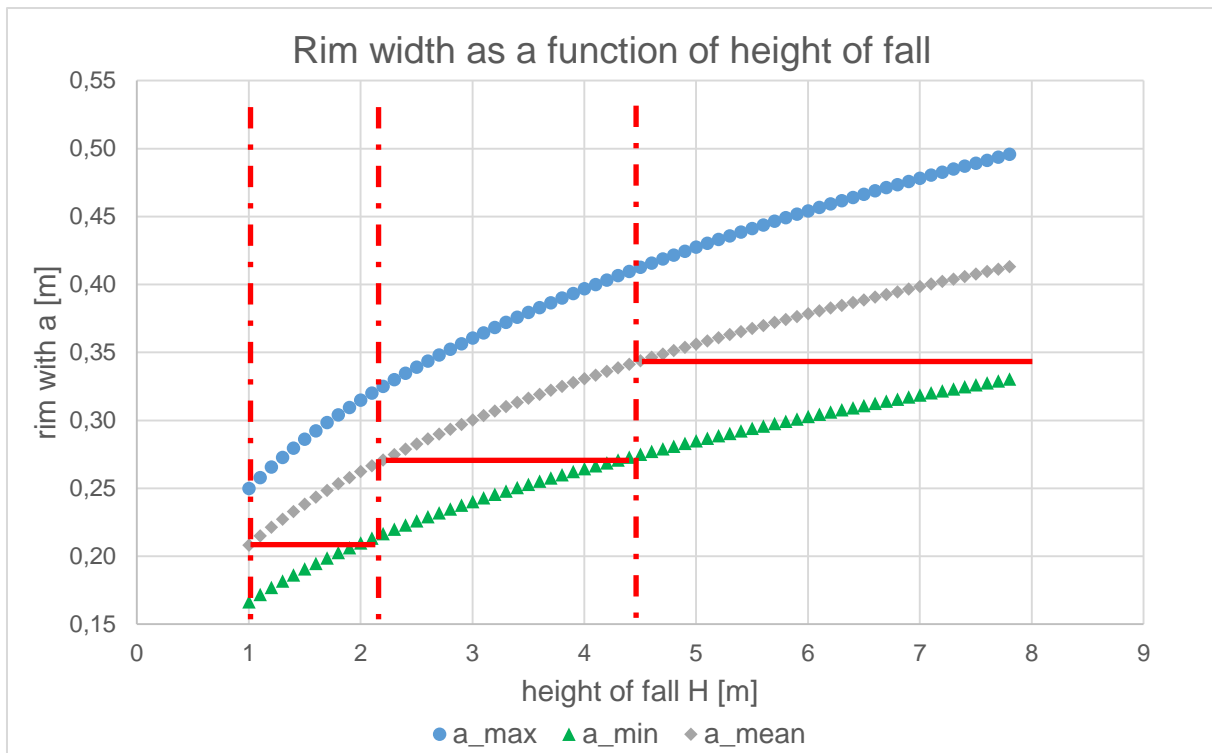
Figure 3-2: Rim width as a function of height of fall according to equation (3-2)

Table 3-2 lists the valid ranges for the chamber sizes, the associated rim widths a and the resulting outer partitions t_o according to equation (3-3)

Table 3-2: Resulting ranges for particular module sizes

Name	Range of H [m]	a [m]	t_o [m]
Size 1	1,0 - 2,1	0,21	0,26
Size 2	2,2 - 4,4	0,27	0,30
Size 3	4,5 - 8,8	0,34	0,36

You can see that the range of validity for module size 1 fits very well to the considered range of the power estimation in paragraph 3.2.1. Since this range of heights of fall fulfil the requirements to cover the electrical energy demand of a rural Nepali household, the focus is set on the design of module size 1 in the following. Anyway, the concept enables the modification of the input parameters later so that an easy adaption to other sizes is possible, if required.

The idea of the modularity of the concept is already described in paragraph 3.1.1. Based on that, the smallest part of the water wheel is one module that depends on the above calculated values for the outer partition and the rim width. The length of the outer partition defines how many segments can be put together in one ring to generate a desired diameter of the water wheel.

Figure 3-3 illustrates that relation abstractly. Both rings are formed by segments of the exact same length at the outer diameter. It is obvious that the left ring with only eight segments has a smaller diameter than the right ring composed by twelve segments. The segment angle ξ decreases with an increasing number of segments.

The maximum height of fall for module size 1 already is identified previously to $H_{max} = 2{,}1\ m$.
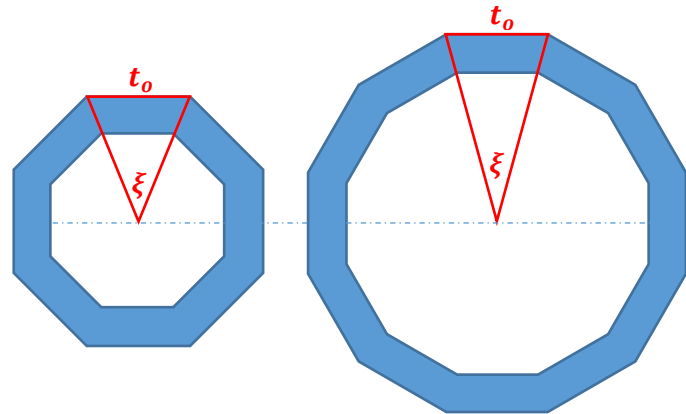
Figure 3-3: Influence of modularity on water wheel diameter

Now, the objective is to find the maximum number of cells that are needed to form a water wheel that still fits to the range. The easiest way to do so is to start with a preferably small number of cells and calculate the associated diameter. Then stepwise rise the number of cells and identify the number of cells that barely fits for the maximum valid height.

The outer diameter of the water wheel as a function of the number of cells is calculated as follows in Formula (3-4).

$$d_o = \left(\frac{t_o}{2 * \sin\left(\frac{\pi}{k}\right)} \right) * 2 \tag{3-4}$$

Using equation (3-4) the values presented in Table 3-3 are calculated. If you compare the calculated values for the outer diameters for different numbers of modules with the maximum height of fall, it is incidental that 25 cells are the maximum usable number of cells for module size 1. The lower boundary is given by the number of modules that for the first time is greater than the minimum valid height of fall. It adds up to 12 cells.

Table 3-3: Water wheel diameter in relation to the number of cells

$k\ [-]$																									
3	4	5	6	7	8	9	10	11	12	13	14	15	16	17	18	19	20	21	22	23	24	25	26	27
0,300	0,368	0,442	0,520	0,599	0,679	0,760	0,841	0,923	1,005	1,086	1,168	1,251	1,333	1,415	1,497	1,580	1,662	1,744	1,827	1,909	1,992	2,074	2,157	2,240

$d_o\ [m]$

3.2.3 Fluid mechanic optimization

After the generic dimensions of the module design are set, the next step is to specify the shape of the cells which requires a little study of the fluid mechanic effects in a water wheel cell.

Generally has to be noticed that a water wheel is a machine that mainly transforms the gravitational energy of the water into usable power [18, p. 210]. Hence the impact of the kinetic energy can be neglected at the optimum operation point. This also was confirmed with simulations of the performance of small scale low-tech water wheels in 2015 [16]. Nevertheless, fluid dynamics play an important role especially at the water entry and during operation aside the optimum conditions.

Therefore, the cell is optimized in respect to fluid dynamic purposes. The basis to do so are the three principle claims that a chamber of a water wheel has to fulfil according to Nuernbergk [11]. Which are:

1. Minimizing the kickback of the water against the paddle.
2. Possibly smooth redirection of the water flow.
3. Keeping the water as long as possible inside the cells before releasing it.

It is not possible to perfectly fulfil all three claims at a time. Thus, the goal is to find the optimal synergy [11, p. 48].

Generating a smooth redirection of the water flow inside the chamber the optimum would be a totally rounded sheet metal structure as shown in Figure 3-4. Thereby, manufacturing the curved shape and assembling the part into the water wheel are the difficulties. According to Brüdern [19] it is principally not possible to realize a loss-free redirection. Thus, to ease the production it is considered as good practise approaching the optimal shape kinking the paddle section twice (Figure 3-5)

Figure 3-4: Optimal shape for the chamber paddle [19, p. 119]

Figure 3-5: Good technical practise for the shape of the chamber paddle [19, p. 119]
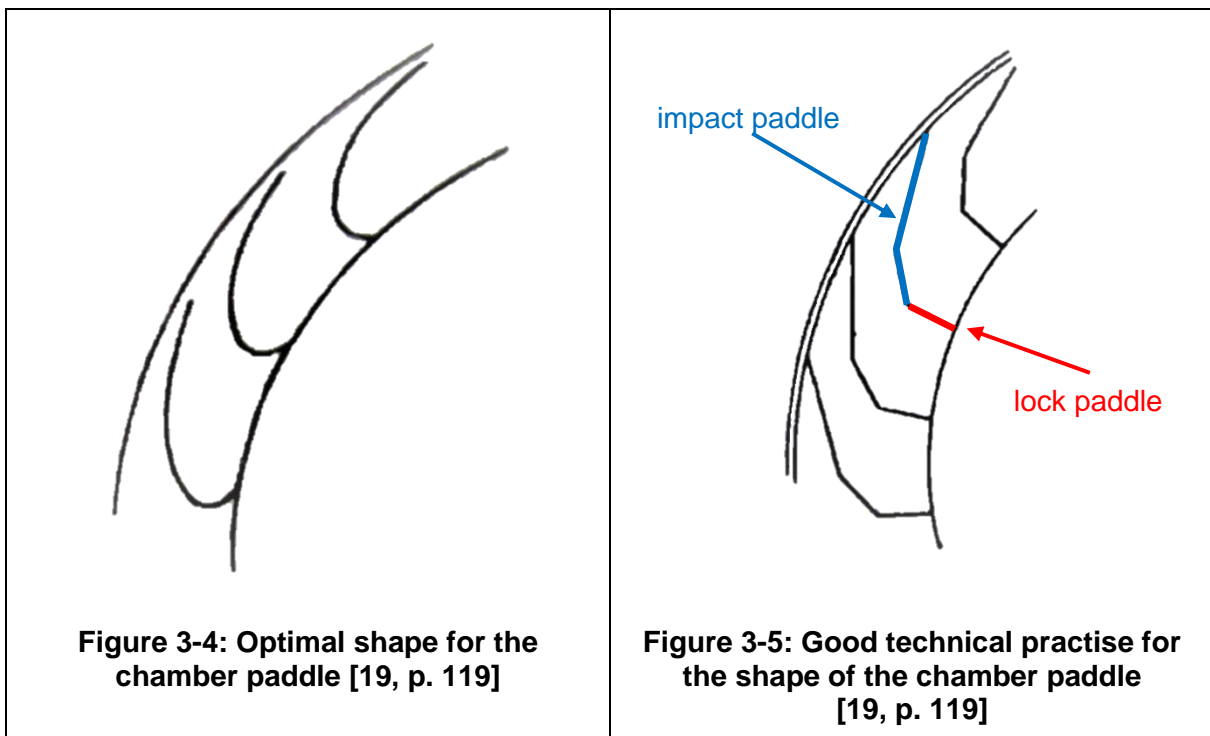
As recommended in [19] the design of the paddle is realized with the explained double kink so that the paddle insists of three sections.

The outer two sections will be referred to as "impact paddle" and the inner section as "lock paddle" (compare Figure 3-5). Correspondent to Henne [10, p. 85] the length of the lock paddle made from sheet metal should be chosen within the interval $l_{lp} \, \epsilon \, [0{,}33 * a; \; 0{,}4 * a]$. To avoid complex values for l_{lp} that might complicate the production, the length of the lock paddle is selected as $l_{lp} = 0{,}4 * a$.

After fixing the value for the lock paddle, the shape of the impact paddle must be cleared. First of all, its end points are given by the general idea of the modular concept. For easily producible, and self-contained modules the whole paddle has to fit inside one of them. Figure 3-6 demonstrates that fact for the temporary shape of the paddle. The paddle (blue) is kept inside the dimensions of one module (black dotted box). As pointed out before, the performance can be raised approaching an optimal curved shape of the paddle creating a double kink. The first kink divides the paddle into lock paddle and impact paddle. The second kink optimizes the shape of the impact paddle. According to Henne [10, p. 86] a good approach is to replace the straight impact paddle by an arc with a radius of two times the length of the straight impact paddle ($l_{ip,st}$). This arc can now be approximated by a kink in the middle of the impact paddle (red) resulting in a relative angle between the two impact paddle segments of $\delta = 14{,}47\,°$. To have straight values for the later production the angel is defined as $\delta = 15\,°$. Figure

$$\delta = \arcsin\left(\frac{0{,}5*l_{ip,st}}{2*l_{ip,st}}\right)$$

$$\delta = \arcsin(0{,}25) = 14{,}47\,°$$

Figure 3-6: Estimation of the paddle shape

3-6 illustrates these relations. As δ is independent from t_o and a the selected value can also be used for other sizes of the design concept specified in paragraph 3.2.1.

Once the design parameters for a smooth redirection of the water in the chambers are fixed the next step is paying attention to the kickback.

The kickback of the water against the paddle is caused by two effects. The first is the relative tangential speed between the water wheel and water flow. The second design influence on the kickback is the relation between the curve of the water flow and the paddle position of the chamber at the entry point.

If the tangential velocity of the water is faster than the rotational speed of the water wheel, it puts a positive impulsive force on the paddle and supports the rotation of the wheel. In case the tangential velocity of the water flow is slower than the wheel a kickback against the rotation is created. The effect caused by the described speed differences depends on the flow velocity of the water in the channel, the entry position of the water into the water wheel and the rotational speed of the water wheel. As the principal effect of the kinetic energy is very little in comparison to the gravitational one it does not make sense to optimise it isolated. Both effects are simulated in the Matlab-model in chapter 4 and the resulting optimal operation point is identified in that way.

According to Müller [20, p. 3] "*the cells are formed in a way so that the water jet from the inflow can enter each cell at its natural angle of fall*". Thus, minimizing the kickback of the water against the paddle additionally the idea is to preferably align the water flow to the paddle. To do so an optimal entry point of the water into the wheel must be found such that the water flow impacts the first section of the impact paddle in an angle smaller than $\omega = 10\,°$ (compare Figure 3-7). The alignment of the water jet and the shape of the cell will be verified in chapter 4.4.2.
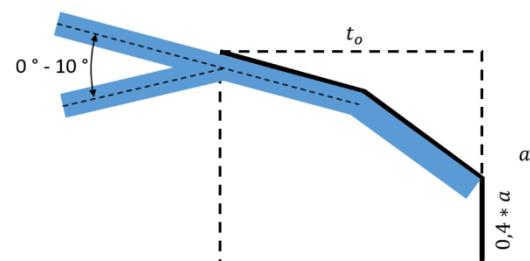
Figure 3-7: Water entry angle restrictions

Furthermore, the entry of the water into the water wheel has to be guaranteed. Meaning, the thickness of the water flow at the entry point must not be greater than the minimum clearance at its way into the chamber. The optimization of both aspects, the right entry angle and the thickness of the water flow, again is executed in the Matlab-tool in chapter 4

The third claim for good chamber design, introduced at the beginning of this chapter, is keeping the water as long as possible inside the water wheel. This is important to extract as much gravitational energy as possible. Thereby, the angle between the entry section of the paddle and the tangent onto the water wheel circle is the determining design criterion. As stated by Brüdern [19, p. 121] two contrary requirements have to be fulfilled. For an optimal entry a preferably big angel ε is claimed. Minimizing the water leak a preferable small angle ε is required. (Compare Figure 3-8). The compromise of these to claims is said to be reached for $20° \leq \varepsilon \leq 30°$.

In the presented concept, equal modules shall be used for different heights of fall. As already mentioned in chapter 3.2.2, different number of cells lead to different segment angles in the water wheel and thus to varying relative position of the cells to each other. As shown in Figure 3-9 this also effects ε. For small water wheel diameters ε is bigger, for greater diameters ε is smaller. To keep the water as long as possible inside the water wheel for all diameters and still allow a good entry of the water in the greatest water wheel of the concept size, the smallest requested value for ε is fixed for the maximum number of modules of the concept size ($\varepsilon_{min} = 20°$). This is implemented during the CAD build (compare chapter 3.3.3.2).
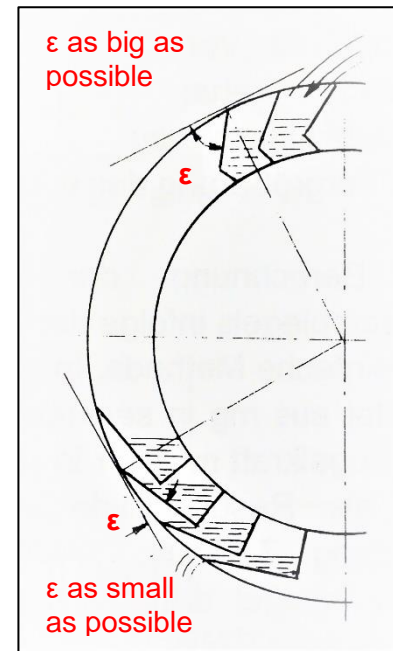
Figure 3-8: Angel of the paddle entry section [7, p. 121]
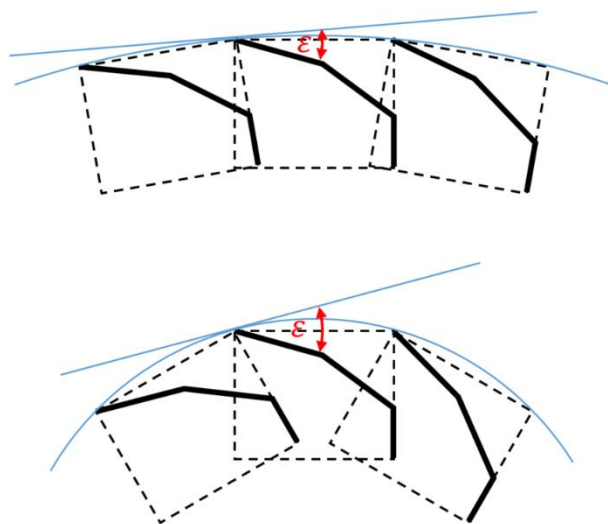
Figure 3-9: Dependency of ε on water wheel diameter

3.2.4 Summary

Since a lot of requirements and parameters have been presented above, they are quickly summarized in this paragraph and illustrated in Figure 3-10.

Material: The modules of the water wheel rim will be produced of sheet metal material, as its processing is easy, it is available for everybody in Nepal at a low prize, and has advantages in the efficiency towards wood.

Concept: The water wheel design bases on a modular concept that enables the use of a single module design for different heights of fall. The determined range of heights of fall is $1{,}0\,m$ to $2{,}1\,m$.

The design criteria are summarized in Figure 3-10:
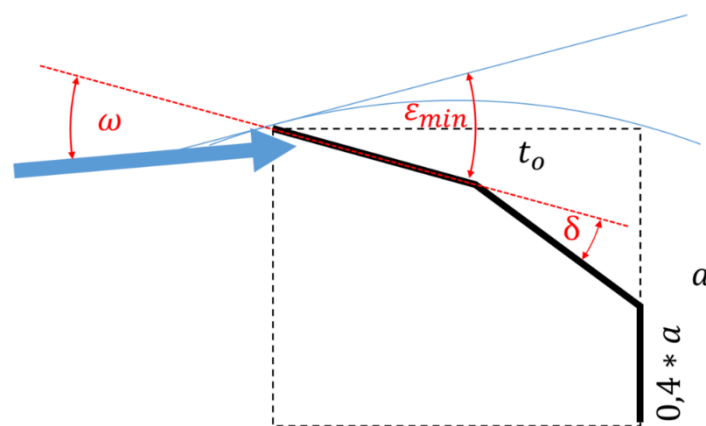
Figure 3-10: Summary of the design criteria

The designed rim with a of the module is addressed as theoretical rim width a_{th} for the rest of this study, because due to the varying numbers modules to form a ring the actually occurring rim width a_{real} differs form a_{th}. a_{real} is calculated in the Matlab-tool in chapter 4 separately for each water wheel diameter.

3.3 Practical design and CAD-implementation

In this paragraph, the concept is specified before is transformed into a CAD-model that enables the variation of the concept parameters and produces drawings which can be used for the production process.

3.3.1 Challenges

The above introduced concept confines itself to optimize the performance, but does not take into account its realization. Thus, the challenge is to integrate the concept into a functional module design that supports manufacturing the cells and assembling the water wheel. Furthermore, a production in developing countries like Nepal has to be ensured.

In addition to these requirements, the manufacturing process of the final design is limited to the use of a metal jigsaw or a plate shear to cut the sheet metal. Furthermore, all holes have to be drilled by a simple hand drill, the joints of the components of a module are managed by

blind rivets, and the connection of the single modules to form a water wheel is done using bolts.

Moreover, the free rotation of the single cells towards each other, assuring the assembly of different numbers of modules in a ring, is a challenge that has to be taken care of. To solve that problem only the outer partition, which is a design criterion, is fixed geometrically.

3.3.2 Setup

Before the detailed constructing can be conducted, the general setup of one module must be determined. It has to be clarified into how many parts one cell needs to be divided to gain manufacturability and to allow the assembly. Different analysed options are presented as follows and are evaluated with respect to their feasibility.

The general principle of the module is a setup as a kind of box with four solid elements containing two side walls, a bottom wall and the paddle. (compare Figure 3-11)
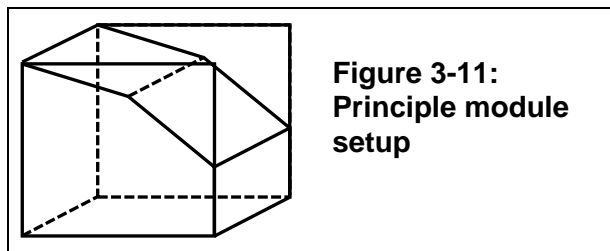
Figure 3-11: Principle module setup

The first setup is a production of the entire module from one piece. In that case the cell must be bend from one flat sheet metal (see Figure 3-12) into a three-dimensional structure.

This setup cannot be manufactured with the required simple bending devices. Thus, the first option cannot be realized.
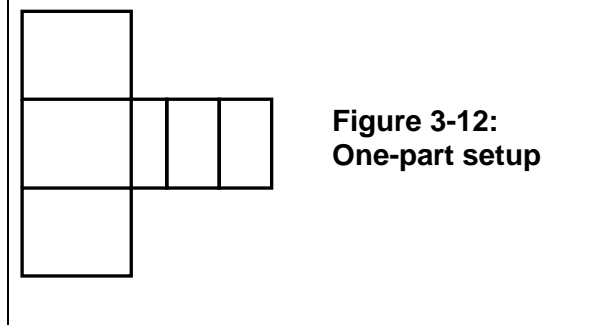
Figure 3-12: One-part setup

The second layout is a separation of the module into two parts, the paddle element and a combined sidewall and bottom section. (see Figure 3-13)

The two-part design is producible with the available machinery, but susceptible for possible manufacturing deviations of the paddle width.
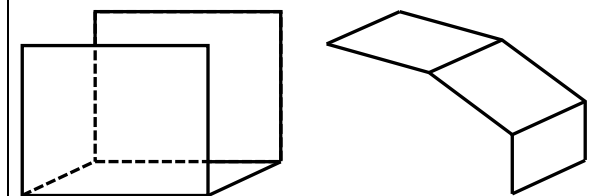
Figure 3-13: Two-part setup

To overcome the difficulties of the first two setups a final layout consisting of four parts is analysed. The four-part design is composed of two identical wall elements, a bottom element and the paddle element. (Figure 3-14)

This design is easy to produce and impervious against manufacturing tolerances. It also offers the greatest flexibility for the concept, because it is also possible to use equal wall elements for different width of the modules.
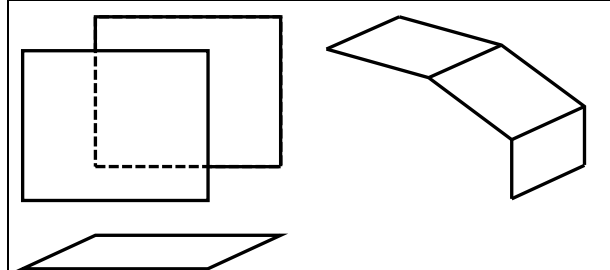
Figure 3-14: Four-part setup

The four-part design is taken as the optimal design choice and transformed into a CAD-Model.

3.3.3 Realization in CAD

The software CATIA P3 V5R20 is used to realize the developed concept in a CAD-Model and thereout create technical drawings for the production. As the entire module is built from sheet metal it is designed within the sheet metal design workspace (Start → Mechanical Design → Sheet Metal Design). The focus is set here on a simple production of the single elements and an easy assemblage of the modules to a water wheel.

3.3.3.1 Component 1 – wall element

The first part to be designed is the wall element, because the dimensions of the paddle and the bottom element are deduced of the wall segment.

To enable the adaptability of the CAD-model to different concepts, first of all, several parameters are created in the specification tree. Figure 3-15 presents the parameters extracted from the Matlab surface of "part 1 – wall".

The required parameters are the rim width a, the outer partition t_o, the minimum number of chambers for the concept size z_{min}, the maximum number of chambers of the concept size z_{max}, the width of the chamber b, which corresponds to the width of the water wheel, the minimal entry section angle towards the water wheel tangent ε_{min}, and the thickness of the sheet metal d, in catia referred to as "Sheet Metal Parameter.1". Table 3-4 lists the parameter values for module size 1.

Table 3-4: Parameters of concept size 1

Parameter	Value
a_{th}	210 mm
t_o	260 mm
z_{min}	12
z_{max}	25
b	30 mm
ε_{min}	20 °
d	0,75 mm
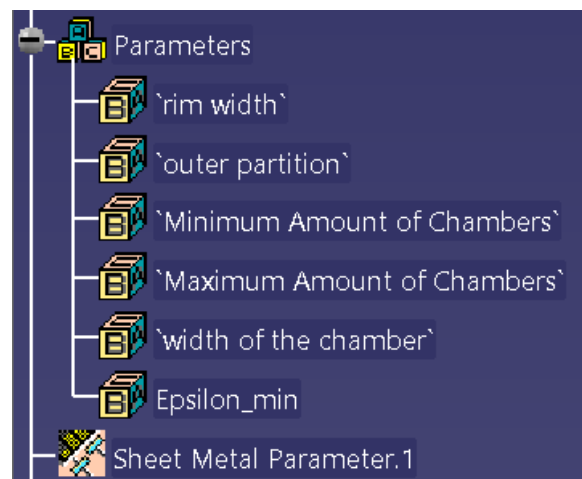
Figure 3-15: Parameters in Catia

The CAD-model of the wall element is illustrated in Figure 3-16. The two horizontally aligned bores fix the outer partition t_o of the water wheel and are used to connect the cells among one another. The modules are in contact at these bores. Thus, also the outer segment length in the water wheel is definite by t_o. The second defined dimension of the wall element is the vertical distance between the right bore and the marked point. This distance is equal to the theoretical rim width a_{th}. The point represents a placeholder for another bore that is later created during the water wheel assembly, because it has to be generated together with the overlapping wall element of the neighbouring cell. That is necessary to allow the use of equal modules in water wheels of different diameters, because for different water wheel diameters

the relative angle between the single modules differs (compare paragraph 3.2.2). Surrounding the holes, the radius $s = 15\ mm$ is set as free zone to ensure an unimpeded access for the tools tightening the screws later. The two horizontal-positioned bores have a larger distance to the top edge than to the side edges. These extended length is required according to Nuernbergk [11, p. 100] as splash water protection and is set to $a_{secure} = 45\ mm$ here. To save material and weight, the outline of the wall segment is not rectangular but has one angular side. The angle is calculated such that for the maximum valid number of chambers of the concept size, the overlap of the modules among each other is minimized.
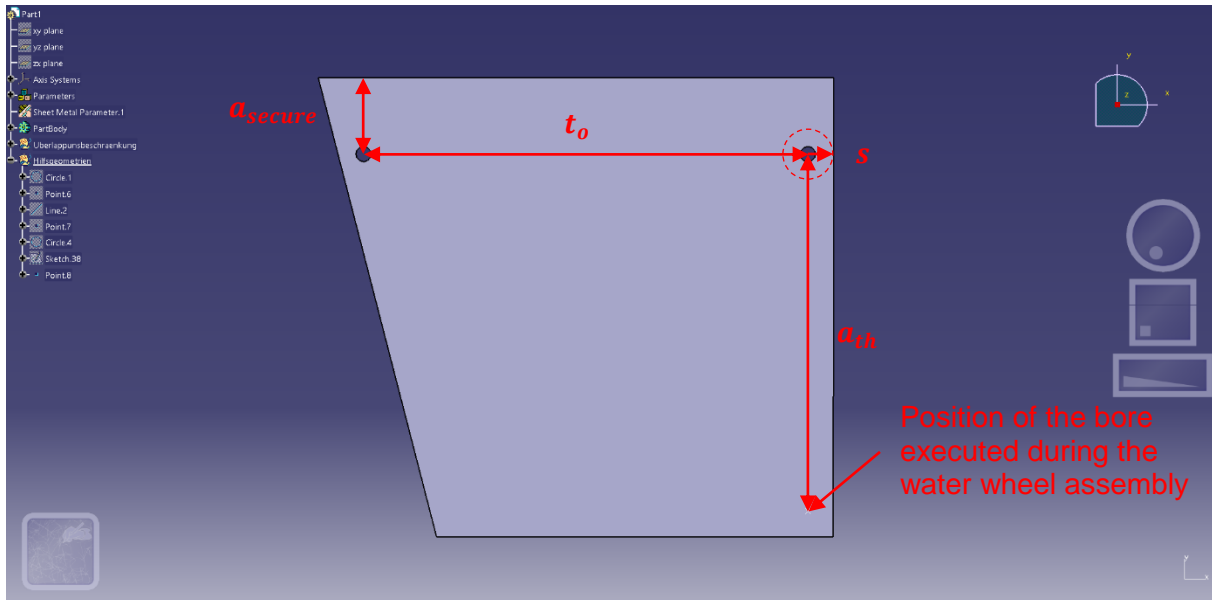
Figure 3-16: CAD-model - part 1 - wall element

3.3.3.2 Component 2 – paddle element

The second part to be transformed into a CAD-model is the paddle element. As the design has to fit to the already created wall element, important references are extracted from the CAD-model of the wall element. These are the positions of the bores and the contour of part 1. The essential work is generating the paddle shape. The challenge is to combine the requirement of the minimal opening angle ε_{min}, between the outer paddle section and the tangent onto the water wheel with the maximum number of chambers. To create that angle, the auxiliary tangent is constructed with respect to the position of the neighbouring cells. To do so, it is necessary to generate an auxiliary line as a straight connection of the two bores left and right of a middle bore which are located as using the maximum number of chambers. This line is parallel to the tangent on the water wheel in the middle bore and is used as a reference to fix ε_{min}. Figure 3-17 shows these dependencies and the construction process.
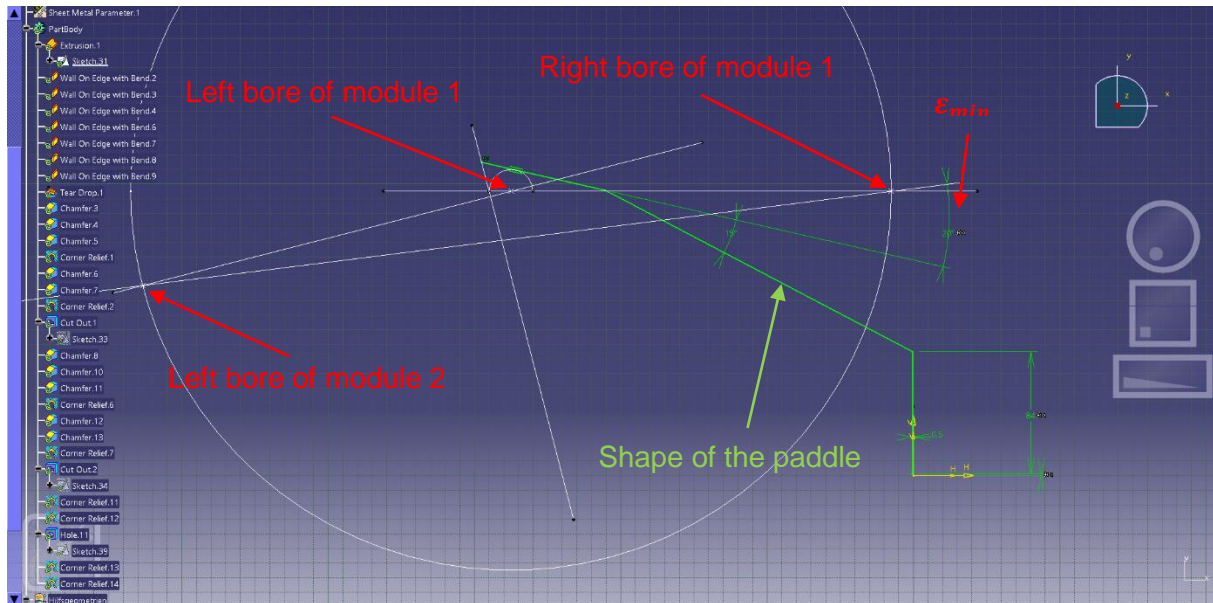
Figure 3-17: Implementation of ε_{min} into CAD-Model part 2

The final three-dimensional model is illustrated in Figure 3-18. After extruding the above developed shape of the paddle to the width of the chamber, the side flaps are attached. They are necessary to connect the paddle with the wall elements and the bottom element using blind rivets. The two holes in the side flaps are aligned with the left bores of the wall segments in the module assembly. The vertical lock paddle section has the in paragraph 3.2.3 described length of $l_{lp} = 0,4 * a_{th}$ and is aligned with the right side of the wall element. The angle between the two sections of the impact paddle is set to $\delta = 15\,°$ (compare paragraph 3.2.3). On the left end of the impact paddle you can see a small flap that is bent about $180\,°$. This tip flap is an additional reinforcement at the entry point of the water flow into the chamber. The experience from former water wheel constructions showed the necessity to provide this here [6].
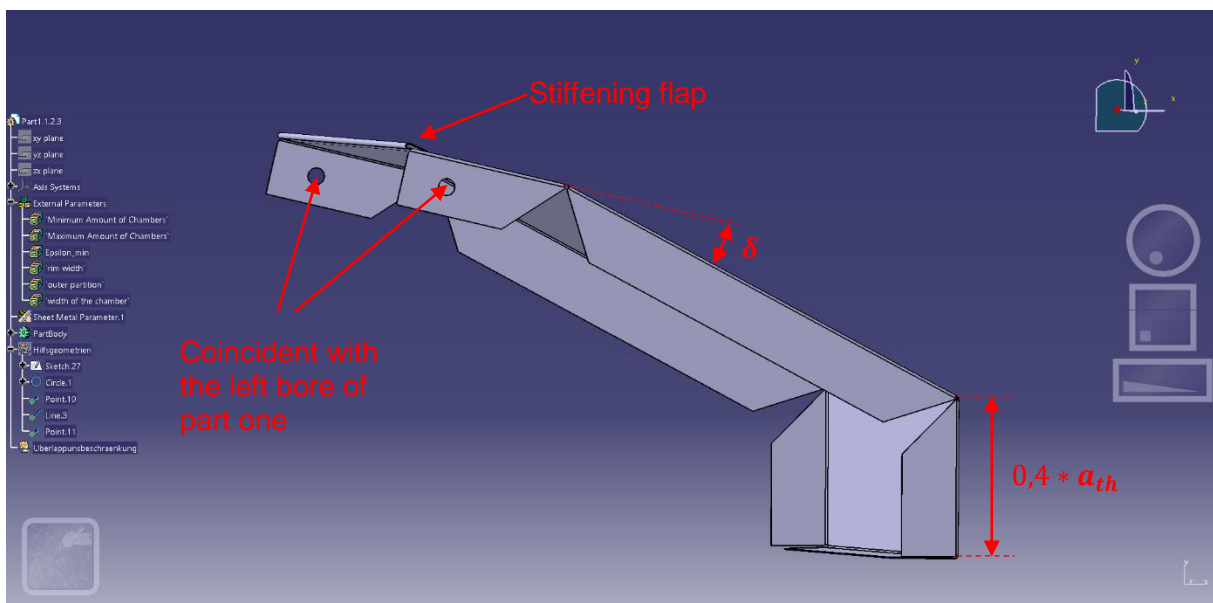
Figure 3-18: CAD-Model - part 2 - paddle element

3.3.3.3 Component 3 – bottom element

The last needed component to build a module is the bottom element. It also depends on the dimensions of the wall segment. Therefore, as already done for the CAD-model of component 2, the main geometric relations are imported from component 1. The challenge in designing component 3 is optimizing its length and thereby minimizing possible water losses to the centre of the water wheel and still enable an unhindered relative rotation of the modules towards each other. Figure 3-19 sketches the limitation. You can see that for smaller diameters of the water wheel the possible bottom length is smaller than for greater diameters. This happens, due to the greater overlap of the cells among each other at smaller diameters. As the designed module shall be applicable for all possible diameters within the concept size, the minimal diameter is the restrictive state.
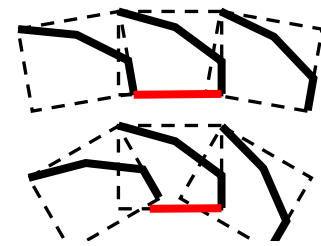
Figure 3-19: influence of the rotation on the bottom length

In the CAD-model the maximum possible length for the bottom element is calculated depending on the parameter of the minimum number of chambers minus a few millimetres of clearance to prevent manufacturing deviations. The angle of the kinked bottom segment is chosen such that with the use of the minimum number of chambers the kinked part is parallel to the bottom element of the adjoining module. The kinked part is added to exhaust the maximal bottom length while minimizing water losses at the inner part of the cell. Like the paddle element the bottom element has side flaps for the blind rivet joints with the wall elements. The flaps are bend downwards keeping the conjunctions to the neighbouring cells outside the closed chamber. That eases the assembly of the modules into a water wheel enormously. This topic is accomplished detailed in paragraph 3.4.1. The marked point in the CAD-model represents, like in component 1 the position of the necessary bore that is drilled during the assembly of the water wheel (compare paragraph 3.3.3.1). The right edge of the bottom element is aligned with the right edge of the side wall element. The lower horizontal edge is adjusted with the lower horizontal edge of component 1. The result is presented in Figure 3-20.
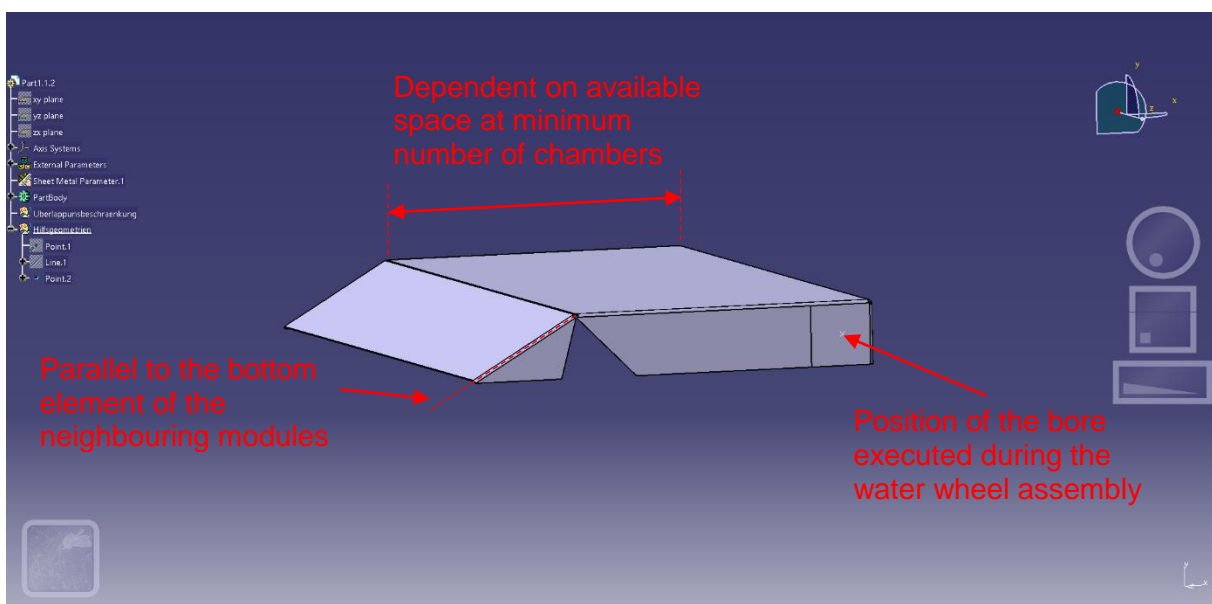
Figure 3-20: CAD-Model - component 3 - bottom element

3.3.3.4 Module assembly

Since all the separate components of the module design have been transformed into CAD-models, they can now be assembled to a complete cell. The result is presented in Figure 3-21. It clearly shows where the points of contact between the elements are. The blind rivets link the elements such that the paddle and the bottom element are connected to each other as well as to both wall elements.
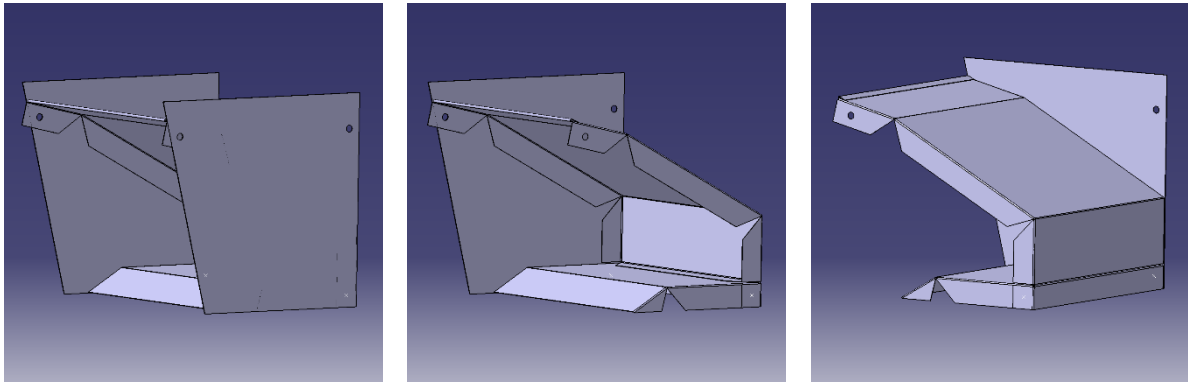
Figure 3-21: Overview - module assembly

Figure 3-22 illustrates the assembled cell and shows the two main designing parameters. As intended the holes in the side wall elements and the paddle element coincide perfectly. The final shape of the cell is marked in black. Accomplishing better accessibility of the bores with tools during assembly of the water wheel, the bottom of the cell has an offset towards the lower edge of the side wall element which is determined by s. The offset is transferred to the paddle element such that the required rim width a_{th} is reached (compare shift of a_{th} between right and lefts side). The outer partition t_o is still defined via the horizontal distance of the two bores. In the picture of the assembled module it becomes clear that the free circle with radius s, introduced in paragraph 3.3.3.1, is preserved in the assembled cell.
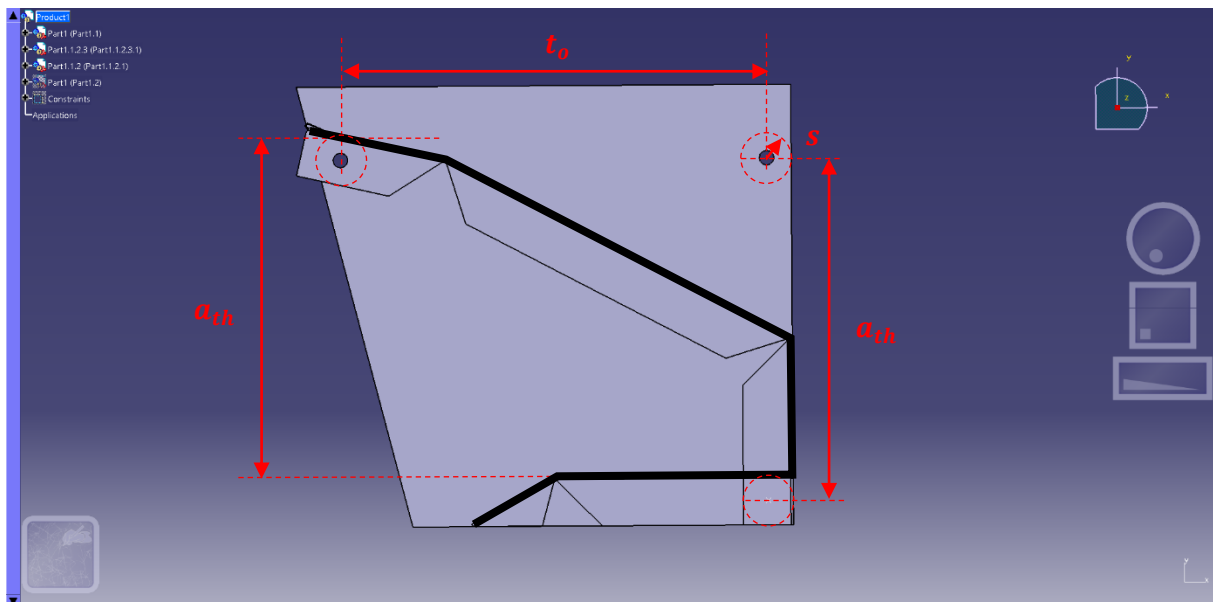
Figure 3-22: Side view of the entire cell

3.4 Water wheel concept

Since the design of the single modules is completed, the next step is to assemble them into the water wheel. The subsequent installation of the water wheel itself includes some restrictions to ensure a proper operation. The current section presents these limiting factors.

3.4.1 Water wheel assembly

Finally, the water wheel can be assembled in CATIA as a three-dimensional model based on the above generated modules. After adding the single cells to a new water wheel product, the relative position to each other has to be defined. Figure 3-23 shows the relative position of two neighbouring modules forming a chamber for the minimum number of chambers $z_{min} = 12$ on the left and for the maximum number of chambers $z_{max} = 25$ on the right. The wall elements in the front plane are suppressed in this figure, to give a better impression of the constellation of the inner parts.
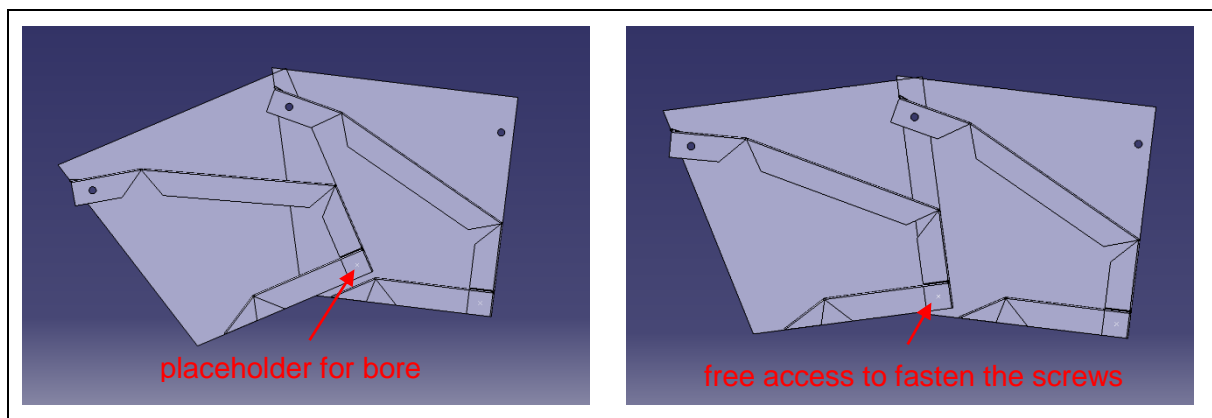
Figure 3-23: Relative position of the modules in the water wheel assembly dependent on different numbers of modules

Figure 3-23 shows that the overlap due to rotation is greater for small water wheel diameters (left picture) and smaller for greater water wheel diameters (right picture). Furthermore, the intended parallelism of the kinked segment of the bottom element and the neighbouring bottom element for the minimum valid number of chambers is fulfilled (left picture). The white point close to the downright edge of each cell still represents the placeholder for the bore finally fixing the relative position of the modules. By analysing Figure 3-23 it can be derived that there is no possibility to prefabricate that hole prior to the assembly because the modules have to be installed in different water wheel diameters. In addition to the flexible application, processing the bore after putting the chambers into their final position prevents upcoming manufacturing divergences. The placing of the bores during the assembly process will be demonstrated within the construction of the prototype in chapter 5.

Also, the position of the bores and thus the offset of the bottom facilitating the assembly is clarified now. The outer ring of screws is tightened from the top, whereas the inner ring of screws is fastened from below the chambers as illustrated in Figure 3-23 (right picture). This way working with tools inside the narrow cells is prevented.

An example of an assembly with enough chambers to form an entire water wheel is illustrated in Figure 3-24.
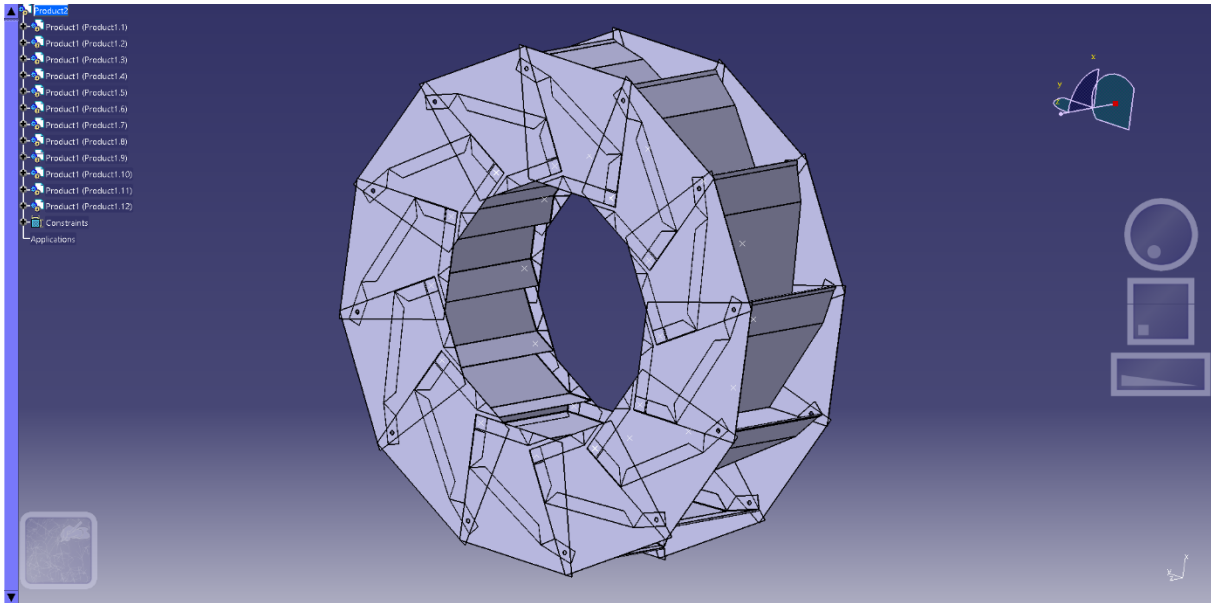
Figure 3-24: CAD-model - water wheel assembly with 12 modules

3.4.2 Installation at operating site

Besides the requirements of the module design, there are some specifications required due to the installation of the water wheel at the operating site.

Most importantly, the unhindered rotation of the water wheel must be assured. Therefore, clearances above (y_{secure}) and beneath (h_{secure}) the water wheel are established as illustrated in Figure 3-25.

The clearance above the water wheel is the distance between the active radius of the water wheel and the lower rim of the water jet. The active radius of the water wheel is determined by the tips of the impact paddles. This space prevents the paddle tips from getting in contact with the channel. The distance should be defined relative to the thickness of the channel bottom and the expectable installation tolerances.

Beneath the water wheel the clearance is identified as the distance between the outer radius of the

Figure 3-25: Clearances

water wheel and the ground. It is very important to refer to the outer radius here as it marks the lowest point of the water wheel.

y_{secure} is a strong condition that always is fulfilled exactly whereas h_{secure} defines a minimum condition that also can be greater dependent on the constellation of height of fall and the optimal water wheel diameter. The clearances should be as little as possible to minimize the losses of height of fall.

The third installation parameter concerns the total width of the water wheel. Besides the use of a single water wheel, it is also possible to operate several water wheels in parallel and thus gathering higher flow rates of water. Figure 3-26 gives an impression of this idea.
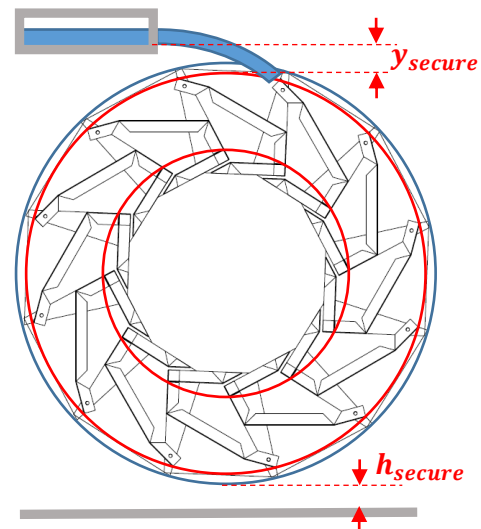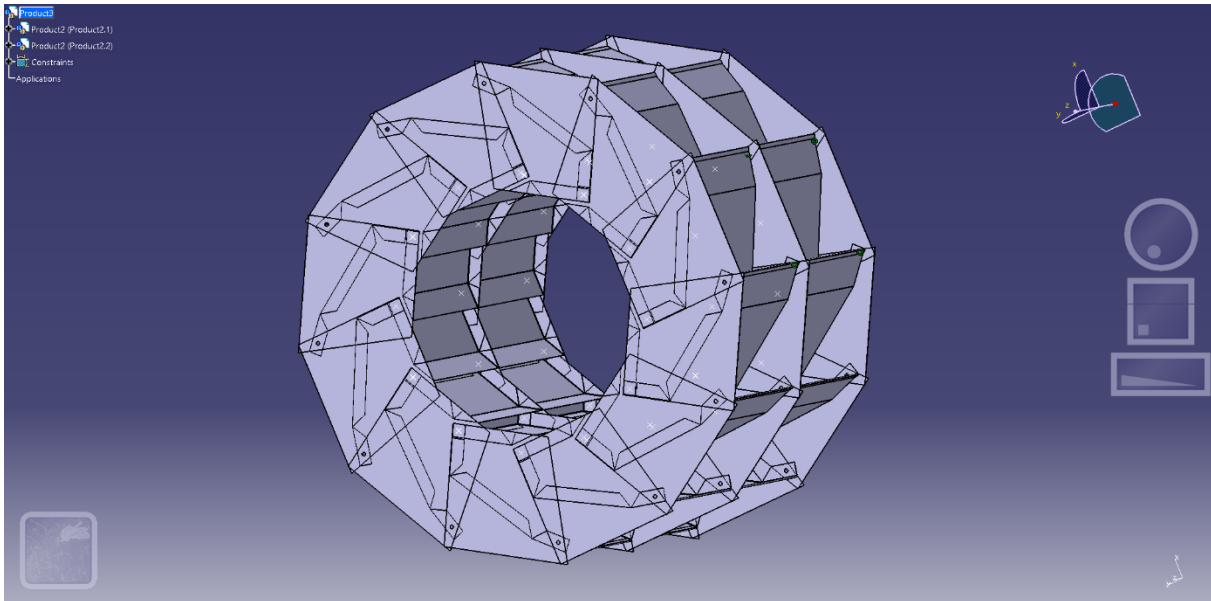
Figure 3-26: CAD-Model - use of two wheels to extend the width

Which combinations of modules are suggestive and how the grouping affects the channel which guides the water to the water wheel is considered in the following.

To achieve a good ventilation, it is generally required that the channel is smaller than the water wheel. For small water wheels, good performances are named for channel widths that are $0,1\ m$ smaller than the water wheel [19, p. 120]. This recommendation is taken into the concept. If the water wheel has a rim in the middle, the channel has to fulfil this requirement for each part of the wheel. This leads to a separation of the water flow into more channels [19, p. 120]. (See Figure 3-27).
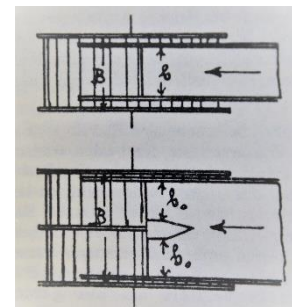
Figure 3-27: Channel width for ventilation [9, p. 14]

Based on this knowledge, the possible water wheel combinations and the related width of the channel can be fixed. The goal is to find a concept that enables a maximum of different possibilities with a minimum of effort. Therefore, as a first step, the minimal width of the channel is restricted to $0,1\ m$. From the above introduced relation of the water wheel width with respect to the channel width it follows that the width of the chamber should be $b_1 = 0,2\ m$. Based on this chamber width the total width of the water wheel grouping can be increased in steps of $0,2\ m$ and, thus, the total channel width increases with $0,1\ m$-steps. Continuing with this concept the total width of the water wheel grouping rises quite fast. Creating a channel width of $0,5\ m$ the water wheel grouping is already $1,0\ m$ wide. To avoid this rapid increase of the total water wheel width, a second module with a different width can be gathered into the concept. The second chamber width is set to $b_2 = 0,3\ m$. With these two module width, it is possible to increase the total channel width by steps of $0,1\ m$ and still keep the total water wheel width smaller, which saves material and simplifies the installation of the water wheel. Possible combinations and resulting total width of the water wheel grouping and the channel are summarised in Table 3-5. $combi$ is the parameter for the combination of the two module widths in the water wheel grouping, B_{WW} is the resulting total width of the water wheel and b_{ch} describes the occurring total channel width. These three parameters will later be used in the Matlab-tool to optimize the water wheel for a certain operating site.

Table 3-5: Module width combinations and resulting total width

$combi$	$B_{WW}\,[m]$	$b_{ch}\,[m]$
b_1	0,2	0,1
b_2	0,3	0,2
$b_1 + b_2$	0,5	0,3
$b_2 + b_2$	0,6	0,4
$b_2 + b_1 + b_2$	0,8	0,5

This agglomeration of water wheels to a wider wheel could be continued endless. To limit the total width at a certain level, it is interrupted here at a total water wheel width of $0,8\,m$.

It has to be taken into account that the possible chamber width also depends on the chosen material. Before going into mass production, it should be verified that the material has the required strength to form solid cells. Sheet metal with a thickness of $0,75\,mm$ fulfils these requirement for modules with a width of $0,2$ and $0,3\,m$.

3.5 Advantages / Disadvantages of the concept

Concluding the chapter "Water wheel concept and design" the advantages and disadvantages of the concept are analysed to enable a sophisticated evaluation.

3.5.1 Advantages

The main advantage, which is also a requirement to the design concept, is the simplicity of the design. The manufacturing can be done with simple machinery that should be available all around the world.

Another benefit relies on the modularity of the concept. It enables the adaptability of a water wheel to different heights of fall within the validity of the concept size, without extensive designing activities. Furthermore, it is possible to exchange single modules in case of a damage. This keeps the maintenance of the water wheels easy. Hopefully that will lead to a continuing operation of the water wheels in contrast to many other more technologically advanced components that lie waste after a damage, because nobody is able to repair it.

Finally, the modularity allows a prefabrication of the single cells. They can be transported easily to the operating site and only need to be joint together using bolts. Thereby, the advantages of a production in an equipped machine shop are harnessed and the restrictions of a rural installation site of the water wheel are reduced.

3.5.2 Disadvantages

The main disadvantage is the possible leaking at the bottom of the chamber, because the modular design prevents a total sealing of the bottom (compare Figure 3-28). This effect is worse for greater water wheel diameters.

Figure 3-28: Leaking at the bottom of the chamber

In addition, for small water wheel diameters, the overlap of the modules due to the relative angle is bigger than necessary for joining the parts. This is required to also use the cells for larger water wheel diameters but creates in many cases an unused material surplus.

At last, the use of equal modules for different sites might lead to a loss of efficiency compared to an optimization of the design for each site separately.

3.5.3 Evaluation

It has to be pointed out that effects that create disadvantages on one side generate advantages on the other side, like the modularity for example.

Besides that, the occurrence of the disadvantages has to be verified in test operation of the water wheel. It depends on the entry point of water flow, the final point of operation and the water wheel diameter whether the disadvantages really appear and how strong they affect the operation. In addition, if the test is negative, the losses could easily be prevented by attaching a small rubber plate to the module, using blind rivets (See Figure 3-29). Furthermore, an opening of the cell to the inside of the water wheel supports the ventilation of the chamber [11, p. 44] and, thus, also can have a positive effect.

rubber plate + blind rivet

Figure 3-29: Suggestion to prevent leaking

It can be concluded that the advantages predominate. The appearance of the disadvantages has to be attempted in a test and can partially be eliminated with simple constructive arrangements. Overall the developed design concept fulfils the requirements for a simple mass-production of water wheels in developing countries.

4 Dimensioning tool for water wheels

After the design concept is completed in chapter 3, the dimensioning tool is developed based on this concept. The task of the dimensioning tool is to adapt the water wheel to the conditions of the operating site. The Matlab-model to achieve this goal is structured in two parts.

The first part contains the geometrical optimization of the water wheel to the installation site. The perfect number of chambers, the total width of the water wheel with the appropriate grouping, and the optimal entry point of the water flow into the water wheel are determined here.

In the second part of the Matlab-tool the optimal operating point is ascertained by calculating the behaviour of the power output of the generated water wheel. This part is based on the Matlab-model for small-scale low-tech water wheels designed in the bachelor´s thesis "Power transmission for a low-tech water wheel" [16].

The current chapter names the required input parameters and explains structure and functionality of the tool.

4.1 Input variables, parameters and constants

First of all, the required information for the calculations have to be fed into the tool. These are the input parameters of the site, the parameters of the module concept as well as additional limits for the water wheel installation and some constants that are needed for the calculations. This chapter gives an overview of all required data.

4.1.1 Input variables

The whole water wheel design presented in the study at hand claims to be as simple as possible for the operator. Therefore, the input variables are reduced to two values. These two values are the free available height of fall and the occurring volume flow rate of water at the site (Table 4-1).

Table 4-1: Input variables of the Matlab-tool

Name / description	Symbol	Unit
Free available height of fall	H	m
Volume flow rate of water	Q	m^3/s

The tool optimizes a water wheel for these two input variables based on the deposited module design. For the installation of a water wheel according to the presented concept for an installation site it is only required to measure these two values and insert them into the code.

4.1.2 Parameters of the module design

Although the user will only have to adjust two variables for a fixed module design concept, another advantage of the Matlab-tool is its easy adaptability to different module concept design sizes (compare paragraph 3.2.1). To enable this flexibility, it is important to allow the variation

of many parameters in the code. As these parameters are already explained in detail in chapter 3 they are only listed here in Table 4-2 and not explained any further. It is referred to chapter 3 for further information.

Table 4-2: Parameters of the module design required in the Matlab-tool

Name / description	Symbol	Unit
Outer partition	t_o	m
Theoretical rim width	a_{th}	m
Thickness of the sheet metal	d	m
Permitted minimum number of chambers	z_{min}	$-$
Permitted maximum number of chambers	z_{max}	$-$
Step range from z_{min} to z_{max}	Z	$-$
Extended length of the wall element as splash water protection	a_{secure}	m
Free radius around the bores	s	m
Minimum angle between tangent on water wheel and the outer paddle section	ε_{min}	°
Angle between the two impact paddle sections	δ	°

4.1.3 Parameters for the water wheel

In addition to the parameters of the module design some specifications assuring a proper assembly and installation of the water wheel are necessary according to chapter 3.4. All the required parameters from the water wheel concept are listed in Table 4-3.

Table 4-3: Parameters of the water wheel optimization requested in the Matlab-tool

Name / description	Symbol	Unit
Clearance between the bottom dead centre of the water wheel and the ground	h_{secure}	m
Clearance between lower rim of the water jet at channel exit and the active upper vertex of the water wheel	y_{secure}	m
Tolerance angle for flow entry into the chamber	ω	°
Width of small module version	b_1	m
Width of broad module version	b_2	m
Possible combinations of the two module width	$combi$	$-$

Name / description	Symbol	Unit
Number of permissible combinations	O	–
Resulting widths of the water wheel	B_{WW}	m
Resulting widths of the channel	b_{ch}	m

4.1.4 Parameters for the power output

All required data processed in the second part of the Matlab-tool are directly computed results of part one. Therefore, just one more parameter is added to complete the required dataset of the Matlab programme part 2. The value does not affect the result of the calculations, but offers an additional output. The input of a value for the dimensioning power P_{Dim} results in the output of the corresponding number of revolutions to facilitate the adaptation of a gearbox in case a generator with a certain input power is available.

Table 4-4: Parameter for the power output in the dimensioning point

Name / description	Symbol	Unit
Dimensioning power	P_{Dim}	W

4.1.5 Constants

For the sake of completeness, Table 4-5 lists the two constants needed for the calculations. They are independent of the site or the used module concept. Thus, it is not necessary to change their values within multiple simulations.

Table 4-5: Necessary constants for the Matlab-tool

Name	Symbol	Value	Unit
Acceleration of gravity	g	9,81	m/s^2
Density of water	ρ_W	999,97	kg/m^3

4.2 Structure of the Matlab model

After summarizing the required input variables, the parameters of the concept and the required constant values, the following chapter describes the functionality of the two parts of the Matlab-tool.

4.2.1 Part 1 – optimized dimensions and installation

The first part addresses the selection of an optimized water wheel for a given operating site, based on the module concept and the water wheel itself. The different steps achieving that target are presented.

4.2.1.1 Optimization of the number of modules

Extracting as much energy as possible from the water, the water wheel has to be as large as possible. Thus, the optimization goal is to find the maximum number of cells that, assembled into a water wheel, fits into the given height of fall and satisfies the constraints of the installation (compare paragraph 3.4.2). Therefore, the total diameter (equation (4-3)) and the active outer diameter of the water wheel (equation (4-2)) are calculated. The active outer diameter is indicated by the tips of the impact paddles. The segment angle $\xi(k)$ is calculated depending on the number of cells k (equation (4-1)) as input value for the determination of the diameters. Figure 4-1 illustrates the calculated values.

$$\xi(k) = \left(\frac{2 * \pi}{k}\right) \tag{4-1}$$

$$D_{active\ out}(k) = \left(\frac{t_o}{2 * \sin\left(\frac{\xi(k)}{2}\right)} + s\right) * 2 \tag{4-2}$$

$$D_{total}(k) = \left(\frac{t_o}{2 * \sin\left(\frac{\xi(k)}{2}\right)} + \frac{a_{secure}}{\cos(\xi(k))}\right) * 2 \tag{4-3}$$
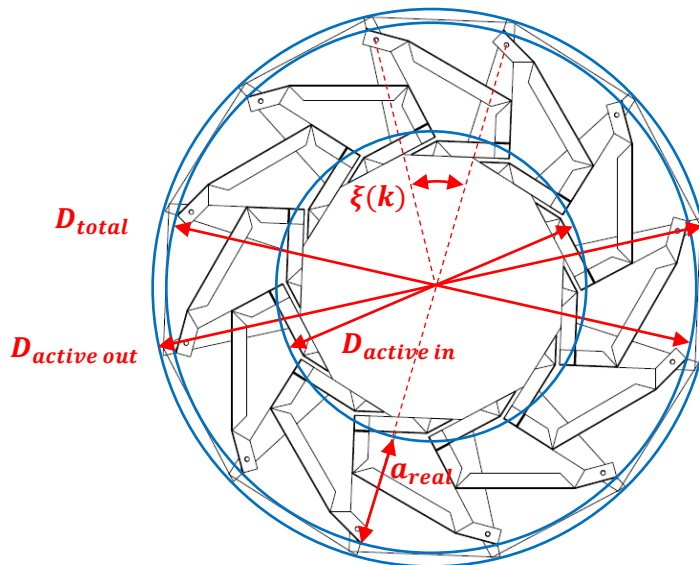
Figure 4-1: Optimized water wheel dimensions

In the next step, the optimal number of cells k_{opt} is calculated with respect to the stated clearances above and beneath the water wheel (compare paragraph 3.4.2) and the allowed step range Z. Z defines the range by which the number of modules can be increased raising k from z_{min} to z_{max}.

In case the introduced height of fall allows a greater number of cells than the concept permits, the message *"The chosen height of fall is greater than the maximum for the given concept. You possibly could extract more energy with a different concept"* is displayed in a textbox and for the further determination $k_{opt} = z_{max}$ is set.

When k_{opt} is smaller than z_{min} the calculation stops and an error with the in information "*The chosen height of fall is too low for the given concept and undercuts z_{min}*" appears in a textbox.

After detecting k_{opt}, the optimal values $\xi_{opt} = \xi(k_{opt})$, $D_{active\ out\ opt} = D_{active\ out}(k_{opt})$, and $D_{total\ opt} = D_{total}(k_{opt})$ are identified. The inner partition t_i of the water wheel is finally calculated depending on t_o, a_{th} and ξ_{opt} as presented in Figure 4-2. Equation (4-4) determines the inner partition t_i.

$$t_i = \left(\left(t_o^2 + a_{th}^2 - 2 * t_o * a_{th} * \cos\left(\frac{\pi}{2} - \xi_{opt}\right) \right) + a_{th}^2 - 2 \right.$$

$$* \left(\left(t_o^2 + a_{th}^2 - 2 * t_o * a_{th} * \cos\left(\frac{\pi}{2} - \xi_{opt}\right) \right)^{0.5} \right) * a_{th} \tag{4-4}$$

$$\left. * \cos\left(\frac{\pi}{2} - \text{asin}\left(a_{th} * \frac{\sin\left(\frac{\pi}{2} - \xi_{opt}\right)}{\left(t_o^2 + a_{th}^2 - 2 * t_o * a_{th} * \cos\left(\frac{\pi}{2} - \xi_{opt}\right) \right)^{0.5}} \right) \right) \right)^{0.5}$$
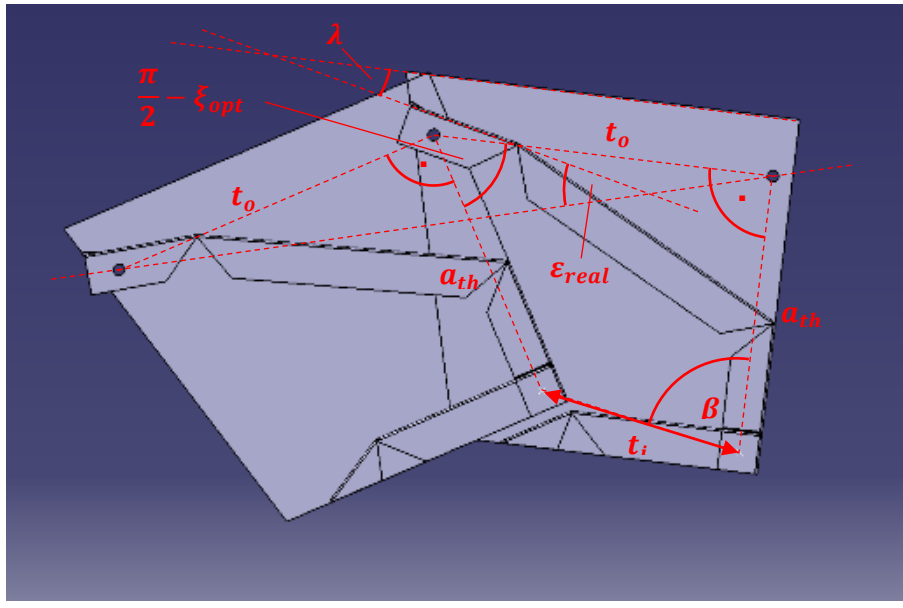
Figure 4-2: Specification of the inner partition

The active inner diameter $D_{active\ in}$ can now be determined based on the previously calculated inner partition of the water wheel (Equation (4-5)).

$$D_{active\ in} = \left(\frac{t_i}{2 * \sin\left(\frac{\xi_{opt}}{2}\right)} + s \right) * 2 \tag{4-5}$$

As the inner and outer active diameter are specified, the resulting real rim width a_{real} is calculated with Formula (4-6). The values are also shown in Figure 4-1.

$$a_{real} = \left(\frac{D_{active\ out\ opt} - D_{active\ in}}{2}\right) \tag{4-6}$$

Furthermore, the real occurring angle ε_{real} between the outer impact paddle section and the tangent on the water wheel is calculated after fixing the optimal number of modules and, hence, the relative position of the modules towards each other Equation (4-7). (See Figure 4-2)

$$\varepsilon_{real} = \frac{\xi_{opt}}{2} + \lambda \tag{4-7}$$

As it is required for later calculations, the angle β, between t_i and the right vertical module edge, is computed as presented in formula (4-8) (compare Figure 4-2).

$$\beta = \arcsin\left(\left(t_o^2 + a_{th}^2 - 2 * t_o * a_{th} * \cos\left(\frac{\pi}{2} - \xi_{opt}\right)\right)^{0,5}\right. $$
$$\left. * \frac{\sin\left(\frac{\pi}{2} - \text{asin}\left(a_{th} * \frac{\sin\left(\frac{\pi}{2} - \xi_{opt}\right)}{\left(t_o^2 + a_{th}^2 - 2 * t_o * a_{th} * \cos\left(\frac{\pi}{2} - \xi_{opt}\right)\right)^{0,5}}\right)\right)}{t_i}\right) \tag{4-8}$$

4.2.1.2 Minimum opening width of the chamber

The minimum opening clearance of the chamber is calculated because it affects the possible thickness of the water flow entering a cell. Hence it is one of the crucial design parameters for the total width of the water wheel and the optimal entry point, which are specified in paragraph 4.2.1.5.

The minimum opening width of the chamber varies with the number of cells in the water wheel due to the different relative position of the modules towards one another. This clearance is calculated using vector geometry. Therefore, the shape of a chamber, created by two modules, is described by vectors as illustrated in Figure 4-3. For each paddle, a relative coordinate system (blue) is set with its origin at the position of the bore created during the water wheel assembly.

The challenge is to describe all the marked points $(P_1, P_2, ..., P_8)$ dependent on the origin (O_1) of the right module.

Referred to O_1, the coordinates of P_1, P_2, the auxiliary points B and C and the directing vectors l_{23d}, for the connection of P_2 and P_3, l_{34d}, for the connection of P_3 and P_4, and l_{rimd}, for the left edge of the right module are defined as follows, based on the information about the module design.

$$\overrightarrow{P_1} = \begin{bmatrix} s \\ s \\ 0 \end{bmatrix}$$

$$\overrightarrow{P_2} = \begin{bmatrix} s \\ 0,4 * a_{th} + s \\ 0 \end{bmatrix} \qquad\qquad \overrightarrow{l_{23d}} = \begin{bmatrix} -\sin(\tau) \\ \cos(\tau) \\ 0 \end{bmatrix}; \ with\ \tau = \frac{\pi}{2} - \delta - \lambda$$

$$\vec{B} = \begin{bmatrix} -t_o \\ a_{th} \\ 0 \end{bmatrix} + s * \begin{bmatrix} \sin(\lambda) \\ \cos(\lambda) \\ 0 \end{bmatrix} \qquad \qquad \overrightarrow{l_{34d}} = \begin{bmatrix} -\cos(\lambda) \\ \sin(\lambda) \\ 0 \end{bmatrix}$$

$$\vec{C} = \begin{bmatrix} -t_o \\ a_{th} \\ 0 \end{bmatrix} + s * \begin{bmatrix} \sin(\chi) \\ \cos(\chi) \\ 0 \end{bmatrix} \qquad \qquad \vec{l}_{rimd} = \begin{bmatrix} -\sin(\chi) \\ \cos(\chi) \\ 0 \end{bmatrix}$$

P_3 is determined by solving linear system (4-9) which describes the intersection of the two straight lines $\overline{P_2 P_3}$ and $\overline{BP_3}$. With the resulting value for the parameter v_1, P_3 is calculated.

$$P_3: \qquad \overrightarrow{P_2} + v_1 * \overrightarrow{l_{23d}} = \vec{B} + v_2 * \overrightarrow{l_{34d}} \qquad \qquad (4\text{-}9)$$

$$\overrightarrow{P_3} = \overrightarrow{P_2} + v_1 * \overrightarrow{l_{23d}}$$

Similarly, P_4 is determined by solving linear system (4-10) which constitutes the intersection of $\overline{BP_3}$ and $\overline{CP_4}$. Again, P_4 is determined using the resulting value for parameter q_1.

$$P_4: \qquad \vec{C} + q_1 * \vec{l}_{rimd} = \vec{B} + q_2 * \overrightarrow{l_{34d}} \qquad \qquad (4\text{-}10)$$

$$\overrightarrow{P_4} = \vec{C} + q_1 * \vec{l}_{rimd}$$

Once all required points of the paddle of the first module are calculated, the points describing the shape of the second paddle are easily determined, because the second paddle has exactly the same relation to O_2 than the first paddle has to O_1. Describing the points of the second paddle relative to O_1 only requires the transformation matrix T between the two module-fixed coordinate systems and the position of O_2 describe in coordinate system 1 ($O_{2\to O1}$). Both parameters are presented below:

$$T = \begin{bmatrix} \cos(\xi_{opt}) & -\sin(\xi_{opt}) & 0 \\ \sin(\xi_{opt}) & \cos(\xi_{opt}) & 0 \\ 0 & 0 & 1 \end{bmatrix} \qquad \qquad \overrightarrow{O_{2\to O1}} = t_i * \begin{bmatrix} -\sin(\beta) \\ \cos(\beta) \\ 0 \end{bmatrix}$$

Based on that, the points P_5, P_6, P_7 and P_8 are calculated referred to coordinate system 1 as follows:

$$\overrightarrow{P_5} = \overrightarrow{O_{2\to O1}} + T * \overrightarrow{P_1} \qquad \qquad \overrightarrow{P_6} = \overrightarrow{O_{2\to O1}} + T * \overrightarrow{P_2}$$

$$\overrightarrow{P_7} = \overrightarrow{O_{2\to O1}} + T * \overrightarrow{P_3} \qquad \qquad \overrightarrow{P_8} = \overrightarrow{O_{2\to O1}} + T * \overrightarrow{P_4}$$
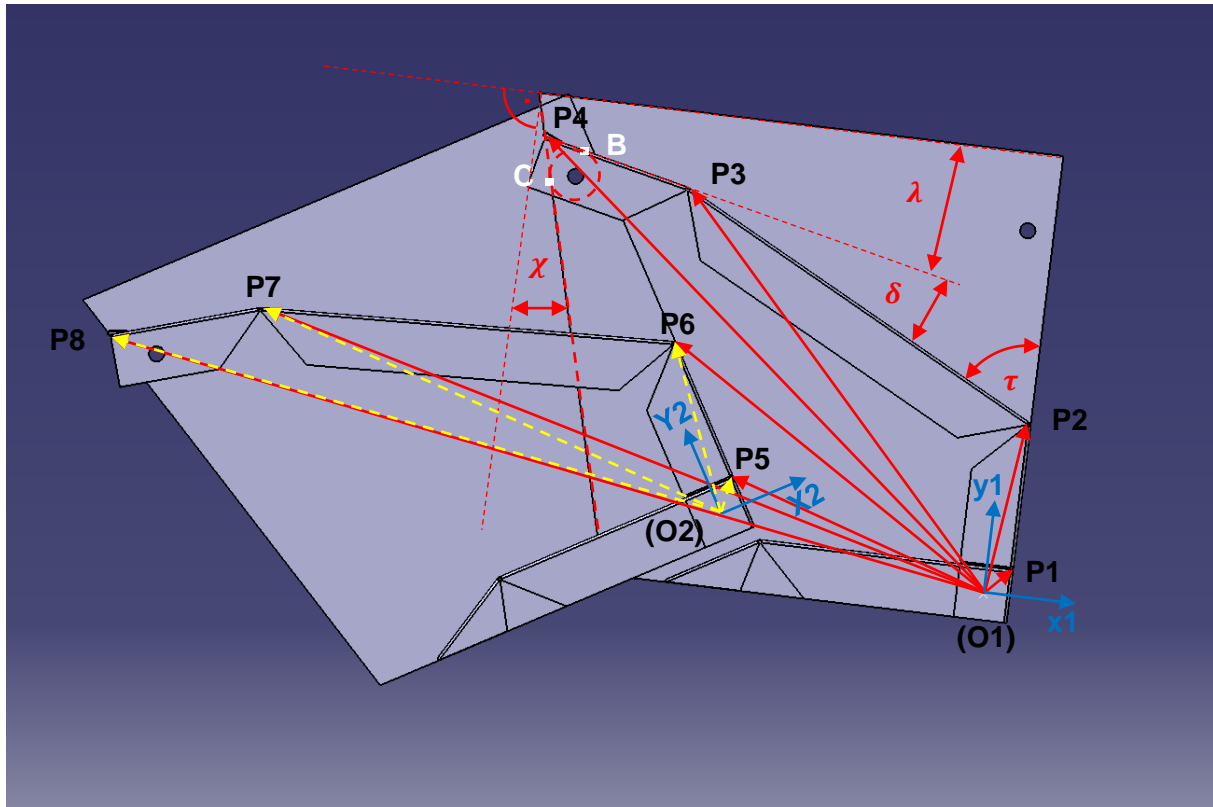
Figure 4-3: Vector description of the chamber shape

Since the coordinates of all relevant points are known, the minimum clearance of a chamber is calculated. Four measurable distances are candidates to represent the minimum opening width. These are the distances of the points P_6 and P_7 to the straight lines $\overline{P_2P_3}$ and $\overline{P_3P_4}$ as shown in Figure 4-4.
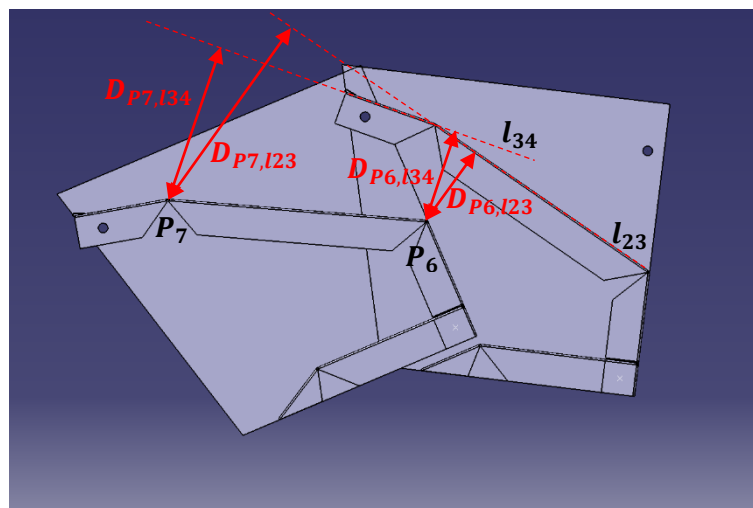
**Figure 4-4: candidates for the minimal opening
distance of the chamber**

In the presented case, it appears that the distances related to P_7 are not relevant for the minimum distance, but this changes for varying numbers of modules and possible other module designs. For that reason, all four distances are taken into account for obtaining the total flexibility of the tool.

If the coordinates are known, the distance of a point to straight line can be computed using the cross product. Thus, the four distances are calculated as follows:

$$D_{P6l23} = \frac{\left|\left(\overrightarrow{l_{23d}} \times (\overrightarrow{P_6} - \overrightarrow{P_2})\right)\right|}{\left|\overrightarrow{l_{23d}}\right|}$$

$$D_{P6l34} = \frac{\left|\left(\overrightarrow{l_{34d}} \times (\overrightarrow{P_6} - \vec{B})\right)\right|}{\left|\overrightarrow{l_{34d}}\right|}$$

$$D_{P7l23} = \frac{\left|\left(\overrightarrow{l_{23d}} \times (\overrightarrow{P_7} - \overrightarrow{P_2})\right)\right|}{\left|\overrightarrow{l_{23d}}\right|}$$

$$D_{P7l34} = \frac{\left|\left(\overrightarrow{l_{34d}} \times (\overrightarrow{P_7} - \vec{B})\right)\right|}{\left|\overrightarrow{l_{34d}}\right|}$$

Finally, the minimum value of these four distances is stated as D_{open}.

4.2.1.3 Calculation of the water flow

Besides the diameter of the water wheel, the optimizing criteria are the optimal entry point of the water flow into the water wheel and perfect total width of the water wheel. To optimize them, the behaviour of the water flow is required. Thus, the stream line and the thickness of the water flow are calculated in this paragraph.

The most important parameter to specify the water flow is the flow velocity in the channel. As explained in chapter 2.2 we use an open channel without slope guiding the water to the water wheel. For this installation, the velocity of the fluid in the channel v_{ch} is approximated using [21, pp. 410-411] and [11, p. 25], as presented in equation (4-11) with the control variable *o* specifying the allowed channel width, as per definition of the water wheel concept.

$$v_{ch}(o) = \left(g * \frac{Q}{b_{ch}(o)}\right)^{\frac{1}{3}} \tag{4-11}$$

Since, the flow velocity is determined, the depth of the water flow in the channel wd_v is calculated (formula (4-12)):

$$wd_v(o) = \frac{Q}{b_{ch(o)} * v_{ch(o)}} \tag{4-12}$$

Based on that, the water stream line, as illustrated abstractly in Figure 4-5, is calculated. The behaviour of the water exiting a levelled channel is described as a horizontal throw.

By putting the origin into the outlet of the channel, the lower edge of the flow line xw in relation to the vertical position y of the water is calculated according to equation (4-13), with e being the control variable for the vertical coordinate. It declares the step range to $0,001\ m$.

$$xw(o,e) = \left(2 * \frac{y(e)}{g}\right)^{0.5} * v_{ch}(o) \tag{4-13}$$

Optimizing the smooth entry point later, the gradient angle $x_{w,rad}$ and the thickness of the water flow orthogonal to the flow direction wd_{orth} is needed. The gradient angle between the water flow line and the horizon is calculated as presented in Formula (4-14).

$$xw_{rad}(o,e) = \arctan\left(\left(\left(0.5 * v_{ch}(o) * \left(\frac{2}{g * y(e)}\right)^{0.5}\right)\right)^{-1}\right) \qquad (4\text{-}14)$$

Equation (4-15) computes wd_{orth} depending on vertical position y, the flow velocity in the channel v_{ch} and the water depth in the channel wd_v.

$$wd_{orth}(o,e) = \cos\left(\arctan\left(\frac{1}{0.5 * v_{ch}(o) * \left(\frac{2}{g * y(e)}\right)^{0.5}}\right)\right) * wd_v(o) \qquad (4\text{-}15)$$

All the correlations explained in this paragraph are illustrated in Figure 4-5. The presented water flow is an example for a certain water depth in the channel $wd_v = 0,13\ m$ and a flow velocity in the channel of $v_{ch} = 1,11\ \frac{m}{s}$.
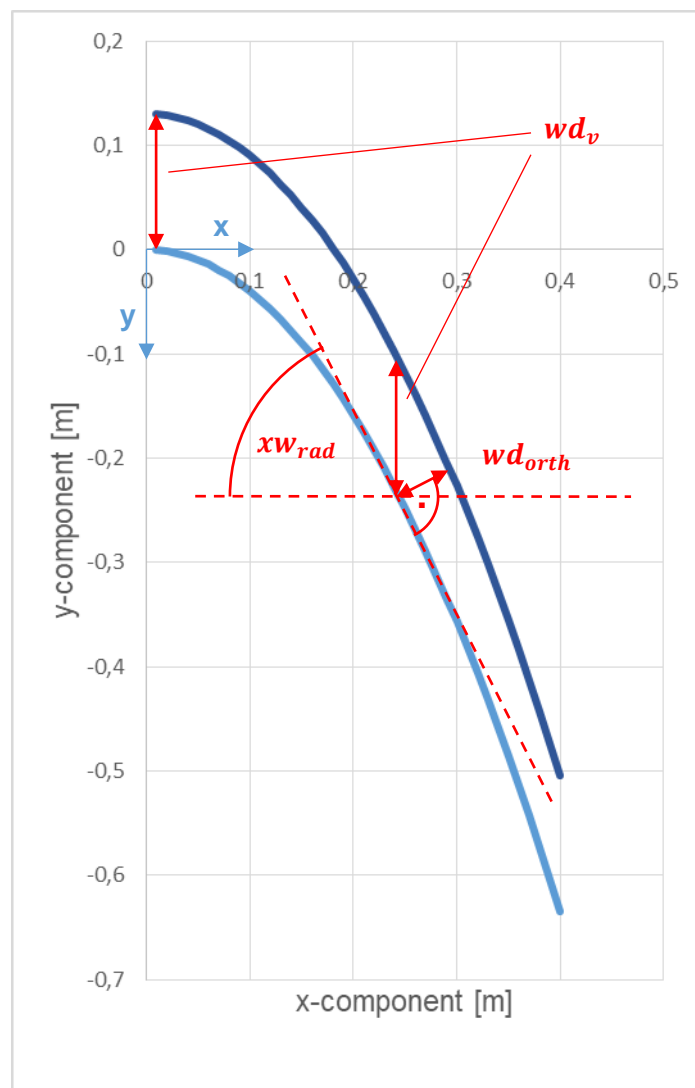
Figure 4-5: Water flow as horizontal throw

4.2.1.4 Position and entry angle of the water wheel

For all possible entry points of the water wheel, the exact position and the corresponding angle of the entry section of the impact paddle relative to the horizontal line is required to adapt them to the values of the water flow in the optimizing process.

Since between the active outer diameter and the lower edge of the water flow the clearance y_{secure} is introduced, no values of the water wheel exist for the interval $y = [0; y_{secure}[$. A second restriction occurs due to the fact that an entry position with an angle of the entry section of the impact paddle relative to the horizontal greater $90°$ shall be suppressed. Thus, borders for the control variable $e = [e_{min}; e_{max}]$ must be set. The restrictions for e_{min} and e_{max} are described in Equation (4-16) and (4-17).

$$y(e_{\min}) = y_{secure} \tag{4-16}$$

$$y(e_{max}) = 0.5 * D_{active\ out\ opt} + y_{secure} - \cos\left(\frac{\pi}{2} - \varepsilon_{real}\right) * 0.5 * D_{active\ out\ opt} \tag{4-17}$$

Figure 4-6 depictures these restrictions. The total circle describing the active outer diameter is highlighted in blue. The red section marks the possible entry points of the water flow into the water wheel according to the above defined limitations. Impinging water on the water wheel left of the vertex is not implicated in the tool as it is not requested due to efficiency purposes [18, p. 211].
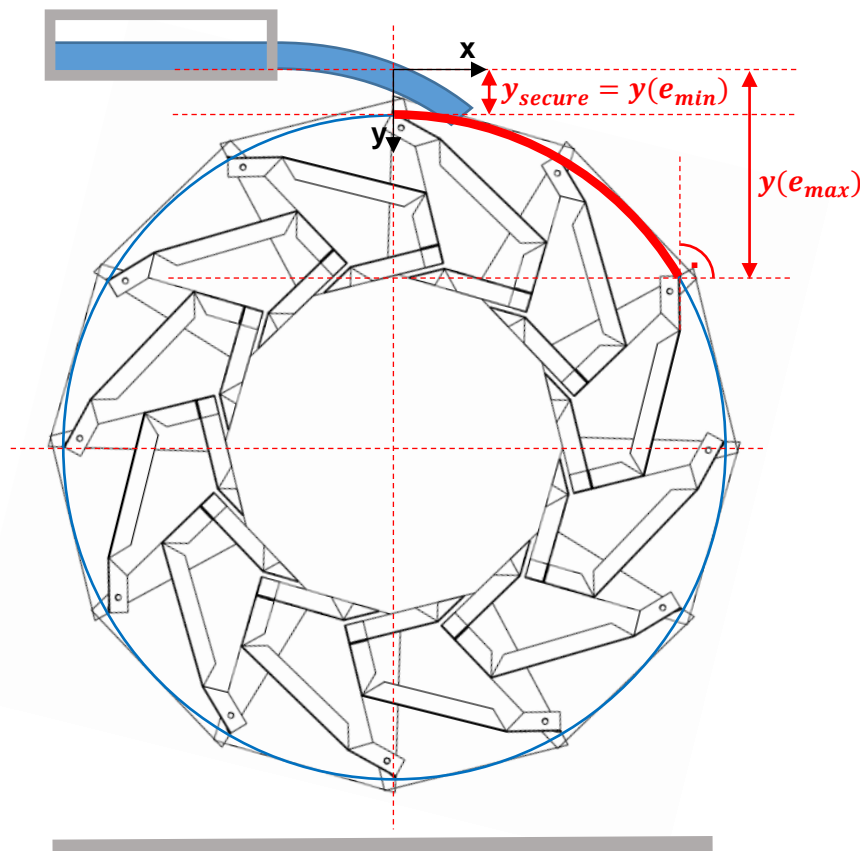
Figure 4-6: Possible entry section

Using these restrictions for e, the possible positions of the entry points xWW dependent on y (Equation (4-18)) and the dedicated angles between the outer impact paddle section and the horizontal xWW_{rad} (Formula (4-19)) are calculated. Figure 4-7 shows all the necessary correlations to form the two equations.

$$xWW(e) = 0.5 * D_{active\ out\ opt} * \sin\left(a\cos\left(\frac{0.5 * D_{active\ out\ opt} - y(e) + y_{secure}}{0.5 * D_{active\ out\ opt}}\right)\right)$$ (4-18)

$$xWW_{rad}(e) = \left(\arccos\left(\frac{0.5 * D_{active\ out\ opt} - y(e) + y_{secure}}{0.5 * D_{active\ out\ opt}}\right) + \varepsilon_{real}\right)$$ (4-19)
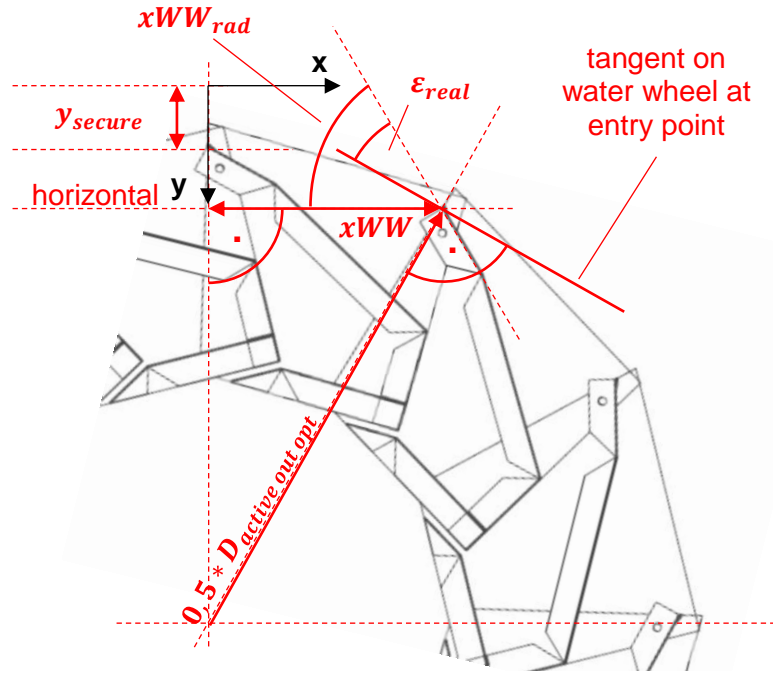
Figure 4-7: Water wheel conditions at entry position

4.2.1.5 Optimisation of the water wheel width and the entry point.

Now all required values to proceed with the final optimisation of the water wheel are known. In this last step, the best combination of the entry point (intersection of the lower water stream line with the active outer diameter of the water wheel) and the total water wheel width are identified. As both of these values influence each other, it is necessary to optimize them together. On the one hand, a small width of the water wheel is targeted to save material, keep the dimensions small and, thus, the installation easier. On the other hand, an entry close to the vertex must be realized to minimize the losses of the height of fall creating a high efficiency.

Conciliating these two optimizing criteria, they are linked in the matrix BX, which rows represent the increasing possible channel width b_{ch}, as defined in the design parameters, referred to by the control variable o. Its columns describe the vertical component y of the entry point indicated by the control variable $e \in [e_{min}; e_{max}]$.

All possible combinations of o and e are tested whether they fulfil the following two requirements. First, the thickness of the water flow has to be smaller than the opening clearance of the chamber. Equation (4-20) presents this limitation.

$$\left(D_{open} - wd_{orth(o,e)}\right) > 0 \qquad (4\text{-}20)$$

The second condition, shown in Formula (4-21), refers to the already in paragraph 3.2.3 mentioned fluid mechanic entry condition, whereupon the water flow and the entry section of the impact paddle preferably should be aligned to minimize the kickback. The allowed angular deviation is defined by ω. To fulfil this requirement, the value of the difference of the angle of water flow to the horizontal line and the angle between the entry section of the impact paddle and the horizontal line has to be between 0° and ω.

$$0 \leq (xw_{rad}(o,e) - xWW_{rad}) \leq \omega \qquad (4\text{-}21)$$

The final optimization is done identifying the minimum value in the matrix BX. Thus, the matrix value is set very high as $BX(o,e) = 10000$ for all combinations that do not fulfil both terms to avoid accidently selecting an illegal combination.

In case a combination meets both requirements, the matrix value is set as described in Equation (4-22):

$$BX(o,e) = e + o * 0.1 * (e_{max} - e_{min}) \qquad (4\text{-}22)$$

The illustrated weighting of the legal combinations is implemented due to the challenge named at the beginning of this chapter to keep the total width of the water wheel small and allow an application close to the upper vertex. Using the current control variable e of the entry point, it is guaranteed that for an equal total width of the water wheel entry points closest to the upper vertex get the smallest value. The second summand defines the weighting of different total width. For each width step o, a factor of 10% of the height difference between the vertex of the water wheel and the lowest allowed entry point (compare paragraph 4.2.1.4) is added to the value e of the position. The result is that a water wheel with a greater total width is selected in the optimisation if it leads to 10% increase of the height of fall according to the allowed height range for the entry points. Thus, very broad water wheels without a significant effect on the efficiency are avoided and appropriate widths for the water wheels are selected.

After the entire matrix BX is filled with the weighted values, the parameters of the optimum combination are identified. This is realised extracting the minimum value of the matrix and reading its row number o and its column number e.

With these two parameters, the optimum values for the following previously introduced arguments $b_{ch,opt}$, $combi_{opt}$, $B_{WW,opt}$, $v_{ch,opt}$, $wd_{v,opt}$ are calculated.

Furthermore, the optimum relative horizontal position of the edge of the channel towards the vertex of the water wheel $x_{rel,opt}$ is determined as presented in Formula (4-23). (See Figure 4-8)

$$x_{rel,opt} = xWW_{opt} - xw_{opt} \qquad (4\text{-}23)$$

The calculation of the power output computed in part 2 of the Matlab-tool requires some additional input information such as the angle between the vertical line and the connection line of the water wheel centre to the optimal entry point. (Equation (4-24); Figure 4-8)

$$\alpha_0 = \arccos\left(\frac{0.5 * D_{active\ out\ opt} - y_{opt} + y_{secure}}{0.5 * D_{active\ out\ opt}}\right) \tag{4-24}$$

Another value, required for part 2, is the flow velocity tangential to the circle of $D_{active\ out\ opt}$ at the optimum entry point. It is defined as follows in Equation (4-25).

$$v_t = \left(\left(\frac{y_{opt} * g}{2}\right) + v_{ch_{opt}^2}\right)^{0.5} * \cos(xWW_{rad} - \alpha_0) \tag{4-25}$$

Finally, Figure 4-8 illustrates these three values.
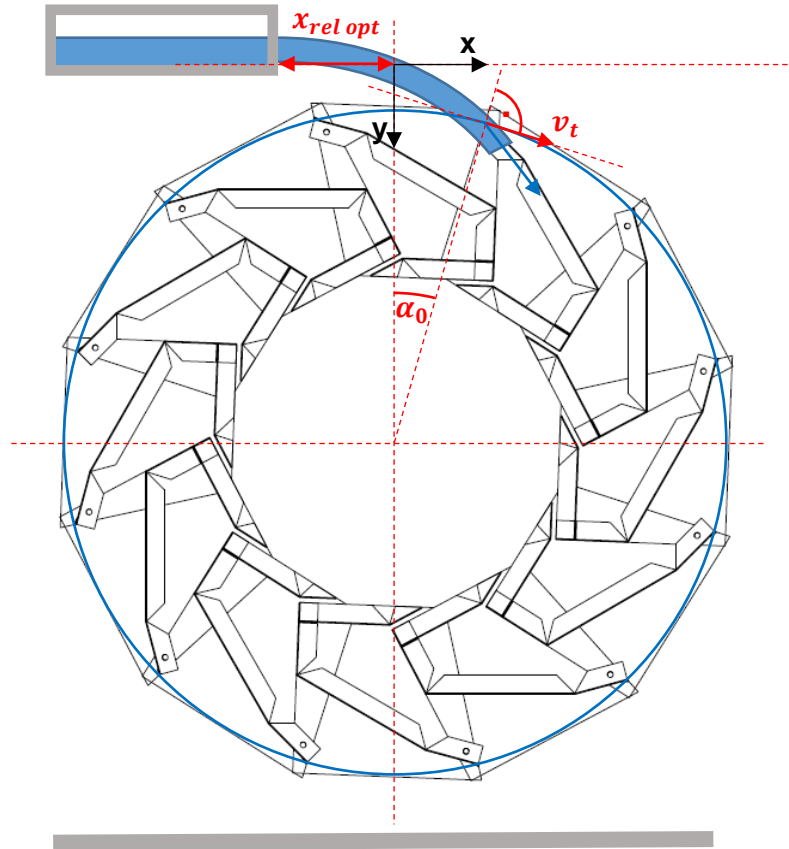
Figure 4-8: Relative position, entry point, tangential flow velocity

In case none of the combinations of o and e fulfil the requirements (4-20) and (4-21) and hence all elements in in the matrix have the value $BX = 10000$, the broadest water wheel possible with the concept is selected with the entry point optimized using only Formula (4-21). Additionally, a warning containing the message "*The chosen flow rate is greater than the maximum flow rate for this diameter of the given concept. Possibly you could extract more energy with a different concept*" is displayed in a text box.

4.2.2 Part 2

The second part of the Matlab-tool contains the calculation of the achievable power output and thereby the identification of the optimal operating point. This part is mainly borrowed from [16]. Thus, only the executed modifications are addressed in the current study, but not the entire functionality. For detailed information about the structure please use [16]. A short overview on the content of part 2 is given at the end of this paragraph.

Generally, two major modifications are implemented into the existing tool for the power output. These are more detailed information about the entry of water and a more exact calculation of holding capacity of the cells.

4.2.2.1 Entry point and flow velocity

In the Matlab-tool from [16], for lack of data, the application of the water wheel with water was standardised at the upper vertex of the water wheel. No considerations were made with respect to the entry angle nor the thickness of the water flow. That was due to the fact that the tool was conceived for yet existing water wheels.

In the present case, we have more information about the design of the water wheel and the optimal entry point. The precise entry position is delivered by α_0 as calculated in paragraph 4.2.1.5.

4.2.2.2 Chamber volume and water content

The second modification touches the estimation of the chamber volume and thereby the amount of water in the water wheel. In [16] the available chamber volume at the entry point was equalized with the maximum chamber volume. From there it decreased linearly until the lowest water interacting chamber.

In the improved Matlab-tool the vector description of a chamber as introduced in paragraph 4.2.1.2 is utilized here as well achieving a more realistic behaviour of the maximum chamber volume from the entry point to the lowest water interacting cell.

First of all, the chamber volume depends on the width of the water wheel and water covered cross sectional area. As the water wheel width is independent of the position of the chamber within the water wheel, the entire scope can be reduced to a two-dimensional consideration.

The maximum holding capacity of a chamber depending on the position of the cell is illustrated in Figure 4-9.

The picture shows obviously that the behaviour of the position dependent holding capacity is not liner from the vertex to the lowest water interacting cell, thus the revision of the concept makes sense.

Moreover, is clarified that the horizontal line is the border for the filling level of the cells. If we consider a single cell moving from the upper vertex downwards, the horizontal is performing a rotation relative to the chamber, with its pivot in the tip of the impact paddle (P_4). (Figure 4-10)

Taking these fact into account, the chamber volume can be detected precisely for each position of the chamber using the already in paragraph 4.2.1.2 introduced vector description of the chamber outline.

Figure 4-9: Position dependent maximal chamber volume

To calculate the volume of the chamber, it is divided into triangles spanned by the vectors form P_4 to the other points of the chamber outline.

One new reference point P_9 must be determined to complete the segmentation. It is defined as the intersection of the straight line $\overline{P_4P_6}$ and the straight line parallel to the x_1-direction through P_1 (compare Figure 4-10). Therefore, linear system (4-26) has to be solved and afterwards P_9 is calculated using parameter s_1.

$$P_9: \qquad \overrightarrow{P_4} + s_1 * (\overrightarrow{P_6} - \overrightarrow{P_4}) = \overrightarrow{P_1} + s_2 * \begin{bmatrix} 1 \\ 0 \\ 0 \end{bmatrix} \qquad\qquad (4\text{-}26)$$

$$\overrightarrow{P_9} = \overrightarrow{P_4} + s_1 * (\overrightarrow{P_6} - \overrightarrow{P_4})$$

Figure 4-10 presents these fragmentations. We can see that only the small striped segment of the total area is not covered by this triangular division based on P_4. This part only values about 2 % of the entire cross section area and thus is neglected for the calculation of the chamber volume.

On that base, the total maximum holding capacity of the chamber $V_{chamber,max,tot}$ occurs when the horizontal line coincides the points P_4 and P_8 as illustrated in Figure 4-10.
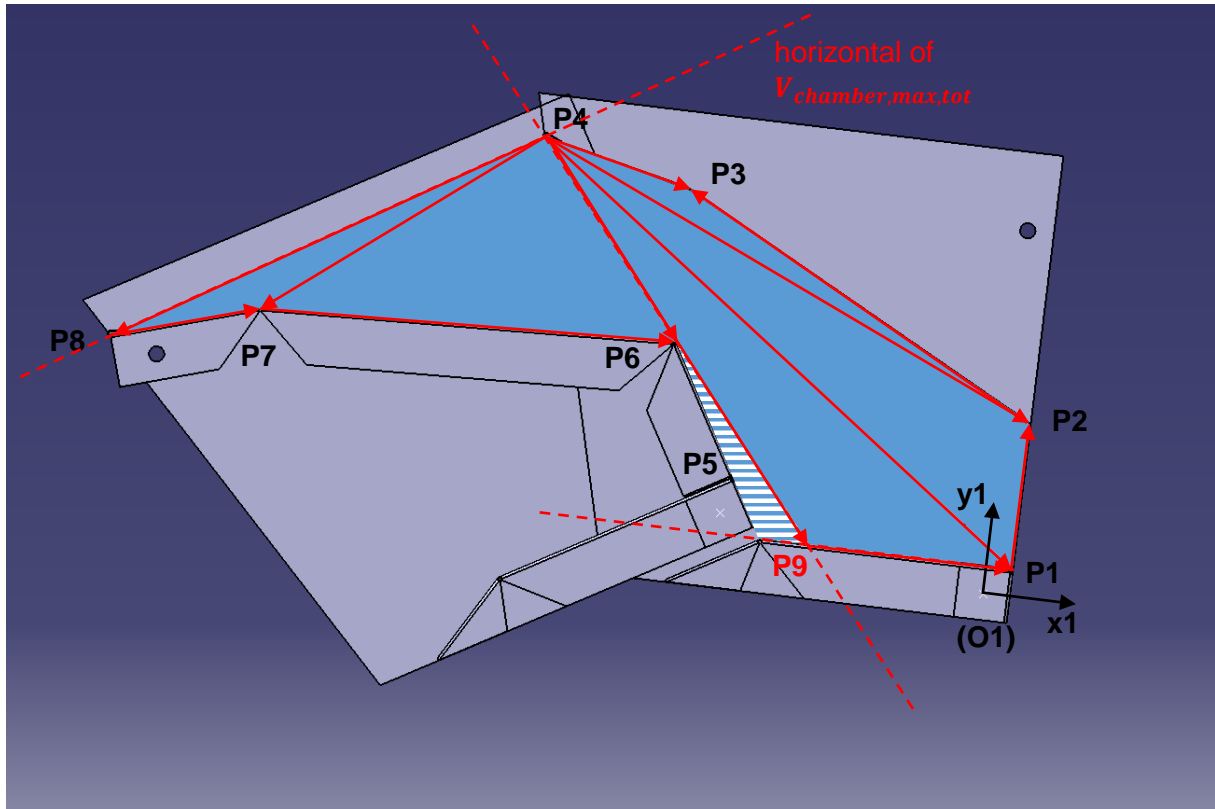
Figure 4-10: Vector description of the maximal chamber volume

Calculating the triangular areas the paling vectors are required. They are compiled and listed below predicated according to the definition $\overrightarrow{v_{bottom\ top}}$:

$$\overrightarrow{v_{p4p3}} = \overrightarrow{P_3} - \overrightarrow{P_4} \qquad \overrightarrow{v_{p4p2}} = \overrightarrow{P_2} - \overrightarrow{P_4} \qquad \overrightarrow{v_{p4p1}} = \overrightarrow{P_1} - \overrightarrow{P_4} \qquad \overrightarrow{v_{p4p9}} = \overrightarrow{P_9} - \overrightarrow{P_4}$$

$$\overrightarrow{v_{p4p6}} = \overrightarrow{P_6} - \overrightarrow{P_4} \qquad \overrightarrow{v_{p4p7}} = \overrightarrow{P_7} - \overrightarrow{P_4} \qquad \overrightarrow{v_{p4p8}} = \overrightarrow{P_8} - \overrightarrow{P_4} \qquad \overrightarrow{v_{p7p8}} = \overrightarrow{P_8} - \overrightarrow{P_7}$$

$$\overrightarrow{v_{p6p7}} = \overrightarrow{P_7} - \overrightarrow{P_6} \qquad \overrightarrow{v_{p1p9}} = \overrightarrow{P_9} - \overrightarrow{P_1} \qquad \overrightarrow{v_{p1p2}} = \overrightarrow{P_2} - \overrightarrow{P_1} \qquad \overrightarrow{v_{p2p3}} = \overrightarrow{P_3} - \overrightarrow{P_2}$$

As next step, the areas of the triangles are computed using the above introduced vectors. The areas are denoted as $A_{numbers\ of\ corner\ points}$ and determined using the cross product of two spanning vectors. The areas are reckoned as follows:

$$A_{p487} = 0.5 * \left| \overrightarrow{v_{p4p8}} \times \overrightarrow{v_{p4p7}} \right|; \quad A_{p476} = 0.5 * \left| \overrightarrow{v_{p4p7}} \times \overrightarrow{v_{p4p6}} \right|; \quad A_{p491} = 0.5 * \left| \overrightarrow{v_{p4p9}} \times \overrightarrow{v_{p4p1}} \right|;$$

$$A_{p412} = 0.5 * \left| \overrightarrow{v_{p4p1}} \times \overrightarrow{v_{p4p2}} \right|; \qquad\qquad A_{p423} = 0.5 * \left| \overrightarrow{v_{p4p2}} \times \overrightarrow{v_{p4p3}} \right|;$$

Approaching the volume more precisely, the reduction of the chamber volume due to the thickness of the material used in the paddle has to be taken into account. For thin sheet metal materials, this effect is quite small, but for thicker metal sheets or other materials it influences the result. To achieve this, the total unfolded length of the paddle is calculated. In order to do this, the distance of the points P_1 and P_2 (D_{P1P2}) as well as the distance of P_2 and P_3 (D_{P2P3}) and P_3 and P_4 (D_{P3P4}) are computed to:

$$D_{P1P2} = 0,4 * a \qquad\qquad D_{P2P3} = \left| \overrightarrow{P_3} - \overrightarrow{P_2} \right| \qquad\qquad D_{P3P4} = \left| \overrightarrow{P_4} - \overrightarrow{P_3} \right|$$

Hence, the total length of the unfolded paddle z equals:

$$z = D_{P1P2} + D_{P2P3} + D_{P3P4} \tag{4-27}$$

Thus, the total maximum absorbable volume of a chamber is calculated according to Equation (4-28). The sum of the triangle areas minus the cross-sectional area of the paddle itself are therefore multiplied with the total width of the water wheel.

$$V_{chamber\,\max\,tot} = \left(A_{p487} + A_{p476} + A_{p491} + A_{p412} + A_{p423} - z * d \right) * B_{WW,opt} \tag{4-28}$$

Since $V_{chamber\,\max\,tot}$ is identified, in the next step, the position depending maximal volume is clarified.

Therefore, for each water interacting chamber $i \in [1; Y]$ from the water entry until the final water exhaust the angle $\Psi(i)$ between the horizontal line and the straight line $\overline{P_4 P_8}$ is needed. With i being the control variable of the position (compare [16]). Due to the angle α_0 for the position of the entry point relative to the vertical, calculated in part 1 of the Matlab-tool, and the correlations presented in Figure 4-11, $\Psi(i)$ is defined as follows in Equation (4-29)

$$\Psi(i) = \alpha_0 + i * \xi_{opt} - \frac{\xi_{opt}}{2} \tag{4-29}$$
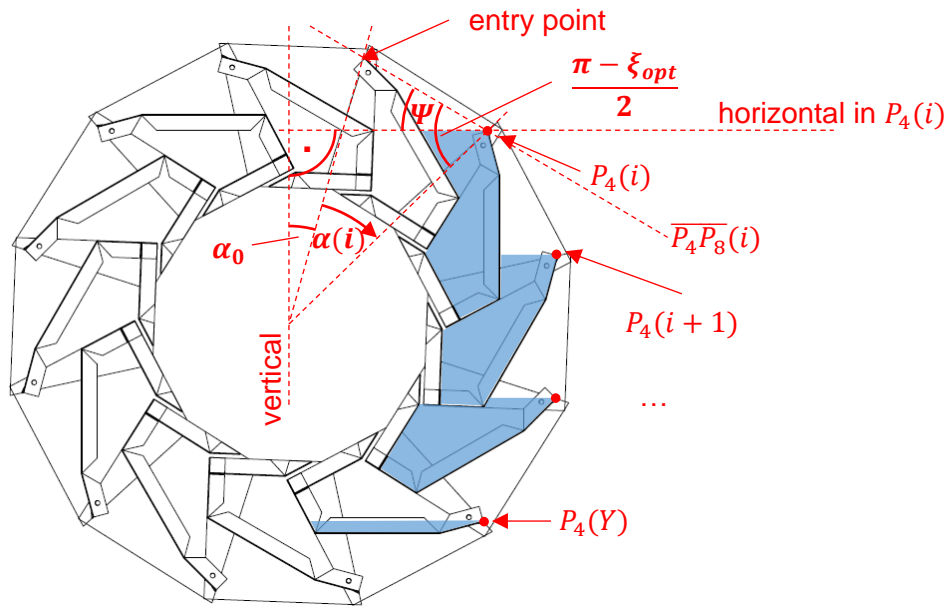
Figure 4-11: Position dependent maximal chamber volume – fixed horizontal

Calculating the position dependent maximum absorbable volume of the chamber, $\Psi(i)$ is transferred into the detailed consideration of a single fixed chamber as illustrated in Figure 4-12.
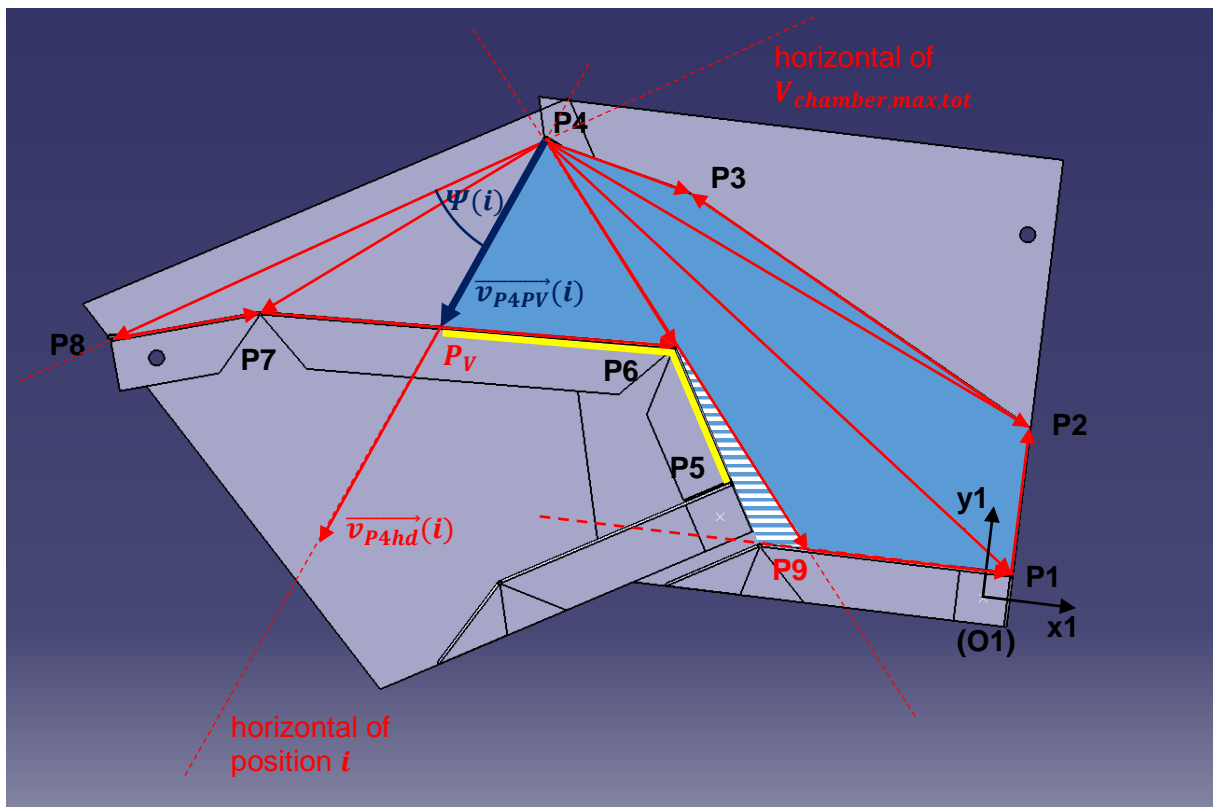
Figure 4-12: Position dependent maximal chamber volume – fixed chamber

The figure emphasises the limitation of the maximum filling level in a chamber by the horizontal of the position. The remaining volume of the chamber is divided in triangular sections like done above for the calculation of $V_{chamber,max,tot}$.

Before the position dependent cross sectional area of the holding capacity for a position can be calculated, the vector from P_4 to the point of intersection P_V of the horizontal line of the position and chamber outline must be defined. P_V can become any point of the line segments $[P_3P_2]$, $[P_2P_1]$, $[P_1P_9]$, $[P_6P_7]$ or $[P_7P_8]$ dependent on $\Psi(i)$.

Identifying the P_V, the directing vector of the horizontal of the position $\overrightarrow{v_{P4hd}}$ is calculate in relation to the fixed chamber dependent on the vector $\overrightarrow{v_{P4P8}}$ to:

$$\overrightarrow{v_{P4hd}}(i) = \begin{bmatrix} \cos(\Psi(i)) & -\sin(\Psi(i)) & 0 \\ \sin(\Psi(i)) & \cos(\Psi(i)) & 0 \\ 0 & 0 & 1 \end{bmatrix} * \overrightarrow{v_{P4P8}}$$

Knowing this vector, P_V is calculated solving a linear system. This process is equal for all positions of P_V, but requires a separate calculation for each line segment.

In the work at hand only the calculation of the case presented in Figure 4-12 with P_V coinciding $[P_6P_7]$ is presented.

The following linear system (4-30) represents the intersection of the horizontal line of the position with $[P_6P_7]$. By solving it P_V and $\overrightarrow{v_{P4PV}}$ are calculated using parameter r_1.

$$P_V: \qquad \overrightarrow{P_4} + r_1 * \overrightarrow{v_{P4hd}}(i) = \overrightarrow{P_6} + r_2 * \overrightarrow{v_{P6P7}} \tag{4-30}$$

$$\overrightarrow{P_V} = \overrightarrow{P_4} + r_1 * \overrightarrow{v_{P4hd}}(i)$$

$$\overrightarrow{v_{P4PV}}(i) = r_1 * \overrightarrow{v_{P4hd}}(i)$$

In the final step, the position dependent maximum holding capacity of a cell $V_{chamber\,max}(i)$ is identified. Therefore, the above for $V_{chamber,max,tot}$ calculated areas A_{p476}, A_{p491}, A_{p412}, and A_{p423} are used completed by the triangular fragment spanned by P_4, P_7 and P_V. Again, the reduction of the volume due to the material thickness of the paddle is taken into account. Only the paddle parts in contact with the water are considered. Compare the yellow highlighting in Figure 4-12.

According to this, the position dependent maximum holding capacity of a chamber is calculated as shown in Equation (4-31).

$$\begin{aligned} V_{chamber\,max}(i) = &\left(A_{p476} + A_{p491} + A_{p412} + A_{p423} - 0{,}5 * |\overrightarrow{v_{P4P7}} \times \overrightarrow{v_{P4PV}}(i)| \right. \\ &\left. - \left(0{,}4 * a_{th} + |\overrightarrow{P_4} + \overrightarrow{v_{P4PV}}(i) - \overrightarrow{P_6}| \right) * d \right) * B_{WW,opt} \end{aligned} \tag{4-31}$$

This modified calculation of the chamber volume is implemented in the underlying Matlab-tool from Geß [16].

4.2.2.3 Short overview of part 2

Based on data for the water wheel dimensions calculated in part 1 of the Matlab-tool, the purpose of part 2 is calculating the behaviour of the mechanical power output. This information can be used for the sizing of a generator and to select a good operating point.

To generate the power output, the gravitational torque, the impulsive forces of the water onto the water wheel, and finally the behaviour of the total mechanical torque are computed.

The maximum power point is identified and on that base the efficiency of the entire installed system respecting the clearances etc. as well as of only the water wheel itself are calculated.

4.3 Data output

Finally, besides displaying the calculated data in screen windows and graphics in the Matlab-surface, an export of the information to a prepared excel-file is implemented in the Matlab-tool. This option must be activated at the very end in the Matlab-code.

4.4 Evaluation

4.4.1 Check of the validity

The assumptions on the possible power output (chapter 3.2.1) are now compared with the achievable power output according to the results of the Matlab-calculations.

Table 4-6 presents the calculated mechanical power output P_{mech}, the optimized total width of the water wheel $B_{WW,opt}$, and the potential electrical power output P_{el}, using an induction generator efficiency of $\eta_{gen} = 0,6$ [17], for various combinations of heights of fall and volume flow rates.

If you compare the respected values for the height of fall with those in paragraph 3.2.1, it can be seen that the probed range does start with 1,3m and not 1,0m. This is, because the clearances due to the installation (see chapter 3.4) used for the prototype (compare chapter 5.1) are taken as a basis. Thus, to achieve the same water wheel diameters as used in rough validity check in paragraphs 3.2.1 and 3.2.2 the heights of fall need to be greater.

The results show that the water wheels generate a higher power output than estimated and thus almost all combinations fulfil the required minimum electrical power supply for a rural Nepali household of $100\ W$. Only the three smallest water wheels possible within the concept combined with a flow rate of $0,02\ m^3/s$ have a power output below that minimum demand.

Water wheels with 23 or more modules and flow rates from $0,09\ m^3/s$ upwards achieve the power demand of $700\ W$ for a household with electrical cooking devices.

Moreover, for small numbers of modules and high volume flow rates up to $Q = 1\ m^3/s$ the allowed total width of the water wheel $B_{WW,opt} = 0,8\ m$ is too narrow to allow a proper entry of the water into the water wheel. The width of the open space for the water to enter the cell decreased with the number of cells. The affected combinations are marked highlighting $B_{WW,opt} = 0,8 +$ reddish. To overcome this limit, wider water wheels have to be enabled an introduced into the input data of the Matlab-tool.

It can be concluded, that the borders for the numbers of modules in a wheel chosen for concept size 1 (compare 3.2.2) are sufficient to provide electrical energy to a rural Nepali household or neighbourhood.

Table 4-6: Computed power output for different H [m] and Q [m³/s] according to the Matlab-tool

$H\,[m]$	1,3	1,4	1,5	1,6	1,7	1,8	1,9	2,0	2,1	2,2	2,3	
k_{opt}	12	14	15	16	17	19	20	21	22	23	25	
0,02	120	142	157	169	178	197	212	228	243	257	288	$P_{mech}\,[W]$
	0,3	0,3	0,3	0,3	0,3	0,2	0,2	0,2	0,2	0,2	0,2	$B_{WW,opt}[m]$
	72	85	94	101	107	118	127	137	146	154	173	$P_{el}[W]$
0,03	181	206	229	251	276	314	335	350	366	380	415	$P_{mech}\,[W]$
	0,5	0,3	0,3	0,3	0,3	0,3	0,3	0,3	0,3	0,3	0,3	$B_{WW,opt}[m]$
	109	123	137	151	166	189	201	210	220	228	249	$P_{el}[W]$
0,04	240	283	320	342	370	417	419	453	483	507	571	$P_{mech}\,[W]$
	0,6	0,5	0,5	0,5	0,5	0,5	0,3	0,3	0,3	0,3	0,3	$B_{WW,opt}[m]$
	144	170	192	205	222	250	251	272	290	304	343	$P_{el}[W]$
0,05	280	368	397	404	443	520	563	593	618	651	664	$P_{mech}\,[W]$
	0,6	0,6	0,6	0,5	0,5	0,5	0,5	0,5	0,5	0,5	0,3	$B_{WW,opt}[m]$
	168	221	238	243	266	312	338	356	371	391	399	$P_{el}[W]$
0,06	345	442	457	502	552	629	631	683	726	765	858	$P_{mech}\,[W]$
	0,8	0,8	0,6	0,6	0,6	0,6	0,5	0,5	0,5	0,5	0,5	$B_{WW,opt}[m]$
	207	265	274	301	331	377	379	410	435	459	515	$P_{el}[W]$
0,07	427	490	550	600	649	715	774	826	865	916	967	$P_{mech}\,[W]$
	0,8+	0,8	0,8	0,8	0,8	0,6	0,6	0,6	0,6	0,6	0,5	$B_{WW,opt}[m]$
	256	294	330	360	390	429	464	496	519	550	580	$P_{el}[W]$
0,08	489	593	584	659	711	838	900	906	966	1014	1133	$P_{mech}\,[W]$
	0,8+	0,8+	0,8	0,8	0,8	0,8	0,8	0,6	0,6	0,6	0,6	$B_{WW,opt}[m]$
	293	356	350	395	427	503	540	544	580	609	680	$P_{el}[W]$
0,09	545	664	722	701	771	915	975	1056	1114	1186	1254	$P_{mech}\,[W]$
	0,8+	0,8+	0,8+	0,8	0,8	0,8	0,8	0,8	0,8	0,8	0,6	$B_{WW,opt}[m]$
	327	399	433	421	463	549	585	634	669	712	752	$P_{el}[W]$
0,1	603	737	798	874	941	979	1050	1136	1308	1271	1431	$P_{mech}\,[W]$
	0,8+	0,8+	0,8+	0,8+	0,8+	0,8	0,8	0,8	0,8	0,8	0,8	$B_{WW,opt}[m]$
	362	442	479	525	442	587	630	682	785	763	859	$P_{el}[W]$

(Row group label: $Q\,[m^3/s]$)

4.4.2 Check of fluid mechanic effects

As described in chapter 3.2.3, the kickback of the water against the water wheel should be kept small to gain a high performance of the water wheel. Achieving that, an optimizing criterion of the Matlab-tool is the selection of the entry point such that the water flow and the outer section of the impact paddle are preferably aligned to prevent a harsh jolt of the water against the paddle.

Based on the mean flow velocity of the water in the channel $v_{ch,opt,mean} = 1,16\frac{m}{s}$ of all the computed cases presented in Table 4-6 the stream line of the flow is compared with the shape of the paddle. Figure 4-14 shows the design of the module as implemented into to tool. The straight length of the impact paddle as well as the relative length of the outer section are market

with arrows. The angel $\delta = 15°$ implemented in the design should to create good performances in redirecting the water in the chamber (see section 3.2.3).

In Figure 4-13 these measurements are transferred to the stream line formed by the mean flow velocity. As done for the prototype the clearance above the water wheel is set as $y_{secure} = 0,05\ m$. To reproduce an entry point close to the upper vertex of the water wheel, the entry point is set to a vertical position of $y = -0,05m$. Projecting the measurements of the impact paddle into the stream line the intermediate angle adds up to $\delta = 13°$.

The conformity of the both angles illustrate that the chosen design fits quite well to the shape of the stream line and, thereby, fulfils the claim to minimise the jolt of the water onto the paddle and eases the water entry.

Figure 4-13: Stream line according to the mean flow velocity

Figure 4-14: Shape of the impact paddle
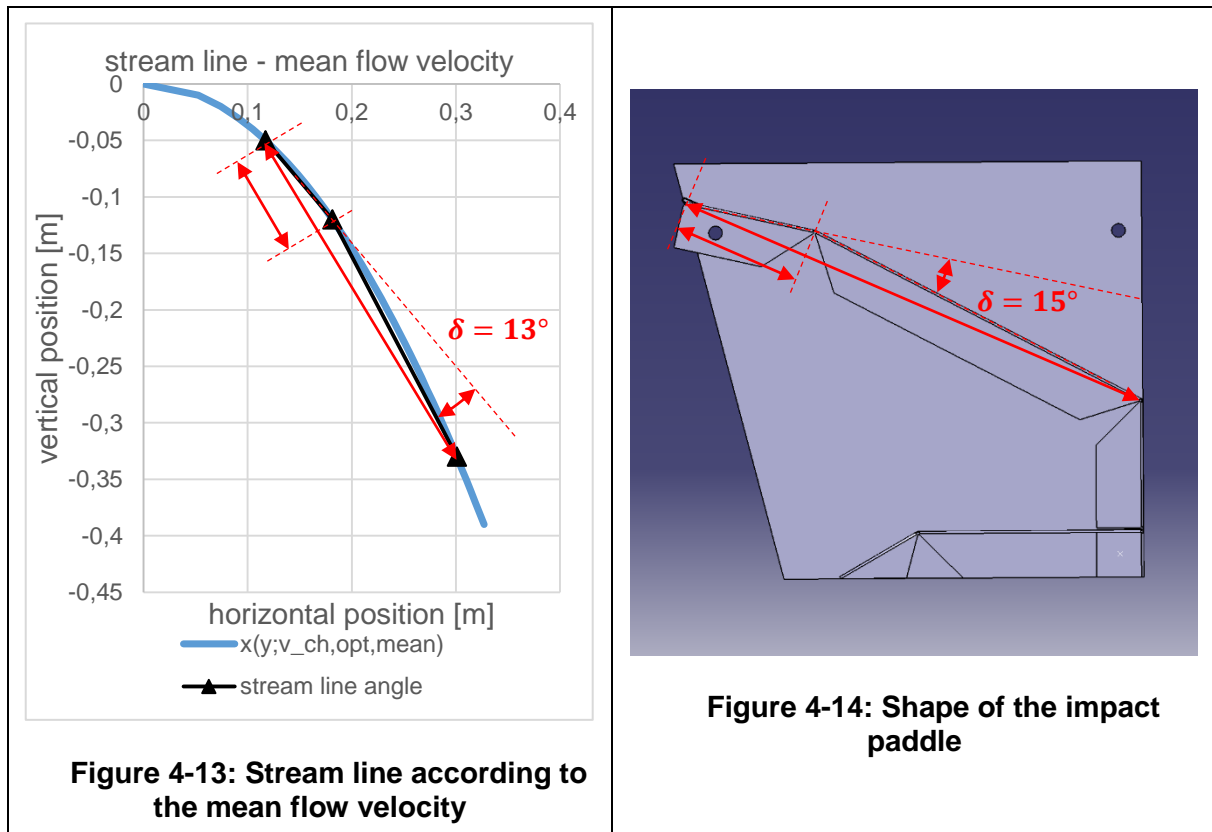
Furthermore, the Matlab-calculations affirmed that the relative angel ε between the outer section of the impact paddle and the tangent onto the water wheel is within the limits for all numbers of modules.

As stated in the design for the maximum number of cells the angle is $\varepsilon_{min} = 20°$. The maximum value for ε is achieved for a water wheel with the minimum number of cells. According to the Matlab-results it adds up to $\varepsilon_{min} = 28°$. Thus, ε lies within the requested interval $\varepsilon \in [20°; 30°]$ for all possible water wheels in concept size 1 as identified in chapter 3.2.3.

4.4.3 Advantages

The developed Matlab-tool enables a simple optimization of a water wheel for a given site based on a set design. Therefore, only the available height of fall and the volume flow rate are required, which can easily be measured by the local people in Nepal. The values are used by the operator of the Matlab-tool to identify how much modules are required.

Moreover, the structure that allows the modification of the entire parameters of the design concept leads to a great flexibility of the concept. Thus, the entire tool easily can be adapted

to new insights in water wheel design. Additionally, an optimization of the concept itself by testing various design parameters and analysing the results is possible with the Matlab-tool.

4.4.4 Disadvantages

The main disadvantages in the Matlab-tool lie in the taken assumptions that differ from the reality. First of all, water losses at the inner side of the water wheel through the clearance at the bottom are neglected.

Another assumption, is that all the water enters the chamber and thereby is generating power. In reality especially for rotational speeds clearly greater than the tangential velocity of the water flow in the entry point the assumption is not valid as much splash water losses occur. For the optimal operating point however the assumption is fine.

Furthermore, only the potential losses at the outlet of the water from the chambers is respected but not the kinetic losses due to the outlet velocity of the water.

Also, mechanical losses of the system are neglected in the calculation, as it is quite difficult to make universal approximations because they depend on many factors like the type of bearings etc.

4.4.5 Evaluation

Finally, can be said that the developed Matlab-tool optimizing the operation offers many possibilities and still reduces the main input parameters to two values.

Surely, some of the made assumptions effect the results of the calculation, but if the losses occur and how they affect the operation has to be verified in a test operation of the prototype as already mentioned in section 3.5.2.

It can be concluded that the Matlab-tool is a good support to adapt the design concept to the requirements of the operating site. Furthermore, it offers the possibility to optimize the module concept and analyse the behaviour of different water wheels with respect to their performance etc.

5 Results and practice

In this chapter, the transformability of the design concept into reality is checked applying the concept to a fictional operating site for a water wheel. The available height of fall adds up to $H = 1,3\ m$ and the water volume flow rate amounts $Q = 0,02\ m^3/s$.

First of all, the design parameters for the concept are stated. Build upon this, an optimum water wheel for the above introduced values for H and Q is computed with the Matlab-tool. Finally, the optimized water wheel will be constructed to verify the manufacturability and detect possible challenges.

In respect to the available sheet metal materials in Nepal for the construction of the prototype a galvanized sheet metal with a thickness of $0,75\ mm$ is used.

5.1 Parameters of the water wheel concept and the module design

To extract the appropriate technical drawings from the CAD-model and simulate the water wheel, all the required parameters of a certain chamber design and the limitations for the installation have to be fixed.

5.1.1 Parameters of the module design

Since, the input data of the operating site of the prototype fit within concept size 1 (compare paragraph 3.2.2), we define concept size 1 for the following executions. Therefore, the corresponding parameters of the module design and their values are listed in Table 5-1.

Table 5-1: Parameters of the module design used for the prototype

Name / description	Symbol	Value	Unit
Outer partition	t_o	0,26	m
Theoretical rim width	a_{th}	0,21	m
Thickness of the sheet metal	d	0,0075	m
Permitted minimum number of chambers	z_{min}	12	–
Permitted maximum number of chambers	z_{max}	25	–
Step range from z_{min} to z_{max}	Z	1	–
Extended wall element length for splash water protection	a_{secure}	0,045	m
Free radius around the bores	s	0,015	m

Name / description	Symbol	Value	Unit
Minimum angle between the tangent on the water wheel and the outer paddle section	ε_{min}	20	°
Angle between the two impact paddle sections	δ	15	°

5.1.2 Parameters of the water wheel

As presented in chapter 3.4 a proper installation of the water wheel and the possible groupings require the definition of further limitations. To ensure an unhindered rotation of the water wheel, the clearances are chosen as shown in the table below such that possible deviations in the installation are compensated for sure. For later constructions, this offers potential to minimize them and thus the losses of height of fall.

The parameters for the grouping are taken unchanged from paragraph 3.4.2.

The parameters are summarized in Table 5-2.

Table 5-2: Parameters of the water wheel used for the prototype

Name / description	Symbol	value	Unit
Clearance between the bottom dead centre of the water wheel and the ground	h_{secure}	0,1	m
Clearance between lower rim of the water jet in the channel and the active upper vertex of the water wheel	y_{secure}	0,05	m
Tolerance angle for flow entry into the chamber	ω	10	°
Width of small chamber version	b_1	0,2	m
Width of broad chamber version	b_2	0,3	m
Possible combinations of the two chamber width	$combi(o)$	{'b1', 'b2', 'b1+b2', 'b2+b2', 'b2+b1+b2'}	–
Number of permissible combinations	O	5	–
Resulting widths of the water wheel	$B_{WW}(o)$	[0.2; 0.3; 0.5; 0.6; 0.8]	m
Resulting widths of the channel	$b_{ch}(o)$	[0.1; 0.2; 0.3; 0.4; 0.5]	m

5.2 Matlab-Simulation of the prototype

Since all required input data are set, the prototype can be adapted to the site and simulated using the developed Matlab-tool. Table 5-3 quotes the two input variables according to the conditions at the operating site of the prototype. The entire calculation of the prototype as processed in Matlab is attached in appendix C).

Table 5-3: Input variables of the prototype operating site

Name / description	Symbol	Value	Unit
Free available height of fall	H	1,3	m
Volume flow rate of water	Q	0,02	m^3/s

5.2.1 Results for the prototype – part 1

The optimized water wheel has following computed dimensions and fluid mechanic values listed in Table 5-4.

Table 5-4: Optimized dimensions and fluid-mechanic values of the prototype

Name / description	Symbol	Value	Unit
Optimum number of modules	k_{opt}	12	–
Active outer diameter	$D_{active\ out\ opt}$	1,035	m
Total outer diameter	$D_{total\ opt}$	1,108	m
Real occurring rim width	a_{real}	0,198	m
Real occurring angle between the tangent of the water wheel and the outer impact paddle section	ε_{opt}	28	°
Optimum grouping	$combi_{opt}$	{'b2'}	–
Optimum width of the water wheel	$B_{WW,opt}$	0,300	m
Related optimum width of the channel	$b_{ch,opt}$	0,200	m
Flow velocity in the channel	$v_{ch,opt}$	0,994	m/s
Water depth in the channel	$wd_{v,opt}$	0,101	m
Tangential flow velocity at entry point	v_t	0,994	m/s
Relative horizontal position of the channel end towards the upper vertex of the water wheel	$x_{rel,opt}$	-0,028	m

According to the output data, a single water wheel build of 12 chambers of the width $b_2 = 0,3\ m$ is optimal to transduce the hydraulic energy potential at the given site into usable power.

An application of the water wheel possibly close to the upper vertex is achieved by a positioning the channel end at $0,028\ m$ left of the vertex. This relative position of the water flow and the water wheel is clarified by illustrating the shape of the flow and the outline of the water wheel for the site of the prototype in Figure 5-1. The origin of the graph coincides with the centre of the water wheel.
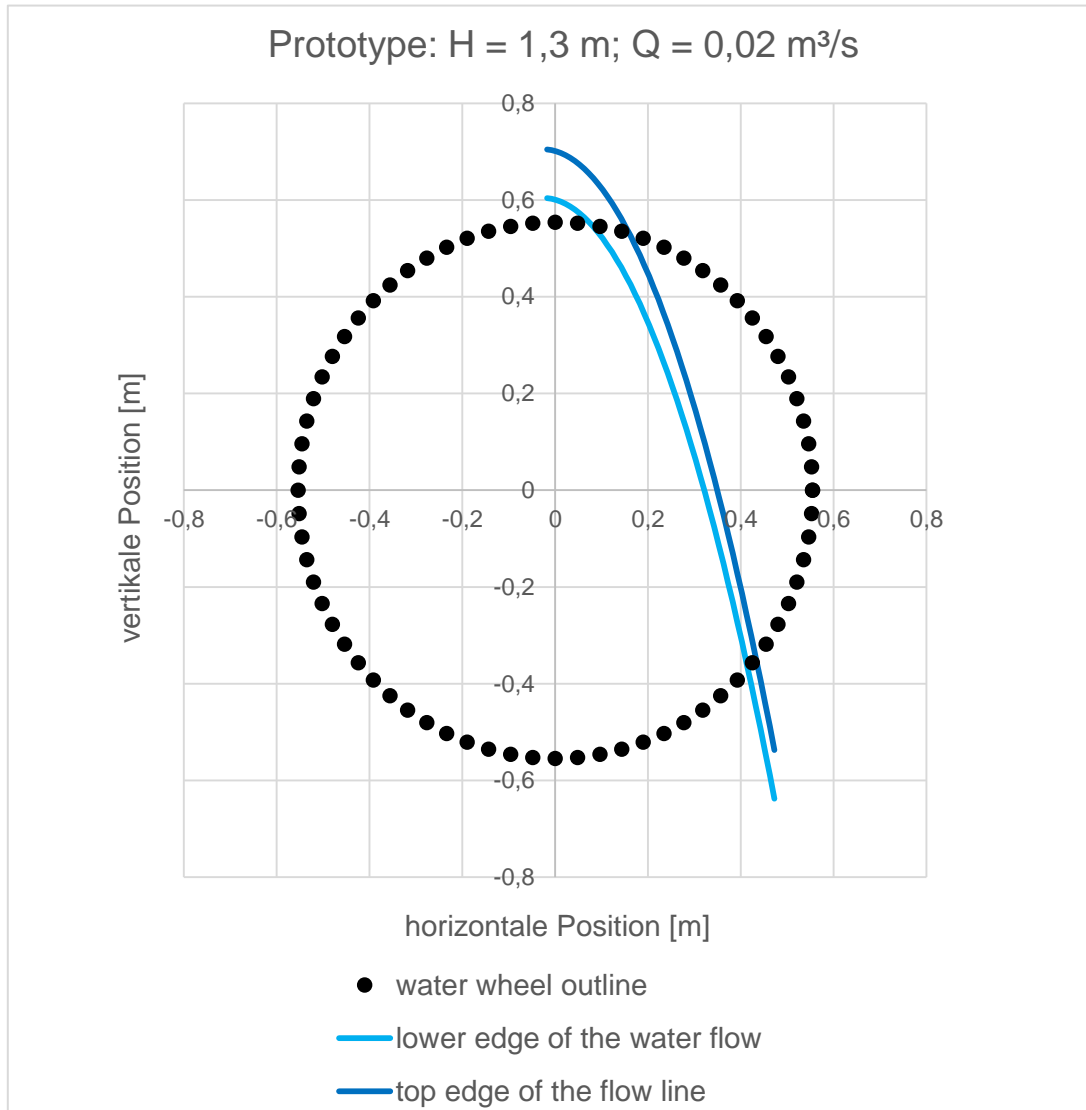
Figure 5-1: Realtive position of the water wheel and the channel respectively the water flow

5.2.2 Results for the prototype – part 2

Figure 5-2 presents the behaviours of the power out and the underlying gravitational and impulsive torques as a function of the number of revolutions.
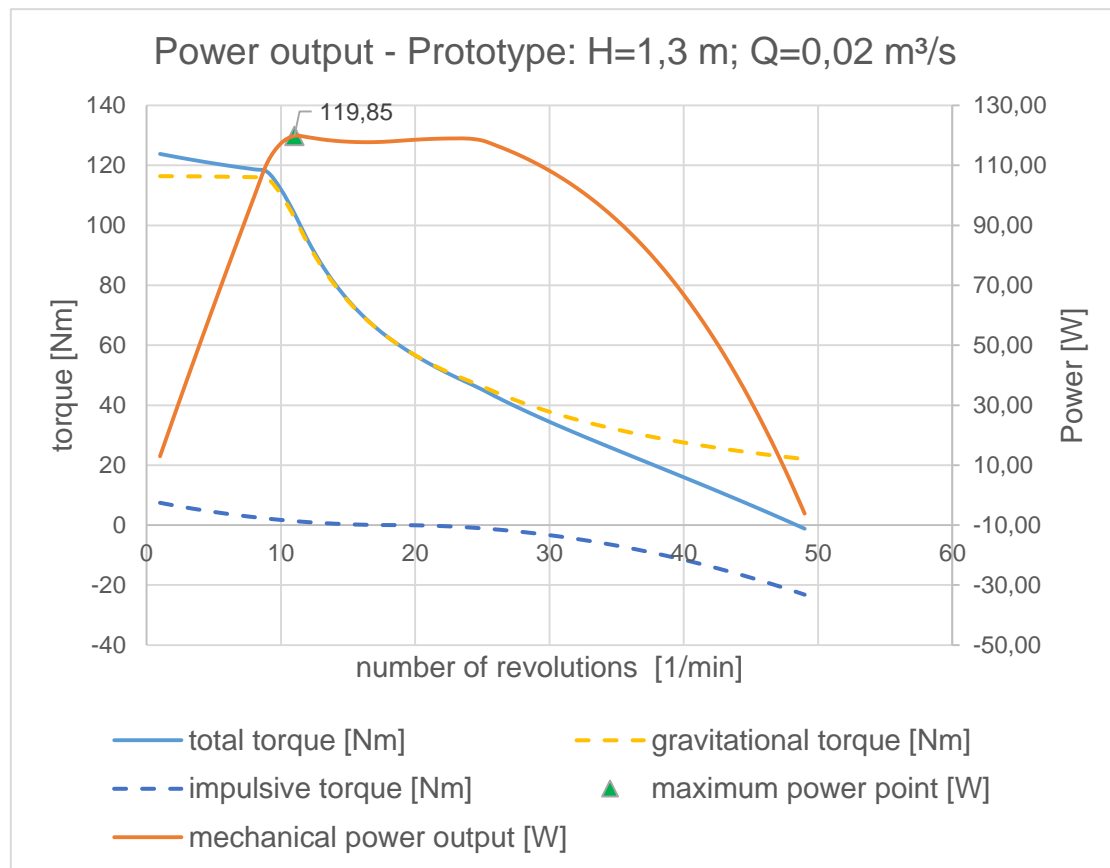
Figure 5-2: Power output of the prototype

The dotted lines in the graph refer to the gravitational torque (yellow) and the impulsive torque (blue). Obviously, the influence of the impulsive torque is much smaller than of the gravitational torque. Whereby the total torque (blue line) mainly follows the behaviour of the gravitational torque. Solely, for numbers of revolutions greater than $n = 30\ rpm$ the impulsive torque has a visible influence and reduces the total torque until it equals $M = 0\ Nm$ at a number of revolutions of $n_{cutout} = 49\ rpm$ which is the idling speed of the prototype. The maximum power output is achieved at a rotational speed of $n = 11\ rpm$ and adds up to $P_{max} = 119{,}85\ W$. The maximum total torque is $M_{max} = 123{,}83\ Nm$ and occurs for a rotational speed close to $n = 0\ rpm$. This value is important for the later dimensioning of the axis.

Furthermore, the Matlab-tool identifies the number of cells interacting with the water at a time to $Y = 5$. This signifies a good operation, because almost all the cells in one half of the water wheel are in contact with water simultaneously which represents an early entry and low exit of the water.

The total efficiency of the installation is $\eta_{tot} = 0{,}45$. Due to the required clearances and the relatively small water wheel diameter in comparison to the rim width, the efficiency is that low. Considering only the efficiency of the water wheel itself by neglecting the losses in height of fall caused by the clearances above and underneath the water wheel, the efficiency of only the water wheel itself is calculated to $\eta_{WW} = 0{,}56$. The divergence of these two efficiencies show the achievable potential by minimizing the clearances.

5.3 CAD-Model and technical drawings of the prototype

According to the optimization of the prototype in section 5.2 a single water wheel with the width $b_2 = 0,3\ m$ is required for the considered operating site. This information and the above described design parameters of the module concept are implemented into the CAD-model of the module parts.

Afterwards, the final technical drawings are derived from the adjusted CAD-models. The resulting technical drawings of the wall element, the paddle element, and the bottom element are attached to this work as appendix D).

5.4 Construction of the Prototype

After identifying the optimal parameters for the prototype and generating the needed drawings, using Matlab and CATIA, the technical realization of the prototype is presented in this chapter. The aim is to process manufacturing and assembly transferrable to a production in Nepal and thereby analyse possible challenges.

The realisation of the prototype is managed with the support of the master student Johannes Eisner, who will install a water wheel based on this concept in Nepal in cooperation with the Kathmandu University in his master thesis.

5.4.1 Required Equipment

First of all, the utilized tools have to be confined due to in Nepal available equipment as explained in paragraph 2.3.2. The used devices and their application are listed in the following.

5.4.1.1 Cutting

To cut the utilized metal sheets, a jigsaw or simple plate shears are used. For small cornered cuttings, a manual notching device is utilized. Figure 5-3 shows these three tools.

Figure 5-3: Cutting devices

5.4.1.2 Drilling

All needed bores are generated using a hand drill as presented in Figure 5-4.

Figure 5-4: Hand drill

5.4.1.3 Bending

Creating the kinks, a manual sheet metal bender is put to use. (Compare Figure 5-5)

Figure 5-5: Sheet metal bender

5.4.1.4 Assembly

For the assembly, clamps, a hand riveter, and suitable wrenches are required. The tools are illustrated in Figure 5-6 below.

Figure 5-6: Assembly devices

5.4.2 Manufacturing steps

Since the utilized tools are clarified, the different steps in the production of the prototype are described in the following section.

5.4.2.1 Basic cut / preparation

As the raw material is delivered in metal sheets of the measurements $2 \times 1\,m$, it is important to identify a good allocation of the single components on the area to minimize the waste of material. To achieve this, the required number of each of the three components of a module is determined and the overall dimensions of these parts are taken from the technical drawings (Appendix D)).

The quantity of the parts to build 12 cells and the corresponding dimensions are presented in Table 5-5.

Table 5-5: List of quantity and dimensions of the components to build the prototype

Component	Dimensions	Quantity
C1 – wall element	$302(232)x270\,mm$	24
C2 – paddle element	$360x233\,mm$	12
C3 – bottom element	$360x452\,mm$	12

The entire components can be manufactured out of three raw metal sheet plates with an arrangement of the components as shown in Figure 5-7 to Figure 5-9. The blue areas represent the remaining material.

Figure 5-7: arrangement for sheet metal plate 1
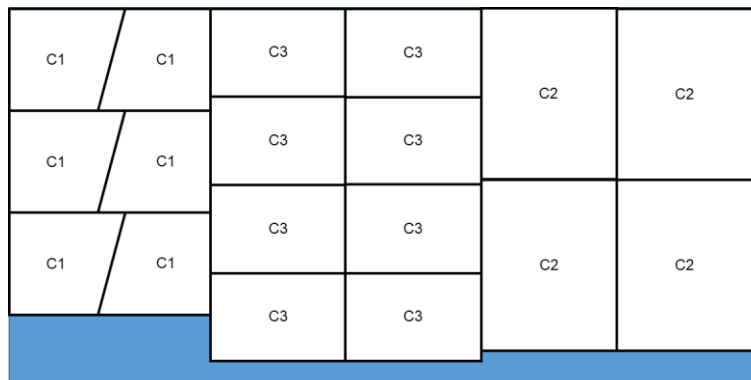
Figure 5-8: Arrangement of sheet metal plate 2
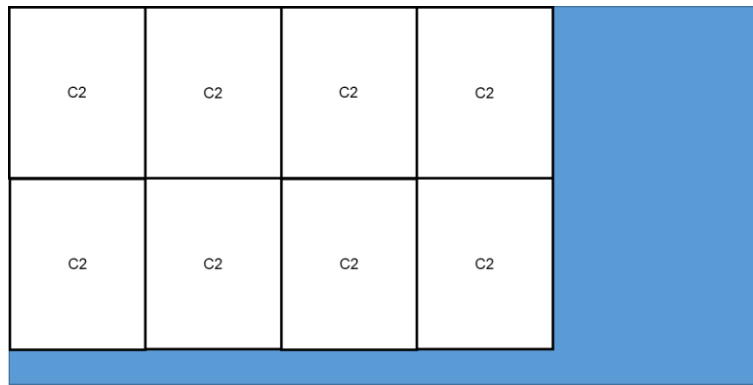
Figure 5-9: Arrangement of sheet metal plate 3

Following this arrangement, the raw sheet metal plates are cut into pieces with the basic measurement of the single components. This step is processed using the jigsaw as presented in Figure 5-10. To support straight cuts, a fence guiding the jigsaw can be applied as illustrated in Figure 5-11 by simply clamping a metal rail parallel to the cutting line.

Figure 5-10: Basic cutting of the components from the raw sheet metal plate

Figure 5-11: Use of a fence to guide the jigsaw

After the basic cut, all components appear in their basic shape without any further cuttings, shearing operations or bores as shown in Figure 5-12.
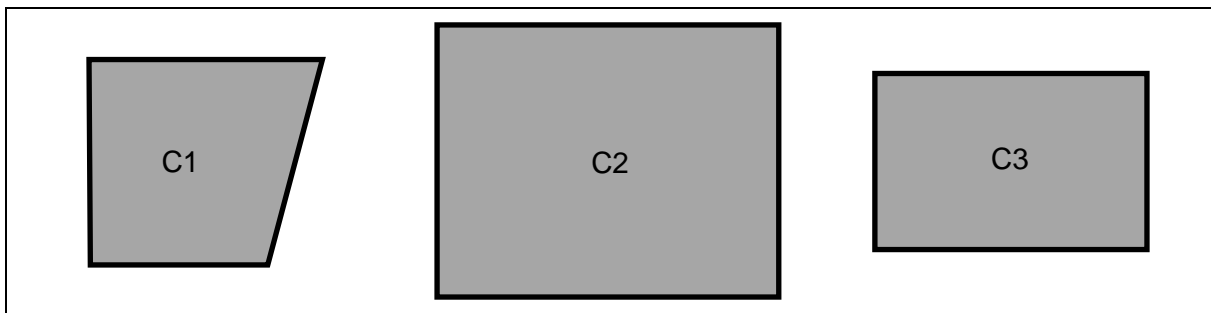
Figure 5-12: shape of the components after the basic cutting

5.4.2.2 Fine cut / holes

In the next step, the fine cuts and the bores are realized to transform the components into their final shape before bending them.

Therefore, the wall element only has to be completed by the two horizontally aligned bores of the distance t_0. Compare the technical drawings in appendix D). It must be kept in mind that two wall elements are opposing parts in a module. Thus, it is essentially to create the holes equally in the two opposing elements of a cell so that the bores of the two wall elements are coincide. This is important to prevent any deformations of the cell due to non-coincide bores. The easiest way achieving that is to drill the holes into stacks of at least pares or multiples of two. Doing that generates always two wall elements for a cell with exactly the same relative position of the bores. Figure 5-13 illustrates these requirements. Once the holes are drilled, the wall element already achieved its final outline and is ready for assembly.
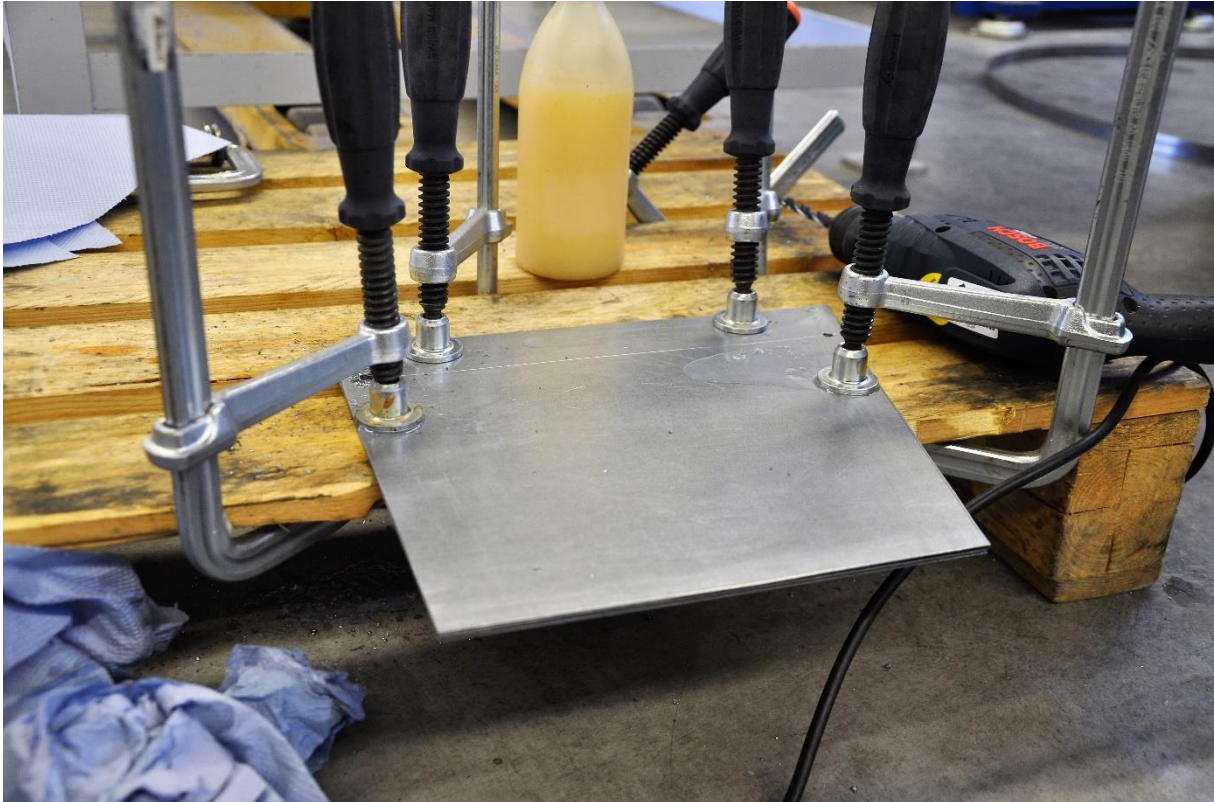
Figure 5-13: Stack of wall elements generating exact positioned bores in opposing elements

The paddle and the bottom element warrant additional to the bores some cornered cuttings which are required to allow processing the kinks in the following steps. These cuttings are created notching them of the pre-cut shape utilizing the notching tool. This process is illustrated in Figure 5-14. If a notching tool is not available all the fin cuts also can be done using the jigsaw or a metal shear.

Figure 5-14: Notching the cornered cuttings

The resulting outlines of the paddle and the bottle element after executing the bores and notches is presented in Figure 5-15. Now both components are ready for the transformation into a three-dimensional shape.

| Paddle element – C2 | Bottom element – C3 |
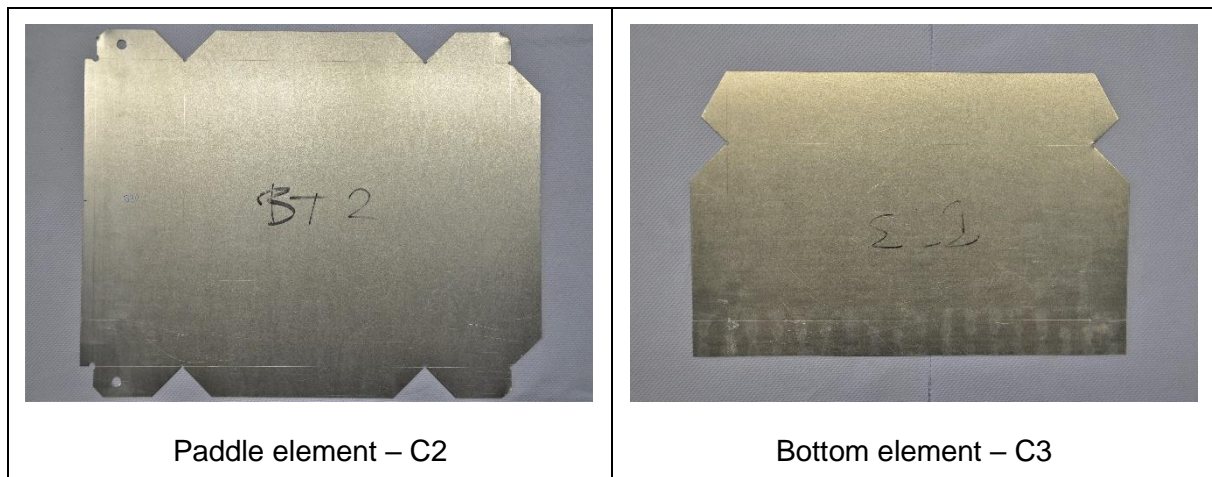
Figure 5-15: shape of paddle and bottom element after fine cutting and processing the bores

5.4.2.3 Bending

Since the two-dimensional silhouettes of the paddle and the bottom element are finalized, they now are transformed into three-dimensional objects creating kinks to achieve the form as defined in the CAD-model.

Due to the manufacturability, it is necessary to perform the required kinks in a special order, because otherwise it is not possible to transform the sheet metal into the right frame.

The steps to reform the paddle are listed below. For each step pictures of the unit interacting with the tool and the result are presented.

1. The first step is bending the side flaps that are required to attach the paddle later to the wall elements. According to the technical drawings they are bend to an angle of 90°.
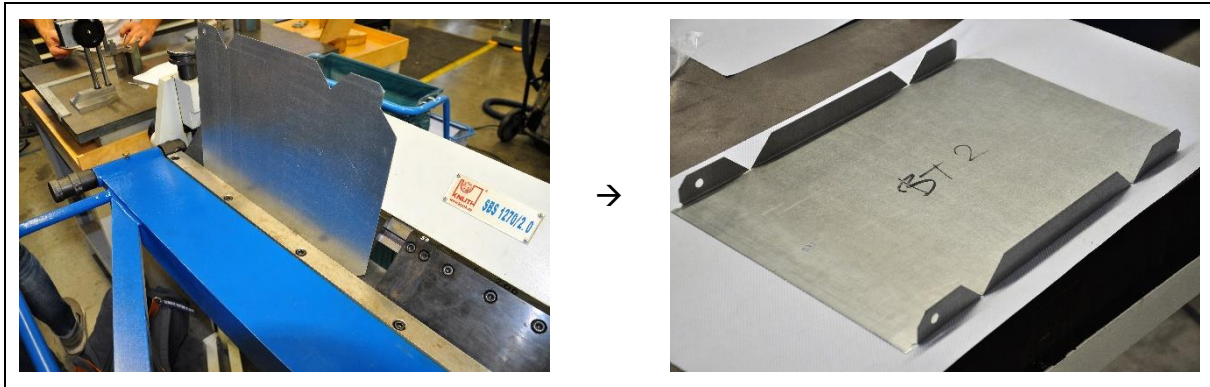
Figure 5-16: Bending of the side flaps

2. The second step is generating the 90° flap to connect the paddle with the bottom element later.
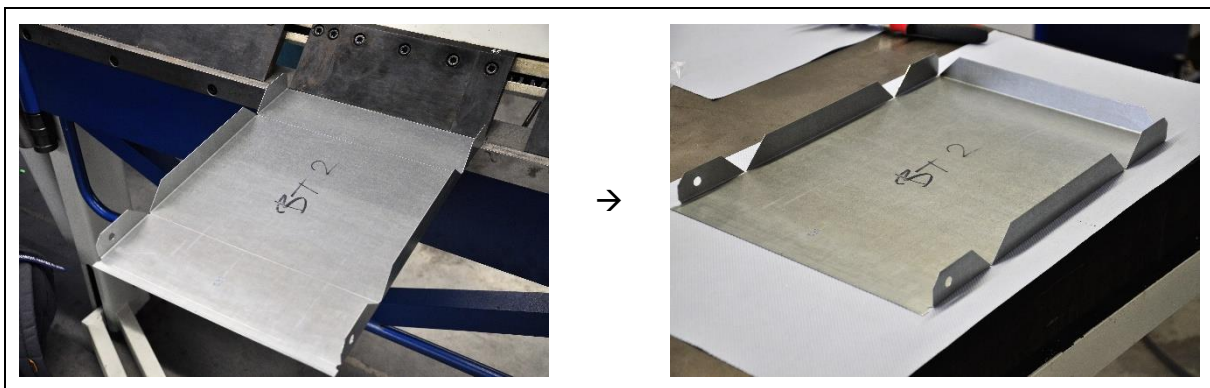
Figure 5-17: Bending of the bottom flap

3. Creating the two kinks to separate the paddle into the two impact paddle sections and the lock paddle section. The required bending angles have to be taken from the corresponding technical drawing (Appendix D)).
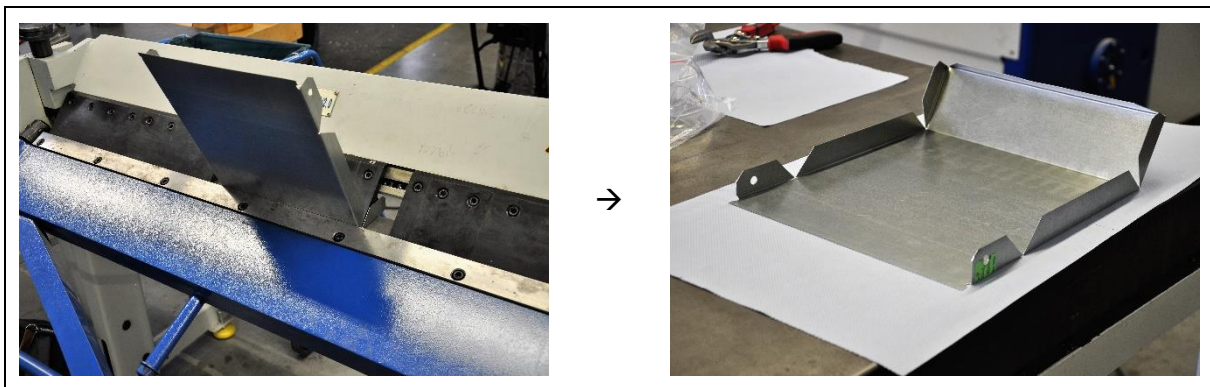
Figure 5-18: Kink to separate impact and lock paddle
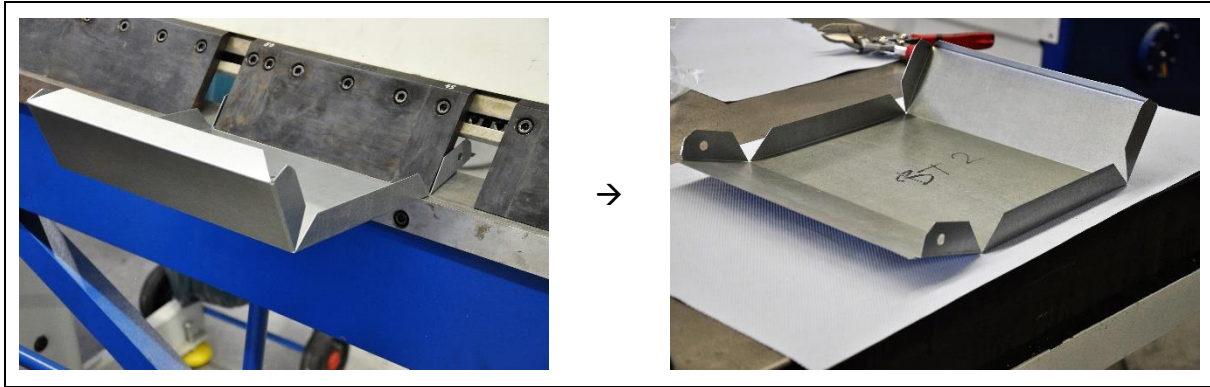
Figure 5-19: Kink to separate the two impact paddle sections

4. The sheet metal bender only allows bending the material into one direction. Therefore, the reverse bent stiffening flap at the top end of the paddle is generated using a hammer.
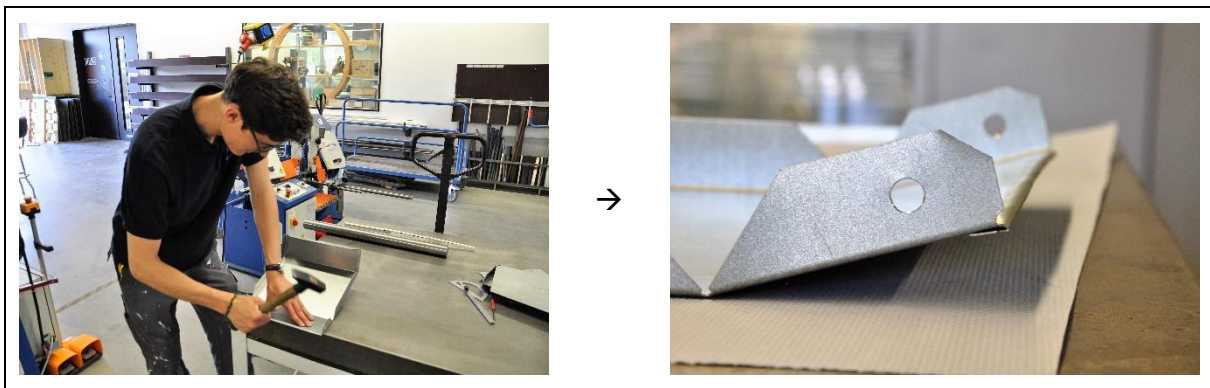
Figure 5-20: hammering the reverse bend stiffening flap

After these four steps, the paddle element is in its final shape.

The second component that requires bending is the bottom element. The successive bending steps are presented equally to the ones of the paddle element.

1. Again, the first step is generating the 90°-bent side flaps, which are required to join the bottom element with the wall elements.
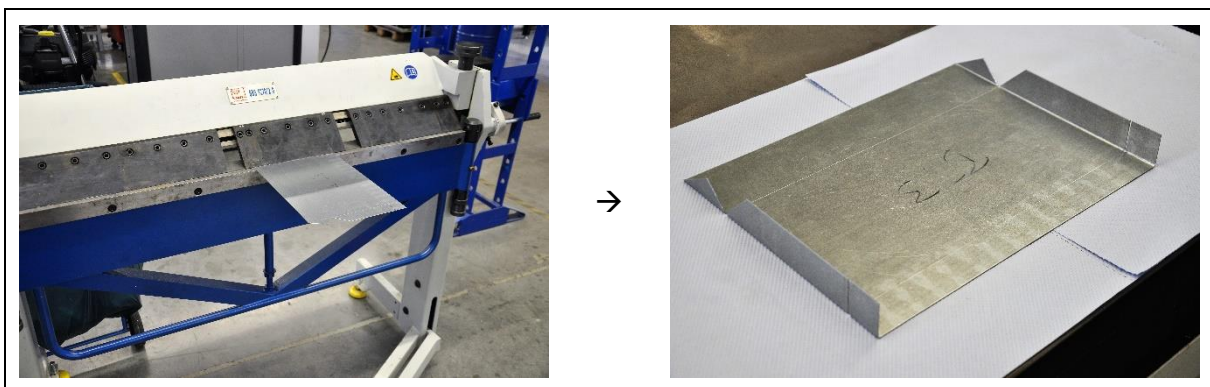
Figure 5-21: Bending the side flap of the bottom element

2. As second step, the angular section of the bottom element is processed. The angle is dependent from the module design and has to be taken from the technical drawing (Appendix D)).
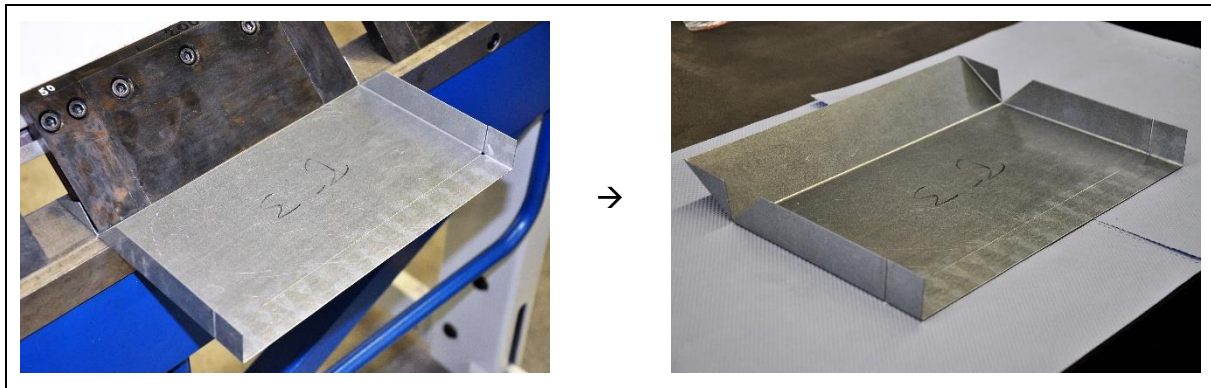
Figure 5-22: hammering the reverse bend stiffening flap

3. The last step in to prepare the bottom element for assembly is bending the 90° back flap that later aligns with the edge of the wall element.
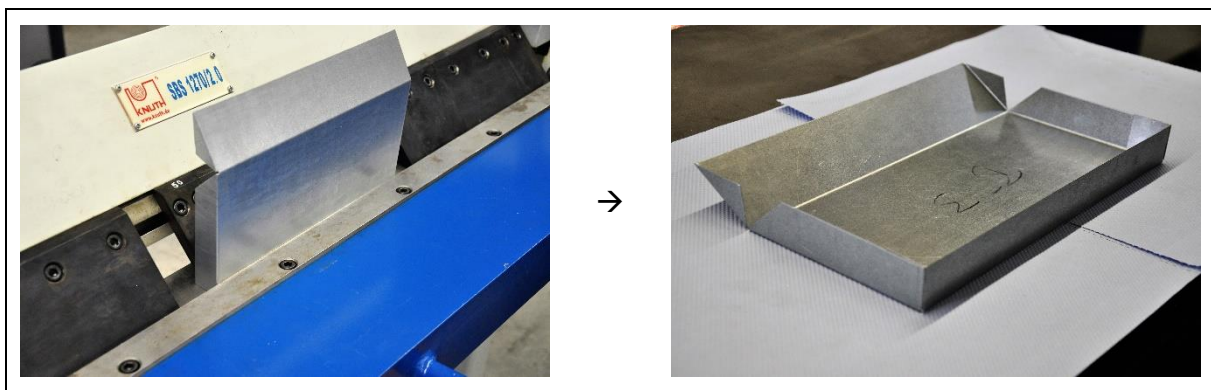
Figure 5-23: hammering the reverse bend stiffening flap

After the bending is completed for all the required elements to build an entire water wheel, the assembly of the single modules is the next step. Figure 5-24 presents all the single elements of the prototype prepared for the module assembly.
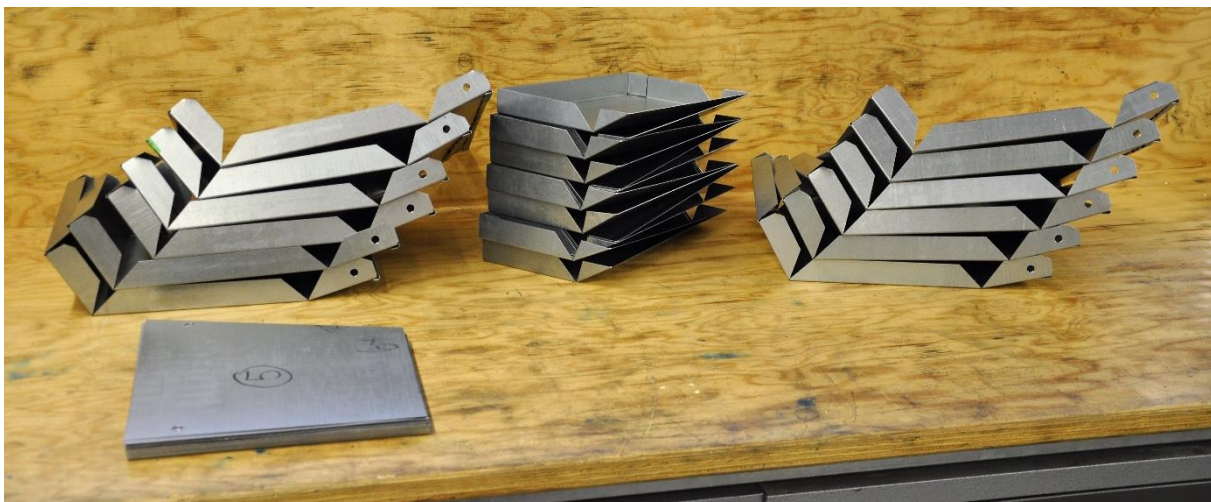
Figure 5-24: Single water wheel elements of the prototype ready for assembly

5.4.2.4 Module assembly

As all the single water wheel elements are ready, they can be assembled to the water wheel modules using blind rivets.

To simplify the assembly of the cells, three wooden templates are created, adapted to the shape of the elements. That enables an easy positioning of the single elements relatively to one another.

The first template is adjusted to the width of the water wheel module and supports the connection of the paddle and the bottom element.

The second template matches to the shape of the paddle. Thereby, it allows an easy conjunction of the paddle with the wall element.

The third template is adapted to the form of the bottom paddle and thus assists linking the bottom element with the wall elements.

The three templates are illustrated in Figure 5-25.

| Template 1 | Template 2 | Template 3 |
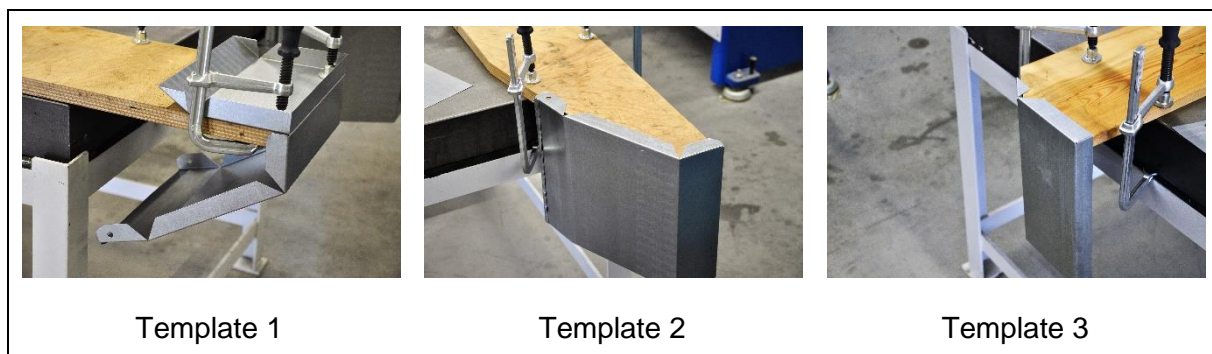
Figure 5-25: Templates to simplify the module assembly

The challenges in the assembly are the right positioning of the elements towards each other and to set the blind rivets into the side flaps and not besides them.

The first elements being joint together are the paddle and the bottom element. Therefore, they have to be levelled such that they are adjusted at their front and positioned equally in their width as shown in Figure 5-26. Generating the bores for the blind rivets, the elements must by clamped together fixing their relative position. With respect to the measurements of the flap, the holes can be drilled. After the bores are processed the blind rivets are used to connect the elements. For a chamber width of $b_2 = 0,3 \ m$ four blind rivets are sufficient. The position of the holes for the blind rivets and the result are presented in Figure 5-27.
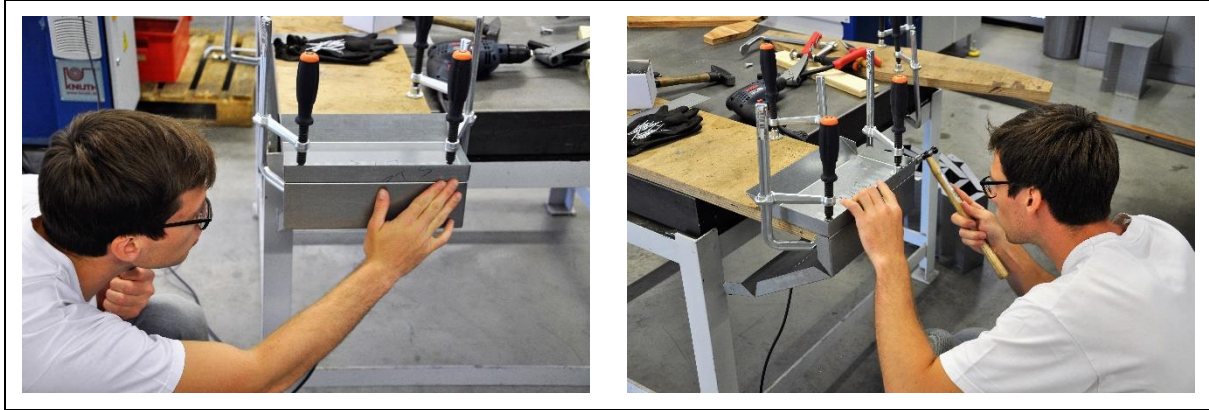
Figure 5-26: levelling of the paddle and bottom element
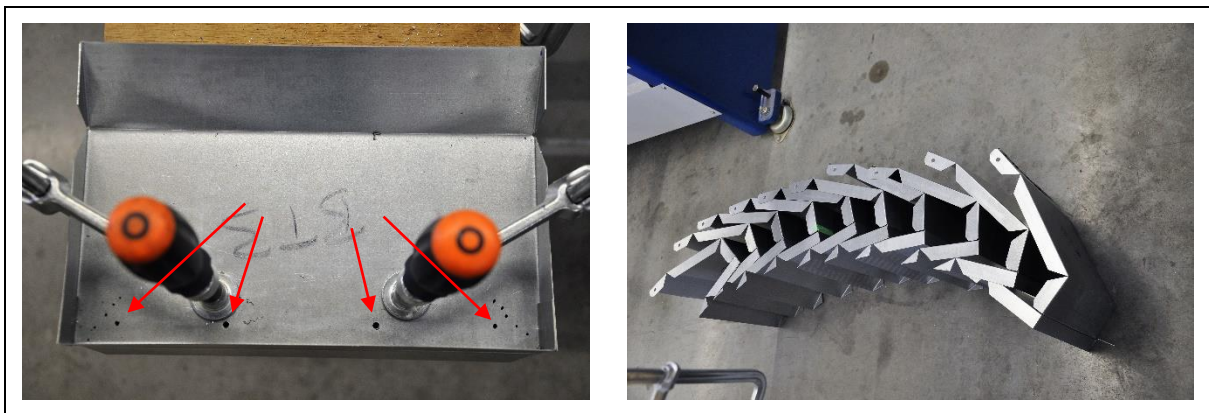
Figure 5-27: bore positions and result

In the next step, the wall elements are attached to the already joined paddle-bottom unit. This is done using template 2 as support structure. The right positon, of the wall element to the paddle-bottom unit depends on three requirements. The bottom edge of the wall element must align the outer edge of the bottom element. The vertical edge of the wall element must match with the rim of the lock paddle section. And third, the bore in the flap of the outer impact paddle section must coincide with the bore in the wall element. (Figure 5-28)
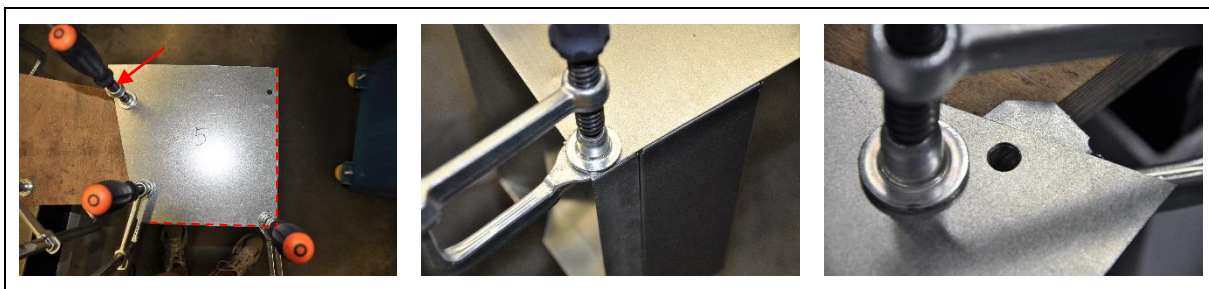
Figure 5-28: Relative positioning of wall element and paddle-bottom unit

The challenge is again to estimate the position of the hidden flaps to drill the bores rightly as shown in Figure 5-29. Also, the fact that the modules are nested into one another in the water wheel assembly has to be taken into account. Doing that, the wall elements of a module are placed between the wall elements and the paddle of the neighbouring cell. A blind rivet placed too close to the tip of the impact paddle might inhibit that. Thus, in the present module design no blind rivets are set into to the flaps of the entry section of the impact paddle (Figure 5-30).

Figure 5-29: Estimating the flap measurements and positioning the bores
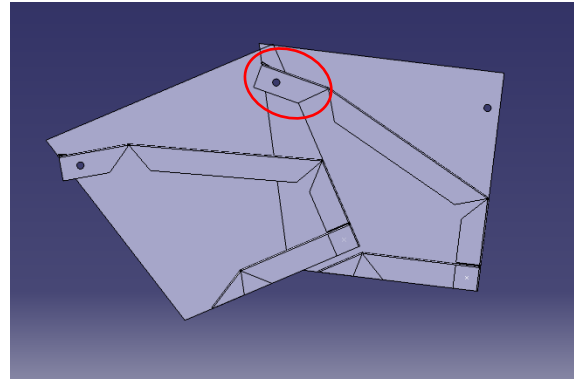
Figure 5-30: Limitations on rivet positions due to modularity – 1

After the positions of rivets are clarified, the bores can be processed and the blind rivets are placed to connect the paddle element with the wall element.

Figure 5-31: bore positions and result

So far only the paddle element is linked with the wall element. Thus, in the next step the wall element also is connected with the side flaps of the bottom element. Supported by template 3, the adjustment of the bottom edge of the wall element and the bottom element is checked and fixed with clamps (Figure 5-32). It must be considered that a bore is placed in the rectangular lower corner of the wall element during the water wheel assembly. Thus, blind rivets must not be placed there (Figure 5-33).

Figure 5-32: Processing the blind rivet holes in wall and bottom element
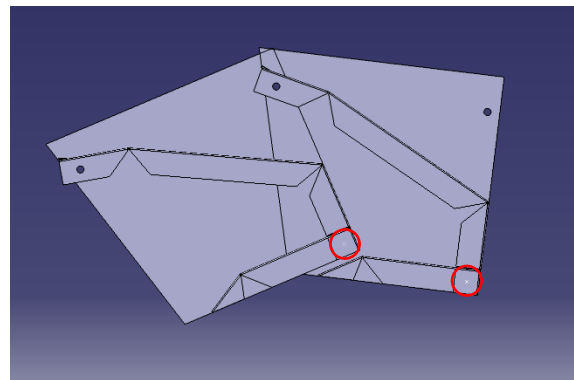
Figure 5-33: Limitations on rivet positions due to modularity – 2

Finally, the holes are processed and the blind rivets are fixed as presented in Figure 5-34.
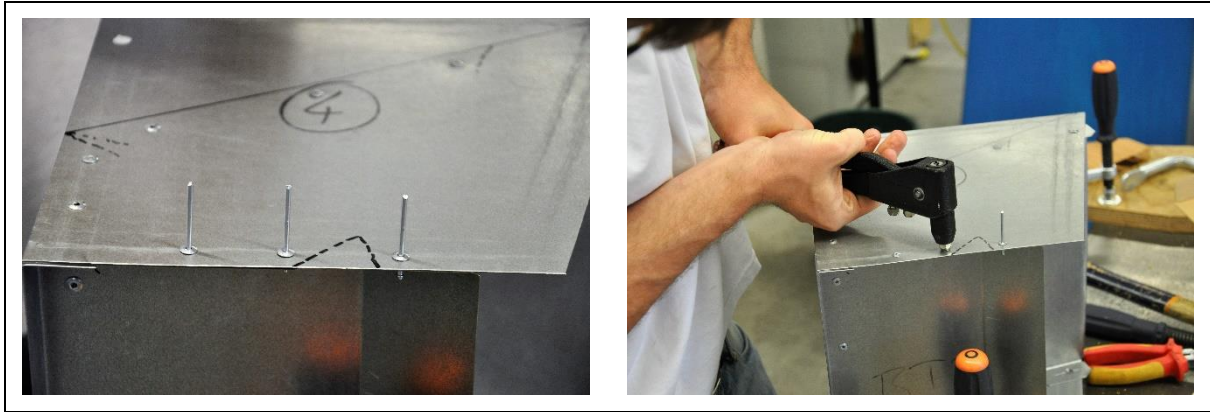
Figure 5-34: Joining wall element and paddle-bottom unit

This work steps are performed equally for both wall elements of one module. It is important to take both wall elements of one module with their bores drilled in the same stack, as explained in section 5.4.2.2, to require the equal relative position of the bores in both wall elements.

The result after assembling all twelve cells of the prototype is illustrated in Figure 5-35.

Figure 5-35: All modules finished

5.4.2.5 Water wheel rim assembly

After all modules are put together, the entire water wheel can be assembled. With the yet existing outer ring of bores the modules are roughly positioned relatively to on another in a circle. Therefore, the cells are loosely bolt together. For the prototype bolts of the measurements $M8 \times 20mm$ are used.
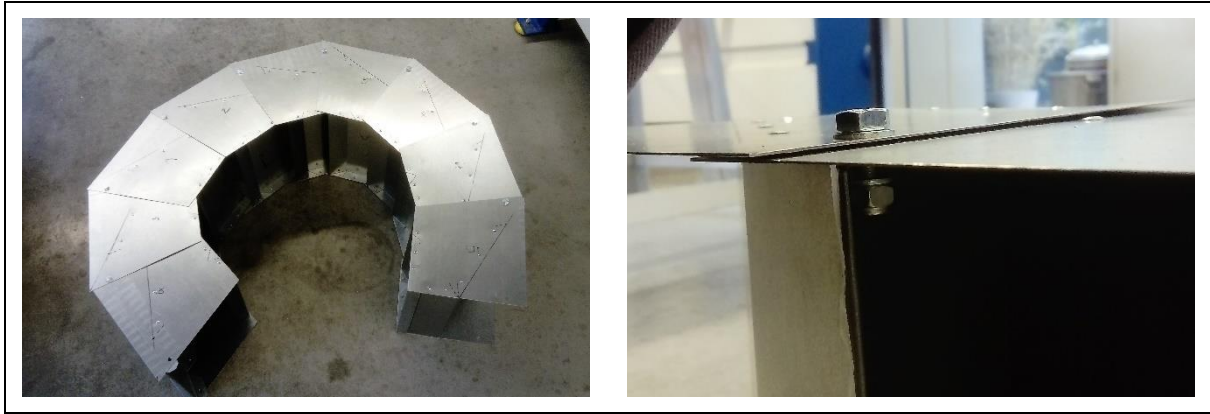
Figure 5-36: Rough positioning of the modules

The exact adjustment then is achieved fixing the angle between neighbouring cells. The angle depends on the number of cells used in the water wheel and is described in Figure 5-37. The final relative position of the modules must be fixed with clamps.
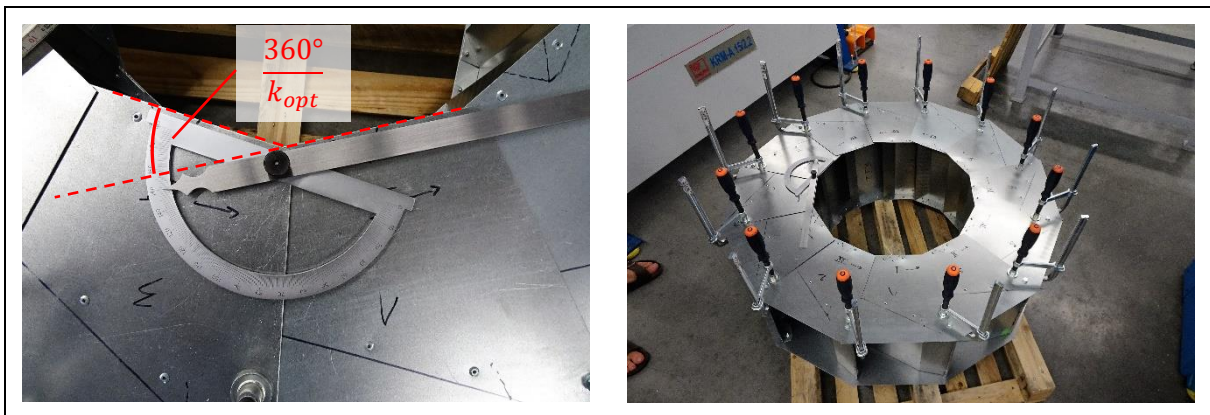
Figure 5-37: Exact positioning of the modules

Once the relative position of all modules is fixed, the inner ring of bores stating the final position is processed. To identify the right position of the bores, the hidden outline of the cells is estimated. (Figure 5-38)
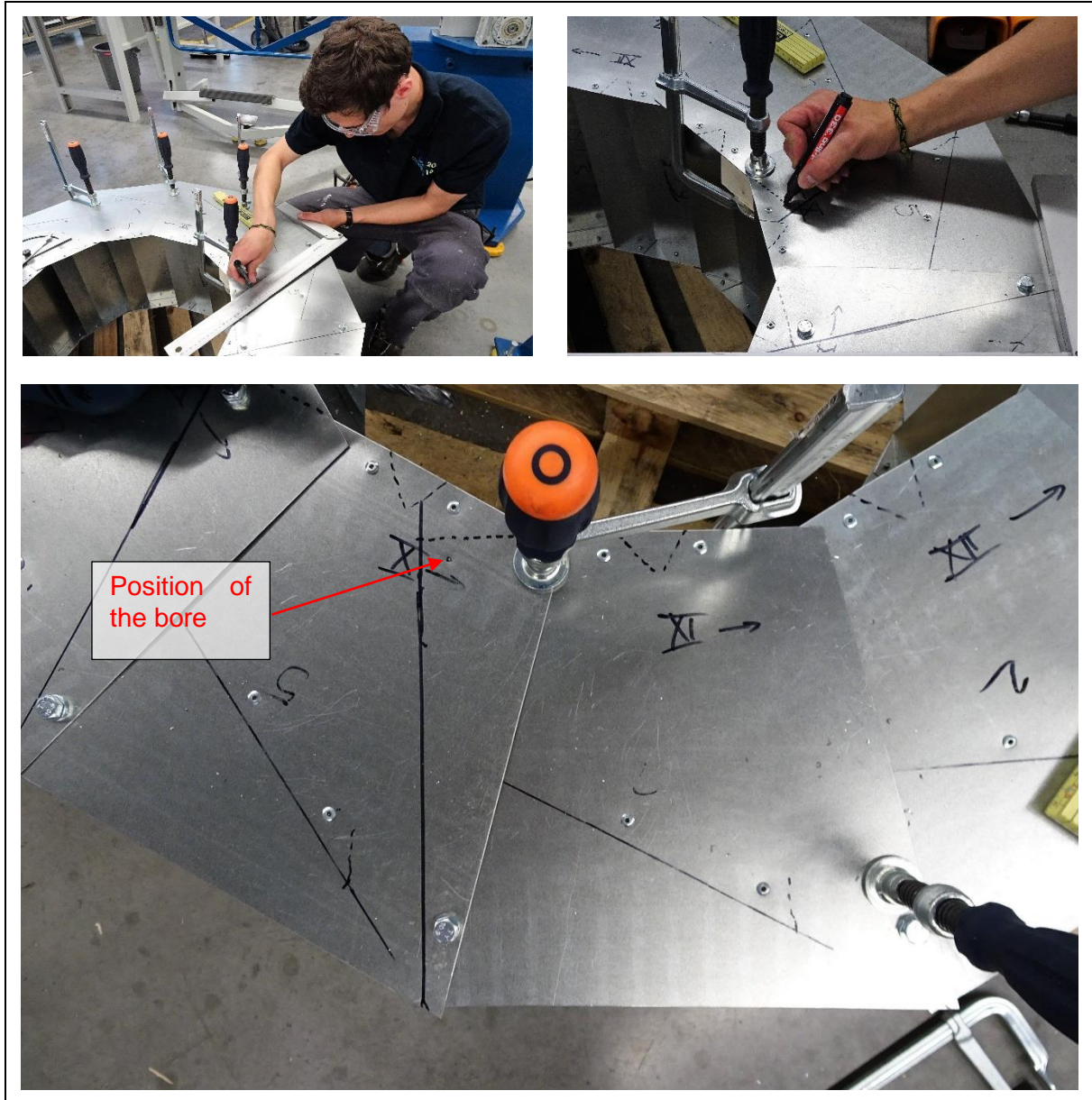
Figure 5-38: Right positioning of the bores

The bores are then processed while clamping a wooden counterpart from below, to prevent the sheet metal flaps from bending away under the pressure of the drill (Figure 5-39). After the bores are placed the bolts are tightened to fix the final shape of the water wheel. (Figure 5-40)
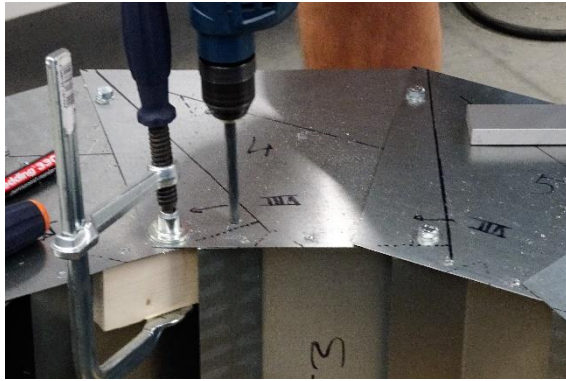
Figure 5-39: Processing the bores using a wooden counterpart

Figure 5-40: bolting the final shape of the water wheel

The entire process of the assembly must be repeated equally for the other side of the water wheel. Finalizing the assembly, the cultrate corners occurring at the overlap of two modules are cut off as shown in Figure 5-41 to obviate injuries.
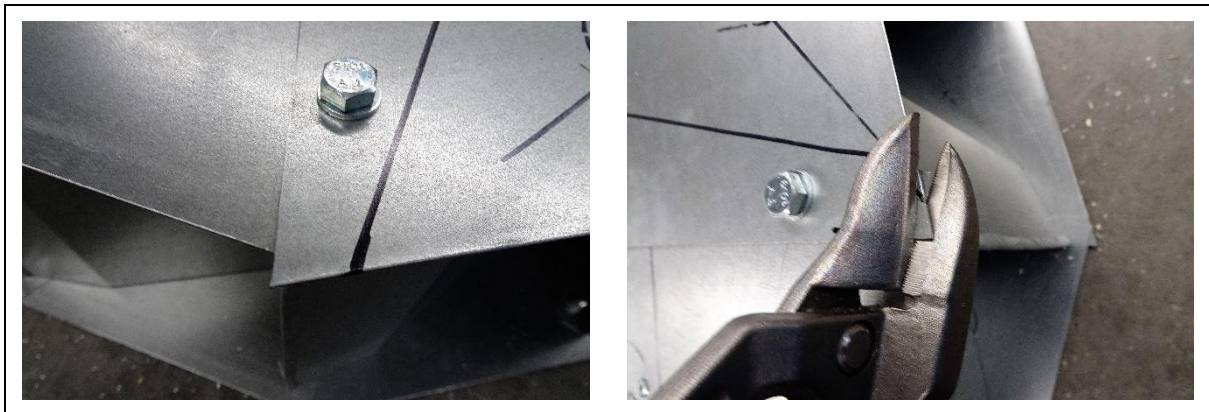
Figure 5-41: Removing cultrate corners

After this work step, the assembly of the water wheel rim of the prototype is completed. The assembled prototype is presented in Figure 5-42.

Figure 5-42: Finalized prototype rim – $H = 1,3\ m$; $Q = 0,02\ m^3/s$

5.4.3 Time estimation

During the total constructing process of the prototype, the working hours were documented. The estimated times for the different process steps are listed in Table 5-6 in person-days (PD).

Table 5-6: Estimation of the required working time

Process	Time
Basic cut / preparation	1,5 PD
Fine cut / notching / bores	1,5 PD
Bending	1 PD
Module assembly	2 PD
Water wheel rim assembly	2 PD
Sum:	**8 PD**

The Table shows that all the different processes in the construction needed a comparable amount of working time. The total time one person requires to build a water wheel of the dimensions of the prototype adds up to eight days. It hast to be mentioned that especially the module assembly warrants the parallel work of two persons and also the water wheel assembly is much easier two by two. Thus, when two people work on the construction full work days in a row, the water wheel rim is completed within four days.

5.4.4   Consideration of costs

Also, the utilized material and the occurring costs are analysed. All the materials are available in Nepal which was a prerequisite of the entire study. The different required materials, their amount and the specific and total prices (net prices) are listed in the table below.

Table 5-7: Cost estimation for the prototype

Material	Specific price		Amount	Total price	
	DE	**NP**		**DE**	**NP**
Raw plain sheet metal plate	$29{,}87\,\frac{€}{1m\times2m\,pcs}$ [1)	$18{,}92\,\frac{€}{4'\times8'pcs}$ 3)	$ca.\,6\,m^2$ $(3\times1m\times2m;$ $2\times4'\times8')$	89,61 €	37,84 €
Blind rivets (package of 500 pcs)	$13{,}13\,\frac{€}{pkg}$ [22]	$13{,}13\,\frac{€}{pkg}$ 2)	$0{,}5\,pkg$ $(only\,240\,pcs)$	6,57 €	6,57 €
Bolts M8x20 (package of 20 pcs)	$4{,}81\,\frac{€}{pkg}$ [23]	$4{,}81\,\frac{€}{pkg}$ 2)	$2{,}5\,pkg$ $(only\,48\,pcs)$	12,03 €	12,03 €
Ring washer 8,4 (package of 100 pcs)	$2{,}74\,\frac{€}{pkg}$ [24]	$2{,}74\,\frac{€}{pkg}$ 2)	$1\,pkg$	2,74 €	2,74 €
Locknuts (package of 100 pcs)	$8{,}09\,\frac{€}{pkg}$ [25]	$8{,}09\,\frac{€}{pkg}$ 2)	$0{,}5\,pkg$ $(only\,48\,pcs)$	4,05 €	4,05 €
Total price:				**115 €**	**63, 23 €**

1) The bill of the sheet metal plates is attached as appendix E)

2) Price set identical to the German price. In reality, it will be a little bit less.

3) Price list of the HULAS STEEL in Pokhara (Nepal) attached in appendix A) converted into € using [26] effective: 2017/07/25

Table 5-7 presents the prices of all components required to build the water wheel rim of the prototype with twelve modules. The net prices in Germany as well as in Nepal are listed. It has to be mentioned that the prices for the material to join the parts in Nepal, like bolts are borrowed from the German values due to a lack of information. This assumption is acceptable, as the main issue is the sheet metal material and the prices for the other parts in reality will be less than in Europe thus underestimating the total costs is prevented.

As the measurements of the raw sheet metal plates are different in Germany and Nepal, only two raw plates are required for the prototype in Nepal instead of three in Germany. The total material price for the water wheel rim in Germany adds up to $115\,€$. In Nepal it would be $63{,}23\,€$. Transferred to Nepalese rupee this is $7591\,NRs$ [27]. Since this is only the price for the water wheel rim more costs for the wheel wrench, the bearings, the generation set, some periphery and the manpower have to be taken into account for a final statement to the investment.

Nevertheless, it is possible to derive some specific prices limited to the costs of the water wheel rim. The specific prices are only presented for the required investment for a production in Nepal. The prototype is assembled of twelve modules, thus the specific price of one module

with the width of $b_2 = 0,3\ m$ within the module size 1 is $5,27\ €/module$. With this module price, for all cases from Table 4-6 that utilize the same modules as the prototype specific prices referring to the electrical power $€/W_{el}$ output are calculated. Thus the cases with $B_{WW,opt} = 0,3\ m$ and $B_{WW,opt} = 0,6\ m$ are respected. The results are illustrated in the graph in Figure 5-43.

Figure 5-43: Specific price for the water wheel rim related to the electrical power output (€ / W_el)

Two facts can be extracted from the graphic. At first the specific costs in general tend to decrease with rising volume flow rates and rising numbers of modules. Second the specific cost reduces with increasing numbers of modules for a constant volume flow rate, but stagnates at a certain value. For example for $Q = 0,03\ m^3/s$ the specific price decreases for rising numbers of cells from 14 to 17, afterwards the specific price is more or less constant.

It can be conclude that the simple design concept using sheet metal offers a low cost power supply that also should be affordable for Nepali people. Besides that, the electrical power output specific costs decrease for greater diameters and higher flowrates. But, to verify this statement it is necessary also to estimate the costs for the smaller module type and complete the consideration for all cases in Table 4-6.

5.4.5 Lessons learned

The construction of the prototype confirmed the functionality of the design concept of the modules as well as of the water wheel itself. The entire construction starting from raw sheet metal plates and finishing the assembly of the water wheel worked without unexpected problems. The construction using very simple tools moreover assured that the concept is unsusceptible to manufacturing deviations.

An important task during the assembly was localizing the hidden side flaps to position the blind rivets right. Using blind rivets was a very good choice, because they allow to process the entire assembly from outside the module and no handling of tools in areas difficult to access is required.

It also is possible generate a solid water wheel based on a thin sheet metal material, due to a stiffening design of elements and module. The only slightly occurring weak point is the long unstiffen distance between the bores at the outer radius of the wall element as illustrated in Figure 5-44. That is generally no problem, because a water wheel is not stressed sideward. Still, this can be corrected by simply attaching an L-kinked sheet metal profile onto the wall element from the outside, if wanted.
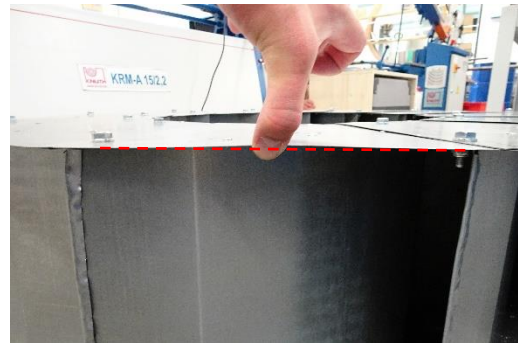
Figure 5-44: Possible weak point

As affirmed in paragraph 5.4.4 the designed concept is a possibility to produce water wheels easily at low cost. That makes it perfectly suitable for an application in Nepal.

Furthermore, the simplicity of the design allows a quite fast realization. Starting from zero the modules can be finished within 6 PD and just another 2 PD are required for the assembly of the water wheel rim at the operating site. The construction of the prototype showed that the assembly processes are much easier to handle working in pairs.

At last has to be mentioned that during the whole manufacturing process, the used galvanized sheet metal gets a lot of scratches all over. To keep the resistivity against rust, the galvanization has to be repeated after the assembly. Other options would be to use stainless steel, if available for an acceptable price, or to colour coat the water wheel.

All in all, the developed design fulfils the expectations that were set in it. Thus, a production in Nepal should be easily possible as assured by Professor Maskey from Kathmandu University, who examined the ready prototype during his visit at the Technical University in June 2017 [3].

5.4.6 Wheel wrench concept

Generally, it has to be pointed out that the workers in Nepal have great skills in constructing wheel structures [6] (e.g. see Figure 5-45). It is not necessary to come up with a prepared concept, but rather suggestive to involve the Nepali into the process and develop a design together based on the water wheel rim instead of presenting a completed design for the wheel wrench. Thus, it is much easier to find a concept that fits to the available techniques in Nepal. That is the reason, why the design of the inner part including the connection of the water wheel with the axis is not a part of this thesis.

Figure 5-45: wheel structures made in Nepal [Stephan Baur]

Nevertheless, a simple concept is sketched, together with Johannes Eisner, which incorporates the bores in the water wheel rim as connecting points. Here as well the concept focuses on a simple realization.

The idea is to connect some bores of the inner circle of the water wheel rim with flat metal bars. At them L-profile metal bars can be positioned and fixed such that they embrace the axis. Thus, it is possible to centre the axis in the wheel without the necessity of an engine lathe.

The advantage of the concept is the easy adaptability to different water wheel diameters.

Figure 5-46 shows a sketch of the concept idea.
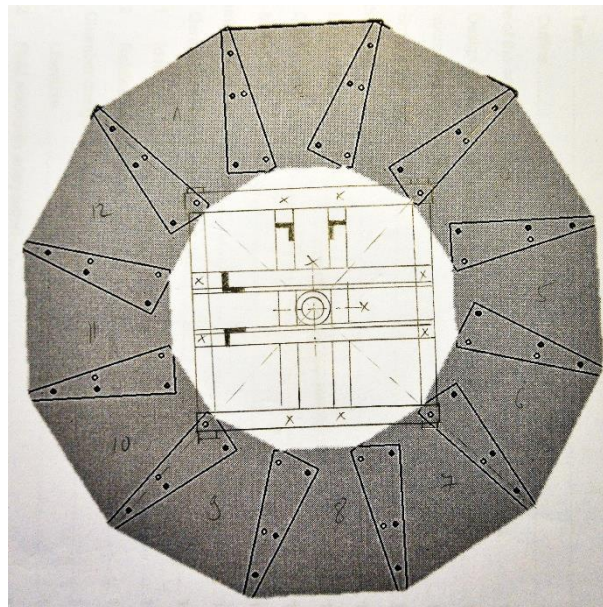
Figure 5-46: Sketch of the wheel wrench concept

The concept was realized by Johannes Eisner. The result is shown in Figure 5-47.
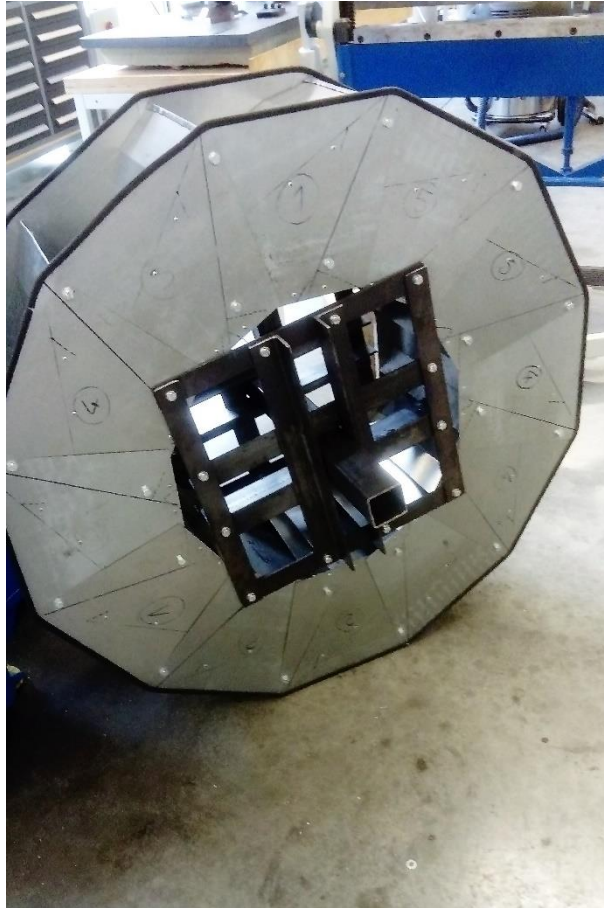
Figure 5-47: Prototype with wheel wrench concept

6 Summary and Outlook

In the work at hand, an entire design concept for overshot water wheels with special consideration to the application in developing countries, on the example of Nepal, has been developed. The focus thereby was set on the special requirements related to the limitations in materials and machinery in Nepal.

Besides these restrictions, the required small-scale demand and the general suitability of overshot water wheel for electrical energy supply in Nepal have been analysed.

Based on that, a modular design concept for overshot water wheels especially for diameters from $1,0$ to $2,1\ m$, has been elaborated. That allows an easy adaptability of water wheels to various operating sites. To automate the optimizing process, a Matlab-tool has been created which calculates the important parameters of the water wheel, like the optimum module number and the appropriate total width of the water wheel, for a fixed module concept. Only two input parameters of the operating site, the height of fall and the water volume flow rate, are required. After computing the optimum values for the water wheel, the Matlab-tool calculates the behaviour of the power output and the occurring mechanical torques as a function of the numbers of rotation in a second part. This information can be used to identify the optimum operation point and for dimensioning the axis.

Finally, the developed design concept and Matlab-tool has been employed on a fictional operating site of a height of fall of $H = 1,3\ m$ and a volume flow rate of $Q = 0,02\ m^3/s$. The results of these calculations have been analysed before the prototype has been constructed. The production process of the prototype has been limited to the equipment that is also available in Nepal to perform a reproducible test of the concept. Thus, it has been possible to affirm the functionality of the designed modular concept for overshot water wheels with different diameters.

As is has not been possible to perform a test operation of the prototype, this is one of the next steps in order to verify the results of the simulation by comparing them with the measurements. This test operation is furthermore quite important to check whether some of the made assumptions, neglecting losses, in the calculation affect the operation or not. Based on results of this analysis, it would be possible to optimize the Matlab-tool.

Besides verifying the Matlab-tool, it could also be used to optimize the entire module concept. This can be done by simulating certain input variables with varying concept parameters. Comparing the results of the simulations, positive or negative effects on the power output can be identified. Apart from the optimizing purpose, the Matlab-tool generally produces a great amount of data for different water wheels. Thus, for example, the behaviour of the efficiency in relation to the height of fall or the total water wheel width etc. could be analysed.

In addition, to verifying the design concept with measurements of the prototype, a far reaching next step is to construct a water wheel based on the developed design in Nepal together with Nepalese workers. This is the final test on whether the concept will be reproducible in Nepal and if it will be accepted by the people.

All in all, the task of the thesis to design a low-tech water wheel concept for Nepal has been fulfilled. The quantity of generated data additionally offers great opportunity for further studies. The construction of the prototype showed the practicability of the concept with simple equipment which indicates that production in Nepal should be easily possible.

Bibliography

[1] Nepal Electricity Authority, "Nepal Electricity Authority - a year in review - fiscal year 2015/2016," Nepal Electricity Authority, Kathmandu, 2016.

[2] Alternative Energy Promotion Centre, "Alternative Energy Prommotion Centre: Renewables: Mini/Micro Hydro Technology," Goverment of Nepal Ministry of Population and Environment, 2013. [Online]. Available: http://www.aepc.gov.np/?option=renewable&page=subrenewable&mid=2&sub_id=14&id=4. [Accessed 19 06 2017].

[3] R. K. Maskey, Interviewee, *Dr.* [Interview]. 28 06 2017.

[4] J. Eisner, "Analysis of the Energy Demand for Designing Off-Grid Energy Systems for Developing Contries Based on the Exapmle of Nepal," TUM, Garching bei München, 2017.

[5] B. Espinar and D. Mayer, "The role of ernery sotrage for mini-grid stabilization; Report IEA-PVPS T11-02:2011," IEA, France, 2011.

[6] S. Baur, Interviewee, *Dipl.-Phys.* [Interview]. 19 7 2017.

[7] F. Tönsmann, "Zeittafeln zur Geschichte der Wasserkraftnutzung (In: Berichtsband zur Tagung Geschichte der Wasserkraftnutzung [Koblenz 1982])," Koblenz, 1985.

[8] C. Bach, Die Wasserräder, Stuttgard: Verlag von Konrad Wittwer, 1886.

[9] W. Müller, Die Wasserräder, 4. Reprint der 2. Auflage von 1939 ed., Detmold: Verlag Moritz Schäfer, 2010.

[10] H. Henne, Wasserräder und Turbinen - ihre Berechnung und Konstruktion, Leipzig: Verlag von Bernh. Friedr. Voigt, 1903.

[11] D. M. Nuernbergk, Wasserräder mit Freihang - Entwurfs- und Berechnungsgrundlagen, Verlag Moritz Schäfer, 2007.

[12] J. Giesecke, S. Heimerl and E. Mosonyi, Wasserkraftanlagen, Berlin Heidelberg: Springerverlag, 2014.

[13] E. Quaranta and R. Revelli, "Output power and power losses estimation for an overshot water wheel," *Renewable Energy,* pp. 978-987, 05 06 2015.

[14] Auswärtiges Amt, "Auswärtiges Amt: Außen- und Europapolitik: Länder: Länderinfos: Nepal: Wirtschaft," 03 2017. [Online]. Available: http://www.auswaertiges-amt.de/DE/Aussenpolitik/Laender/Laenderinfos/Nepal/Wirtschaft_node.html. [Accessed 21 07 2017].

[15] H. Drews, "Segmentkranz-Wasserrad," [Online]. Available: http://www.wasserrad-drews.de/. [Accessed 24 07 2017].

[16] L. Geß, "Powertransmission for a low-tech water wheel," -, Garching bei München, 2015.

[17] P. Hench, "Bachelorarbeit: Wirkungsgrad einer Assynchronmaschine als Generator in Inselsystemen," München, 2017.

[18] C. Jehle, Bau von Wasserkraftanlagen - Praxisbezogenen Planungsgrundlagen, 5. überarbeitet und erweiterte Auflage Hrsg., Berlin: VDE Verlag GmbH, 2011.

[19] R. Brüdern, Wie man Wasserräder Baut, Rothemühle: Dipl. Ing. Richard Brüdern, 2006.

[20] G. Müller, "Water Wheels as a Power Source".*Renewabel Energy.*

[21] G. Bollrich, Technische Hydro-mechanik-1; Grundlagen, Berlin: HUSS-MEDIEN GmbH, 2007.

[22] Rivet-Expert, "Rivet-Expert: Home:Materailien: Blindnieten: Riv-linkstandard Blindnieten: Standard Blindniet offen Flachrundkopf Stahl/Stanl," [Online]. Available: https://www.rivet-expert.com/de/materialien/blindnieten/standard-blindnieten/standard-blindniet-offen-flachrundkopf-stahl-stahl/#1277. [Accessed 19 07 2017].

[23] Wegertseder GmbH, "Wegertseder.com: Direktbestellung: Schrauben: Sechskanntschrauben: mit Gewinde bis Kopf: Regelgewinde," [Online]. Available: https://wegertseder.com/ArticleDetails.aspx?AKNUM=2748&Diameter=8. [Accessed 19 07 2017].

[24] Wegertseder GmbH, "Wegertseder.com: Direktbestellung: Scheiben: Standardscheiben ohne Fase," [Online]. Available: https://wegertseder.com/ArticleDetails.aspx?AKNUM=1490&Diameter=8,4. [Accessed 19 07 2017].

[25] Wegertseder GmbH, "Wegertseder.com: Direktbestellung: Muttern: Sicherungsmuttern: Kunststoff-Ring: niedrige Form (Standard): Regelgewinde," [Online]. Available: https://wegertseder.com/ArticleDetails.aspx?AKNUM=3340&Diameter=8. [Accessed 19 07 2017].

[26] finanzen.net, "Home: Währungsrechner: Nepalesische Rupie - €," 25 07 2017. [Online]. Available: http://www.finanzen.net/waehrungsrechner/nepalesische-rupie_euro. [Accessed 25 07 2017].

[27] finanzen.net, "Home: Währungsrechner: Euro - Nepalesische Rupie," 25 07 2017. [Online]. Available: http://www.finanzen.net/waehrungsrechner/euro_nepalesische-rupie. [Accessed 25 07 2017].

Appendix

A)   Overview on sheet metal prices from HULAS STEEL in Pokhara, Nepal

HULAS GURANS

Galvanized and Color Coated Sheets

Consumer Price List For HULAS STEEL Authorized Depot At: **Pokhara**

Valid from 4th Srawan 2074 (19th July 2017)   **Rs / Bdl Incl VAT**

Base Metal mm	Avg.Wgt	Mark / stamp For GP GC	GC Sheet	GP Sheet	GI Heritage	GI H Span	Colour coat	CC Heritage	CC H Span	Ridge
1.20	189	1.20 mm	23990	23990						
1.10	172	1.10 mm	22120	22120						
0.90	142	0.90 mm	18270	18270						
0.80	127	0.80 mm	16450	16450			18990			
0.75	119	0.70 mm	15510	15510	16550		17890	19080		
0.60	96	22 (6)	12580	12580	13420		14700	15680	21030	
0.55	86		11340	11420	12100		13350	14240	18950	
0.52	83	24 Heavy	10750	10820			12740			
0.50	79	24 Medium	10410	10470	11100	14885	12310	13130	17610	
0.45	71		9410	9470	10040	13454	11310	12060	16170	
0.41	65	26 Heavy	8670	8740		12400	10540		15080	2940
0.38	61	26 H	7930	7990			9730			2690
0.35	55	26 Light	7560	7620			9260			2570
0.31	50	28 Heavy	6820	6890			8380			2320
0.28	45	28 Medium	6210	6270			7760			2120
0.26	42	28 Light	6860	5900			7350			2000
0.24	39	30 Heavy	5580	5630			6970			1910
0.22	36	30 Medium	5160	5210			6560			1770
0.20	32	30 Light	4780	4780			6180			1630
0.18	29	32 Gauge	4430	4430			5760			1520
0.15	25	32 CQ	3900	3900						1340
0.13	22	0.15 MM	3460	3460						1200
0.12	21	0.14 MM	3370	3370						

4' WIDE plain sheets

			Rs / Pc GP Sheet	Rs / Pc Colour coat
1.10	26.11	1.10 mm	3230	
0.90	21.45	0.90 mm	2680	3020
0.80	19.11	0.80 mm	2420	2740
0.75	17.95	0.75 mm	2280	2580
0.70	16.75	0.70 mm	2120	2490
0.62	14.88	0.62 mm	1900	2230
0.55	13.25	0.55 mm	1710	2010
0.50	12.08	0.50 mm	1560	1830
0.48	11.59	0.48 mm	1490	1760
0.45	10.89	0.45 mm	1410	1660
0.42	10.17	0.42 mm	1330	1550
0.40	9.72	0.40 mm	1270	1540
0.37	8.99	0.37 mm	1180	1440
0.35	8.52	0.35 mm	1130	1380
0.30	7.36	0.30 mm	980	1220
0.28	6.89	0.28 mm	930	1160

GI EXPANDED METAL MESH

Thk mm	width	Rs / m
1.20	3'	130
1.20	4'	180
1.00	3'	110
1.00	4'	150
0.90	3'	100
0.90	4'	140

Hulas LifesTile Profile

Thk. mm	Weight	Rs./Bdl
0.40	87.56	15740

Weight Tolerances ± 0.50Kg. Per Bdl.

B)   Calculation to select the different module sizes

H	a_min	a_max	a_mean	t_mean
1	0,17	0,25	0,21	0,26
1,1	0,17	0,26	0,22	0,26
1,2	0,18	0,27	0,22	0,27
1,3	0,18	0,27	0,23	0,27
1,4	0,19	0,28	0,23	0,27
1,5	0,19	0,29	0,24	0,28
1,6	0,19	0,29	0,24	0,28
1,7	0,20	0,30	0,25	0,29
1,8	0,20	0,30	0,25	0,29
1,9	0,21	0,31	0,26	0,29
2	0,21	0,31	0,26	0,30
2,1	0,21	0,32	0,27	0,30
2,2	0,22	0,33	0,27	0,30
2,3	0,22	0,33	0,28	0,31
2,4	0,22	0,33	0,28	0,31
2,5	0,23	0,34	0,28	0,31
2,6	0,23	0,34	0,29	0,31
2,7	0,23	0,35	0,29	0,32
2,8	0,23	0,35	0,29	0,32
2,9	0,24	0,36	0,30	0,32
3	0,24	0,36	0,30	0,33
3,1	0,24	0,36	0,30	0,33
3,2	0,25	0,37	0,31	0,33
3,3	0,25	0,37	0,31	0,33
3,4	0,25	0,38	0,31	0,33
3,5	0,25	0,38	0,32	0,34
3,6	0,26	0,38	0,32	0,34
3,7	0,26	0,39	0,32	0,34
3,8	0,26	0,39	0,33	0,34
3,9	0,26	0,39	0,33	0,35
4	0,26	0,40	0,33	0,35
4,1	0,27	0,40	0,33	0,35
4,2	0,27	0,40	0,34	0,35
4,3	0,27	0,41	0,34	0,35
4,4	0,27	0,41	0,34	0,36
4,5	0,28	0,41	0,34	0,36
4,6	0,28	0,42	0,35	0,36
4,7	0,28	0,42	0,35	0,36
4,8	0,28	0,42	0,35	0,36
4,9	0,28	0,42	0,35	0,37
5	0,28	0,43	0,36	0,37
5,1	0,29	0,43	0,36	0,37
5,2	0,29	0,43	0,36	0,37
5,3	0,29	0,44	0,36	0,37
5,4	0,29	0,44	0,37	0,37
5,5	0,29	0,44	0,37	0,38
5,6	0,30	0,44	0,37	0,38

H	a_min	a_max	a_mean	t_mean
5,7	0,30	0,45	0,37	0,38
5,8	0,30	0,45	0,37	0,38
5,9	0,30	0,45	0,38	0,38
6	0,30	0,45	0,38	0,38
6,1	0,30	0,46	0,38	0,39
6,2	0,31	0,46	0,38	0,39
6,3	0,31	0,46	0,38	0,39
6,4	0,31	0,46	0,39	0,39
6,5	0,31	0,47	0,39	0,39
6,6	0,31	0,47	0,39	0,39
6,7	0,31	0,47	0,39	0,39
6,8	0,32	0,47	0,39	0,40
6,9	0,32	0,48	0,40	0,40
7	0,32	0,48	0,40	0,40
7,1	0,32	0,48	0,40	0,40
7,2	0,32	0,48	0,40	0,40
7,3	0,32	0,48	0,40	0,40
7,4	0,32	0,49	0,41	0,40
7,5	0,33	0,49	0,41	0,41
7,6	0,33	0,49	0,41	0,41
7,7	0,33	0,49	0,41	0,41
7,8	0,33	0,50	0,41	0,41
7,9	0,33	0,50	0,41	0,41
8	0,33	0,50	0,42	0,41
8,1	0,33	0,50	0,42	0,41
8,2	0,34	0,50	0,42	0,42
8,3	0,34	0,51	0,42	0,42
8,4	0,34	0,51	0,42	0,42
8,5	0,34	0,51	0,43	0,42
8,6	0,34	0,51	0,43	0,42
8,7	0,34	0,51	0,43	0,42
8,8	0,34	0,52	0,43	0,42
8,9	0,35	0,52	0,43	0,42

C) Matlab dimensioning tool – computing the prototype

Sizing of overshot water wheels based on a modular water wheel concept

The tool is structured in two parts. The first part is the actual sizing of the overshot water wheel based on a modular chamber concept. The second part is the calculation of the power output of the water wheel selected in part 1.

```
clc
clear all
close all
```

Input variables of the site

The water wheel concept is optimized for the application with these variables

```
H=1.3; %m % free available height of fall
Q=0.02; %m^3/s % volume flow rate of water
```

Activation of the export to Excel

This option is generally switched of. If an export to Excel is requested, you have to activate the code lines at the very end of the code. The "filename" and the "sheet number" of the Excel file must be inserted.

```
%N_sheet=1; % sheet number for export to Excel
```

Parameters for water wheel sizing - part 1

Contains all important parameters of the concept etc. that are necessary for the calculations in part 1

These parameters are now set for a potential height of fall from 1.0 m to 2.1 m. For heights of fall beyond this interval it is possible to vary these parameters.

```
% main geometrical parameters of the concept
t_o=0.26; %m % outer partition of the chambers
a_th=0.21; %m % theoretical rim width
a_secure=0.045; %m %extended length over active radius;
s=0.015;  %m % free radius around screw holes to guarantee assembly

% material parameters
d=0.00075; %m % thickness of sheet metal material;
%            also possible for other materials

% Restrictions according to the interval of the valid heights of fall
% of the concept
z_min=12; %- % permitted minimum number of chambers in a ring
z_max=25; %- % permitted maximum number of chambers in a ring
Z=1; %- % step range from z_min to z_max
```

```
% Parameters of the paddle design (module element 2)
Epsilon_min=20; %° % angle between chamber entry section and tangent on the
%                    active water wheel circle
Delta=15; %° anlgle between the two impact paddle sections

% Parameters of the installation concept to ensure functionality
h_secure= 0.10; %m %clearance between the bottom dead centre of the
%                    water wheel and ground to ensure unhampered movment
y_secure=0.05; %m % only possible in steps of 0.001m
%                    clearance between the lower rim of the water flow
%                    and the active uppervertex of the water wheel

% Parameter for entry angle tolerance
Omega=10; %° % positive entry tolance angle between water flow line and
%              first paddle section

% Parameters for possible width of the chambers
% generally two different width to combine
b1=0.2; %m % width of small module version
b2=0.3; %m % width of broad module version
combi={'b1','b2','b1+b2','b2+b2','b2+b1+b2'}; % enabled combination of
%                                              the chamber versions to
%                                              generate the neccesarry
%                                              width of the channel
B_WW=[0.2;0.3;0.5;0.6;0.8]; %m % resulting width for defined chamber
%                                variations and enabled combinations
b_ch=[0.1;0.2;0.3;0.4;0.5]; %m % possibel width of the channel according
%                                to chamber variations and enabled
%                                combinations
O=5; %- % number of enabled combinations
```

Parameter for calculation of the power output - part 2

These parameters are requested for the calculation of the power output in part 2 beside the results from part 1

```
nMax=250; %1/min % Maximum considered number of revolutions;
%                  fictional value to restrict the calculations
%                  before knowing nCutOut

PDim=0; %W % Special output of the number of revolutions for the choosen
%            power value to ease the selection of a generator
%            and a gearbox. It always will be set at n_Dim > n_max
```

Constants

```
g=9.81; %m/s^2 % acceleration of gravity
rhow=999.97; %kg/m^3 % density of water
```

Part 1

Optimization of the water wheel for the chosen site

Calculation of necessary values based on the chamber design

```
chi=2*pi/z_max; %rad % angle of the side element of the chamber;
%                    equivalent to xi(z_max)
Lhamda=Epsilon_min-360/z_max/2; %° %angle between entry and
%                                   outer module line
lhamda=Lhamda/180*pi; %rad % angle between entry and outer module line
tau=(360-180-Delta-90-Lhamda)/180*pi; % rad % angle between the inner impact
%                                            paddle section and the lock paddle
omega=Omega/180*pi; %rad %positive entry tolance angle between
%                   water flow line and first paddle section
i=z_min:Z:100; %- % control varable for the number of chambers
z_max_p=i>z_max; %- % modification of z_max for the calculation
%                   according to step range Z
z_max_p=min(i(z_max_p)-Z); %- %modification of z_max for the calculation
%                              according to step range Z
```

Optimization of the number of chambers

The tool selects the maximal possible amount of chambers so that the water wheel fits below the given height of fall with respect to the postulated clearances.

```
% angle of one chamber segment from hole to hole
xi=0;
for k=z_min:Z:z_max_p
    xi(k)= 2*pi/k   ; %rad % angle of one chamber segment in ring
end

% active outer diameter of the water wheel (tip of paddle)
D_active_out(k)=0;
for k=z_min:Z:z_max_p
D_active_out(k)=(t_o/(2*sin(xi(k)/2))+s)*2;
end

% total outer diameter of the wahter wheel
D_total_out(k)=0;
for k=z_min:Z:z_max_p
    D_total_out(k)=D_active_out(k)-2*s+2*a_secure/cos(xi(k));
end

% select optimal number of chambers
% if H is greater than the maximum possible diameter with given concept -->
% chose maximumm permitted number of chambers and display information in a
% text box
if D_total_out(z_max_p)/2+h_secure+D_active_out(z_max_p)/2+y_secure < H
    box1=msgbox('The chosen height of fall is greater than the maximum diameter of the given
concept. You possibly could extract more energy with a different concept','advice');
    k_opt=z_max_p; %- % optimized number of chambers = max. number
%                     if H greater than the concept interval
else
    k_opt=find(D_total_out/2+h_secure+D_active_out/2+y_secure > H );
    k_opt=min(k_opt)-Z; %- % optimized number of chambers
```

```
end

% Check if H is inside the valid interval
% If H is to small for the concept --> interrupt calculation and display
% error information in text box
if k_opt<z_min
    box2=msgbox('The chosen height of fall is too low for the given concept and undercuts
z_min','Error','error');
    error('The chosen height of fall is too low for the given concept and undercuts z_min')
else
```

Calculation of the optimized values for the water wheel

The optimal values for the water wheel are calculated based on the previously identified optimum number of chambers

```
D_total_opt=D_total_out(k_opt); %m % optimum total outer diameter
D_active_out_opt=D_active_out(k_opt); %m % optimum of the
%                                      active outer diameter
xi_opt=xi(k_opt); %rad % optimum segmet angle
t_i=((t_o^2+a_th^2-2*t_o*a_th*cos(pi/2-xi_opt))+a_th^2-2*((t_o^2+a_th^2-2*t_o*a_th*cos(pi/2-
xi_opt))^0.5)*a_th*cos(pi/2-asin(a_th*sin(pi/2-xi_opt)/((t_o^2+a_th^2-2*t_o*a_th*cos(pi/2-
xi_opt))^0.5))))^0.5;
            %m % inner partition of the water wheel form hole to hole
D_active_in=(t_i/(2*sin(xi_opt/2))+s)*2; %m % active inner diameter of
%                                      the water wheel
a_real=(D_active_out_opt-D_active_in)/2; %m % real rim width dependet from
%                                      theoretical rim width of the
%                                      concept and the optimal
%                                      amount of chambers

% geometrical support value
c=(t_o^2+a_th^2-2*t_o*a_th*cos(pi/2-xi_opt))^0.5; %m % varable diagonal of
%                                      the chamber side
%                                      element (hole to hole)

% occurring angle between tanget to water wheel and the entry section
% of the paddle
epsilon_real=xi_opt/2+lhamda; %rad
Epsilon_real=epsilon_real/pi*180; %°
```

Specification of the chamber design by using vectors

This specification is necessary to calculate the minimum opening distance and the holding capacity of the chambers later.

```
%point 1
p_1=[s;s;0];
%point 2
p_2=[s;0.4*a_th+s;0];
%point3
l_23d=[-sin(tau);cos(tau);0]; % directing vector p_2 to p_3
B=[-t_o;a_th;0]+s*[sin(lhamda);cos(lhamda);0]; % support point for straight line p_3 p_4
l_34d=[-cos(lhamda);sin(lhamda);0]; % directing vector of straight line 34
```

```matlab
syms v1 v2 %point 3 as intersection  of line 1_23 and line l_34
eqns = [p_2(1)+v1*l_23d(1)==B(1)+v2*l_34d(1),p_2(2)+v1*l_23d(2)==B(2)+v2*l_34d(2)];
S = solve(eqns, [v1 v2]);
v1=vpa(S.v1);
v2=vpa(S.v2);


p_3=p_2+v1*l_23d; % vector to p_3

%point 4
C=[-t_o;a_th;0]+s*[-cos(chi);-sin(chi);0]; % support point for straight line
%                                       rim (rim of module side element)
l_rimd=[-sin(chi);cos(chi);0]; % directing vector of module side element
%                           line through p_4

syms q1 q2 %point p_4 as intersection of straight line 34 and straight line rim
eqns = [C(1)+q1*l_rimd(1)==B(1)+q2*l_34d(1),C(2)+q1*l_rimd(2)==B(2)+q2*l_34d(2)];
S = solve(eqns, [q1 q2]);
q1=vpa(S.q1);
q2=vpa(S.q2);


p_4=C+q1*l_rimd; % vector to point 4

%point 5
p_5=[t_i*(-sin(asin(c*sin(pi/2-asin(a_th*sin(pi/2-xi_opt)/c))/t_i)));t_i*(cos(asin(c*sin(pi/2-
asin(a_th*sin(pi/2-xi_opt)/c))/t_i)));0]+[cos(xi_opt) -sin(xi_opt) 0;sin(xi_opt) cos(xi_opt)
0;0 0 1]*p_1;
%point 6
p_6=[t_i*(-sin(asin(c*sin(pi/2-asin(a_th*sin(pi/2-xi_opt)/c))/t_i)));t_i*(cos(asin(c*sin(pi/2-
asin(a_th*sin(pi/2-xi_opt)/c))/t_i)));0]+[cos(xi_opt) -sin(xi_opt) 0;sin(xi_opt) cos(xi_opt)
0;0 0 1]*p_2;
%point 7
p_7=[t_i*(-sin(asin(c*sin(pi/2-asin(a_th*sin(pi/2-xi_opt)/c))/t_i)));t_i*(cos(asin(c*sin(pi/2-
asin(a_th*sin(pi/2-xi_opt)/c))/t_i)));0]+[cos(xi_opt) -sin(xi_opt) 0;sin(xi_opt) cos(xi_opt)
0;0 0 1]*p_3;
%point 8
p_8=[t_i*(-sin(asin(c*sin(pi/2-asin(a_th*sin(pi/2-xi_opt)/c))/t_i)));t_i*(cos(asin(c*sin(pi/2-
asin(a_th*sin(pi/2-xi_opt)/c))/t_i)));0]+[cos(xi_opt) -sin(xi_opt) 0;sin(xi_opt) cos(xi_opt)
0;0 0 1]*p_4;
```

Minimum clear width of opening

The minimum clear width of the opening depends on the number of chambers in a ring.

```matlab
% Distance of point 6 to straight line 23
D_p6l23=norm(cross(l_23d,p_6-p_2))/norm(l_23d);
% Distance of point 6 to straight line 34
D_p6l34=norm(cross(l_34d,p_6-B))/norm(l_34d);
%Distance of point 7 to straight line 23
D_p7l23=norm(cross(l_23d,p_7-p_2))/norm(l_23d);
D_p7l23=vpa(D_p7l23);
%Distance of point 7 to straight line 34
D_p7l34=norm(cross(l_34d,p_7-B))/norm(l_34d);
D_p7l34=vpa(D_p7l34);
% minimum clear width of the chamber
D_open=[D_p6l23 D_p6l34 D_p7l23 D_p7l34];
D_open=min(D_open); % find the minimum of the 4 possible cases
D_open=vpa(D_open); %m %miminum clear open width of the chamber
```

Calculation of the water flow line

The water flow line is calculated as a horizontal throw

```matlab
% water flow velocity in the channel
v_ch=0;
for o=1:1:o % control varable of the channel variations
    v_ch(o)=(g*Q/b_ch(o))^(1/3); %m/s % possible flow velocities according
    %                                  to given channel width of concept
end
% vertical depth of the water flow according to the channel width
wd=0;
for o=1:1:o
    wd_v(o)=Q/b_ch(o)/v_ch(o); %m % possible vertical water depth according
    %                             to given channel width of concept
end
% calculation of water flow line
xw=0;
y=0.001:0.001:1; %m %y-coordinate interval for calcualtion of the water curve

% bottom water flow line
for o=1:1:o
        for e=1:1:1000 % target is to put the water in the wheel close
            %             to the highest point
            xw(o,e)=(2*(y(e))/(g))^0.5*v_ch(o); %m % bottom water flow line
        end
    end

% gradient angle of the bottom water flow line relative to horizon
for o=1:1:o
        for e=1:1:1000 % target is to put the water in the wheel close
            %             to the highest point
            x_w_rad(o,e)=atan(((0.5*v_ch(o)*(2/(g)/(y(e)))^0.5))^(-1)); %rad
        end
end

% Restricions for the y-values by y_secure and gradient angle of chamber <90°
% Because of y_secure the water flow only kann have the first possible
% contact with the water wheel after falling for a heigt differenc equal to
% y_secure
% The restriction of gradient angle of the camber < 90° is to minimize the
% hit of water on the paddle.
y_grenz=0.5*D_active_out_opt+y_secure-cos(pi/2-epsilon_real)*0.5*D_active_out_opt;
y_grenz=round(y_grenz-0.005,2);
e_max=y_grenz/(0.001); % mimimum y-coordinate of water flow to hit the
%                        water wheel
e_min=y_secure/0.001; % maximum y-coordinate of water flow to enter the
%                        chamber properly

% thickness of the water flow othogonal to flow direction
for o=1:1:o % control variable for channel width
    for e=e_min:1:e_max % control variable for y-coordinate of water flow
        wd_orth(o,e)=cos(atan((0.5*v_ch(o)*(2/(g)/(y(e)))^0.5)^(-1)))*wd_v(o); %m
    end
end
```

Calculation of the chamber entry

```
%Position
for e=e_min:1:e_max % control variable for y-Koordinat of water flow
    xWW(e)=0.5*D_active_out_opt*sin(acos((0.5*D_active_out_opt-
y(e)+y_secure)/(0.5*D_active_out_opt)));
end
%gradient angle of the chamber entry section relative to the horizontal line
for e=e_min:1:e_max % control variable for y-Koordinat of water flow
    x_WW_rad(e)=(acos((0.5*D_active_out_opt-
y(e)+y_secure)/(0.5*D_active_out_opt))+epsilon_real);
end
```

Optimization of water entry point and width of the water wheel

The water entry point and the necessary width of the water wheel are influencing each other. Therefore they are optimized together. The optimization is based on two requirements. If both requirements are fulfilled the combination of width and entry point is activated. The goal is to find an option that enables an early entry of the water in to the wheel and still keeps the water wheel width as small as possible.

```
% creating of high array values for |y|<y_secure to enable search for
% minimum value later
for o=1:1:O % control variable for channel width
    for e=1:1:e_min-1 % control variable for y-Koordinat of water flow
        BX(o,e)=10000;
    end
end

% link of the two criteria
% First criterion: thicknes of the water flow in entry is smaller than the
% clear width of the chamber opening
% Second criterion: water flow has to hit the entry paddle section at an
% angle within an interval of 0° to Omega
for o=1:1:O % control variable for channel width
    for e=e_min:1:e_max % control variable for y-coordinate of water flow
        if (D_open-wd_orth(o,e))>0
            if 0<=(x_w_rad(o,e)-x_WW_rad(e)) && (x_w_rad(o,e)-x_WW_rad(e))<=omega
                BX(o,e)=e+o*0.1*(e_max-e_min); % only weighting of the
                %height of entry in to the wheel; step to the next wider
                %opton only if it gains a certain persental of the usable height
            else
                BX(o,e)=10000; % if the criteria are not fulfilled, the array
                %               value is set very high to enable an
                %               optimization searching the minimum
                %               value of the matrix
            end
        else
            BX(o,e)=10000; % if the criteria are not fulfilled, the array
            %               value is set very high to enable an
            %               optimization searching the minimum
            %               value of the matrix
        end
    end
end
```

```matlab
% calcualtion of the coordinates of the optimum water entry point and the optimum width of the
% channel by identifying the minimum value of the matrix BX
for e=1:1:e_min-1 % control variable for y-coordinate of water flow
        AX(e)=10000; % additional parameter for optimization in case choosen water flow rate Q
is to great for the concept
end

for o=1:1:O % control variable for the channel width
    for e=e_min:1:e_max % control variable for y-coordinate of the water flow
        if min(BX(:))==10000
            u1=O;
            if 0<=(x_w_rad(5,e)-x_WW_rad(e)) && (x_w_rad(5,e)-x_WW_rad(e))<=omega
                AX(e)=e;
            else
                AX(e)=10000;
            end
            u2=find(AX==min(AX(:)));
        else
            [u1,u2]=find(BX==min(BX(:))); % coordinates for the optimal entry point
        end
    end
end

% Text output in case chosen water flow rate Q is too great for the concept
if min(BX(:))==10000
    box3=msgbox('The chosen flow rate is greater than the maximum flow rate for this diameter
of the given concept. Possibly you could extract more energy with a different
concept','Warning','warn');
end
```

Calculation of the optimum values for further calculations

```matlab
alpha_0=acos((0.5*D_active_out_opt-y(u2)+y_secure)/(0.5*D_active_out_opt)); %rad %angle
between the vertical line and the entry pointd
b_ch_opt=b_ch(u1); %m %optimal width of the channel
combi_opt=combi(u1); %resulting combination of the enabled combinations of the chamber
variations
B_WW_opt=B_WW(u1); %m %reslulting width of the water wheel
v_ch_opt=v_ch(u1); %m/s %resulting flow velocity in the channel
wd_v_opt=wd_v(u1); %m %resulting water depth in the channel
v_t=((y(u2)*(g)/2)+v_ch_opt^2)^0.5*cos(x_WW_rad(u2)-alpha_0); %m/s %tangential flow velocity
at the entry point
x_rel_opt=xWW(u2)-xw(u1,u2); %m %optimal location of the end on the channel relative to the
crest of the water wheel
```

Preparation of output to Excel - part 1

```matlab
excel_1=[H;Q;k_opt;D_active_out_opt;D_total_opt;h_secure;y_secure;b_ch_opt;B_WW_opt;v_ch_opt;w
d_v_opt;v_t;x_rel_opt;a_real;t_o;Epsilon_real;d];
```

Plot of the results of part 1

Plot of water wheel in relation to water flow

```matlab
% additional data to plot the water wheel
waterwheel=[D_active_out_opt*0.5*cos(linspace(0,2*pi,100))-
x_rel_opt;D_active_out_opt*0.5*sin(linspace(0,2*pi,100))+D_active_out_opt*0.5+y_secure];
% additional data to plot the bottom water stream line
xwb=xw(u1,:);
% additional data to plot the top water stream line
for e=1:1:1000
    xwt(e)=(2*(y(e)+wd_v(u1))/(g))^0.5*v_ch(u1);
end

figure()
% plot of water wheel and flow
% inputs in are plottet over -y to turn it upside down
plot(xwb,-y,'b.','LineWidth',2)
grid on
title('Positioning of the Water Wheel relative to the channel')
xlabel('distance [m]')
ylabel('distance [m]')
xlim([-(D_active_out(k_opt)+h_secure+y_secure+wd_v(u1))*0.5-x_rel_opt
(D_active_out(k_opt)+h_secure+y_secure+wd_v(u1))*0.5-x_rel_opt])
ylim([-D_active_out(k_opt)-h_secure-y_secure wd_v(u1)])
hold on
plot(xwt,-y,'b.','LineWidth',2)
hold on
plot3(waterwheel(1,:),-waterwheel(2,:),3*ones(100,1), 'r-','LineWidth',2)
hold off
```
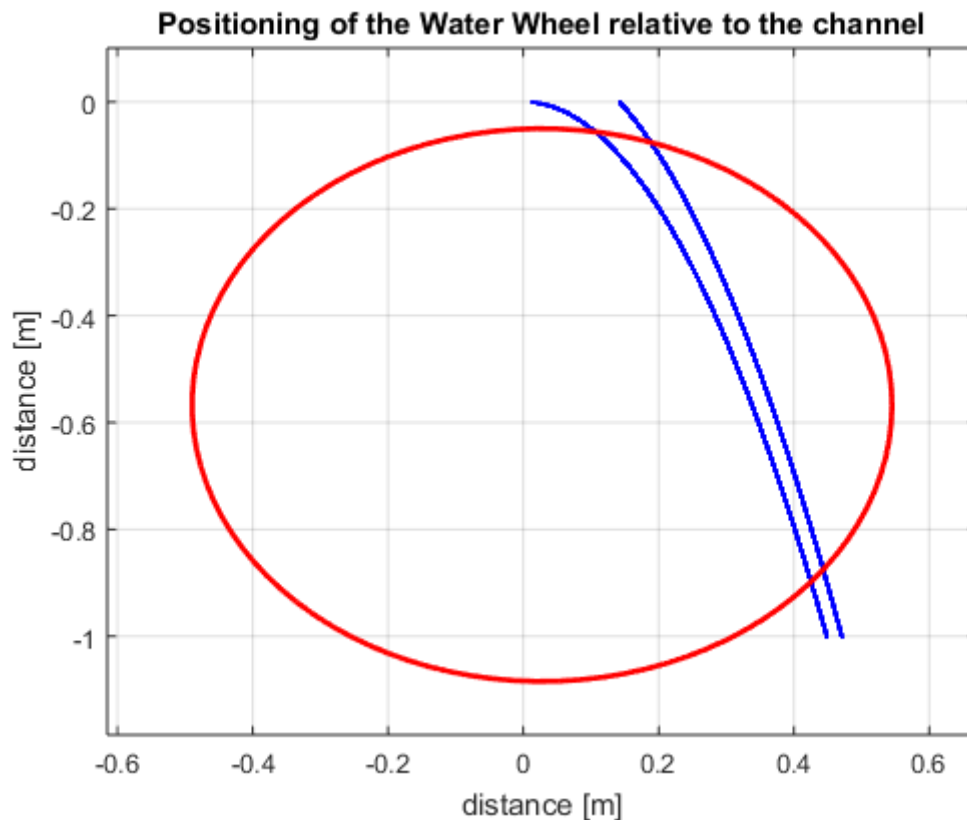
Output of input variables and calculated values

```matlab
% output of input variables
str4 = sprintf('Input variables:\n\nH [m]\t\t\t%.2f\nQ [m^3/s]\t\t\t%.4f',H,Q);
figure,
uicontrol('Style','edit','min',1,'max',10,...
        'String',[str4],...
        'Enable','inactive',...
        'Units','Normalized','Position',[.2,.1,.65,0.8])


% output of calculated values
str5 = sprintf('calculated values:\n\noptimum amount of chambers:\nk_opt [-
]\t\t\t%.f\n\nresulting diameters:\nD_active_out_opt [m]\t\t\t%.2f\nD_total_opt
[m]\t\t\t%.2f\n\noptimal width of the channel:\nb_ch_opt [m]\t\t\t%.2f\nflow velocity in the
channel:\nv_ch_opt [m/s]\t\t\t%.2f\n\nneccessary chamber combination for optimal channel
width:\ncombi_opt [-]\t\t\t%s\n\nresulting width of the water wheel based on chamber
combination:\nB_WW_opt [m]\t\t\t%.2f\n\nrelative position of channel to water
wheel:\nx_rel_opt
[m]\t\t\t%.2f',k_opt,D_active_out_opt,D_total_opt,b_ch_opt,v_ch_opt,combi{u1},B_WW_opt,x_rel_o
pt);
figure,
uicontrol('Style','edit','min',1,'max',10,...
        'String',[str5],...
        'Enable','inactive',...
        'Units','Normalized','Position',[.2,.1,.65,0.8])
```

```
                        Input variables:                              ^

                H [m]        1.30
                Q [m^3/s]    0.0200









                                                                      v
```

```
              calculated values:

          optimum amount of chambers:
              k_opt [-]        12

            resulting diameters:
        D_active_out_opt [m]        1.03
          D_total_opt [m]      1.11

          optimal width of the channel:
          b_ch_opt [m]        0.20
           flow velocity in the channel:
          v_ch_opt [m/s]        0.99
      neccessary chamber combination for optimal channel width:
          combi_opt [-]        b2

      resulting width of the water wheel based on chamber combination:
          B_WW_opt [m]        0.30

          relative position of channel to water wheel:
          x_rel_opt [m]        -0.03
```

```
end
```

Part 2

Calculation of the expected power output for the chosen site based on the model for overshot water wheels created in the bachelor thesis "Kraftübertragung für ein Low-Tech Wasserrad" (by Lukas Gess,2015)

Calculation of necessary basic values

```
R_active_out_opt=0.5*D_active_out_opt; %m % active outer radius of the
%                                       water wheel
alpha=xi_opt; %rad % anlge for steps between the mass centers of der
%                   chambers
gamma=pi-alpha_0-epsilon_real; %rad % total angle of water interacting cells
l=2*R_active_out_opt*pi/k_opt-d; %m % arc lengs of the outer partition
Y=round(k_opt*gamma/(2*pi)); %- % number of the cells interacting with
%                               water
n=1:1:nMax; %1/min % temporary interval of number of revolutions of the
%                   water wheel
Pref_tot=Q*rhoW*(g*H+0.5*v_ch_opt^2); %W % reference power; total given
%                                       power by potential and kinetic
%                                       energy of the water
Pref_WW=Q*rhoW*(g*D_active_out_opt+0.5*v_ch_opt^2); %W % reference power
%                                       relative to water wheel diameter
```

Chamber volume

The volume of the cells are calculated based on the specification of the chamber design by using vectors (part 1). The maximum volume is calculated for every cell position of the water interacting cells.

```matlab
% total length of the unfolded paddle
% Distance of point 2 to point 3
D_p2p3=norm(p_3-p_2);
% Distance of point 3 to point 4
D_p3p4=norm(p_4-p_3);
D_p3p4=vpa(D_p3p4);
% total length of the unfolded paddle
z=0.4*a_th+D_p2p3+D_p3p4;
z=vpa(z);


% Calculation of point 9
syms s1 s2 %point 9 as intersection of line 1_46 and line l_p1_parallel_x
eqns = [p_4(1)+s1*(p_6(1)-p_4(1))==p_1(1)+s2,p_4(2)+s1*(p_6(2)-p_4(2))==p_1(2)];
S = solve(eqns, [s1 s2]);
s1=vpa(S.s1);
s2=vpa(S.s2);


p_9=p_4+s1*(p_6-p_4); % vector to p_9


% Calculation of the total volume of a chamber
% vectors of the different volume sections
v_p4p3=p_3-p_4; %vector of point 4 to point 3
v_p4p2=p_2-p_4; %vector of point 4 to point 2
v_p4p1=p_1-p_4; %vector of point 4 to point 1
v_p4p9=p_9-p_4; %vector of point 4 to point 5
v_p4p6=p_6-p_4; %vector of point 4 to point 6
v_p4p7=p_7-p_4; %vector of point 4 to point 7
v_p4p8=p_8-p_4; %vector of point 4 to point 8
v_p7p8=p_8-p_7; %vector of point 7 to point 8
v_p6p7=p_7-p_6; %vector of point 6 to point 7
v_p1p9=p_9-p_1; %vector of point 1 to point 5
v_p1p2=p_2-p_1; %vector of point 1 to point 2
v_p2p3=p_3-p_2; %vector of point 2 to point 3


% total area of the segments
A_p487=0.5*norm(cross(v_p4p8,v_p4p7));
A_p476=0.5*norm(cross(v_p4p7,v_p4p6));
A_p491=0.5*norm(cross(v_p4p9,v_p4p1));
A_p412=0.5*norm(cross(v_p4p1,v_p4p2));
A_p423=0.5*norm(cross(v_p4p2,v_p4p3));
% total volume of the cell
V_chamber_max_tot=(A_p487+A_p476+A_p491+A_p412+A_p423-z*d)*B_WW_opt;
V_chamber_max_tot=vpa(V_chamber_max_tot);

% calculation of the position dependent maximum volume of the chamber
% angles of the volume secitons
iota_487=acos(v_p4p8'*v_p4p7/norm(v_p4p8)/norm(v_p4p7));
iota_487=vpa(iota_487);
iota_476=acos(v_p4p7'*v_p4p6/norm(v_p4p7)/norm(v_p4p6));
iota_476=vpa(iota_476);
iota_491=acos(v_p4p9'*v_p4p1/norm(v_p4p9)/norm(v_p4p1));
```

```matlab
iota_491=vpa(iota_491);
iota_412=acos(v_p4p1'*v_p4p2/norm(v_p4p1)/norm(v_p4p2));
iota_412=vpa(iota_412);
iota_423=acos(v_p4p2'*v_p4p3/norm(v_p4p2)/norm(v_p4p3));
iota_423=vpa(iota_423);

% filling angle psi
for i=1:1:Y
    psi(i)=alpha_0+i*alpha-alpha/2;
end

% vector relative to vector v_p4p8
% directiing vektor of water horizon according to cell position
for i=1:1:Y % control variable for the water interacting cells
    v_p4hd(1,i)=[cos(psi(i)) -sin(psi(i)) 0]*v_p4p8;
    v_p4hd(2,i)=[sin(psi(i)) cos(psi(i)) 0]*v_p4p8;
    v_p4hd(3,i)=[0 0 1]*v_p4p8;
end

% Calculation of the maximum volume according to cell postition by using
% vector geometry
for i=1:1:Y
    if (0<=psi(i))&&(psi(i)<iota_487)
        syms r1 r2 %point p_V as crossing
        eqns =
[p_4(1)+r1*v_p4hd(1,i)==p_7(1)+r2*v_p7p8(1),p_4(2)+r1*v_p4hd(2,i)==p_7(2)+r2*v_p7p8(2)];
        S = solve(eqns, [r1 r2]);
        r1=vpa(S.r1);
        r2=vpa(S.r2);
        v_p4pV(:,i)=r1*v_p4hd(:,i); % vector from point 4 to point V (volume)
        V_chamber_max(i)=(A_p487+A_p476+A_p491+A_p412+A_p423-(norm(p_4+v_p4pV(:,i)-
p_7)+D_p3p2+0.4*a_th)*d-0.5*norm(cross(v_p4p8,v_p4pV(:,i))))*B_WW_opt;

    elseif (iota_487<=psi(i))&&(psi(i)<iota_487+iota_476)
        syms r1 r2 %point p_V as crossing
        eqns =
[p_4(1)+r1*v_p4hd(1,i)==p_6(1)+r2*v_p6p7(1),p_4(2)+r1*v_p4hd(2,i)==p_6(2)+r2*v_p6p7(2)];
        S = solve(eqns, [r1 r2]);
        r1=vpa(S.r1);
        r2=vpa(S.r2);
        v_p4pV(:,i)=r1*v_p4hd(:,i); % vector from point 4 to point V (volume)
        V_chamber_max(i)=(A_p476+A_p491+A_p412+A_p423-(0.4*a_th+norm(p_4+v_p4pV(:,i)-p_6))*d-
0.5*norm(cross(v_p4p7,v_p4pV(:,i))))*B_WW_opt;

    elseif ((iota_487+iota_476)<=psi(i))&&(psi(i)<(iota_487+iota_476+iota_491))
        syms r1 r2 %point p_V as crossing
        eqns =
[p_4(1)+r1*v_p4hd(1,i)==p_1(1)+r2*v_p1p9(1),p_4(2)+r1*v_p4hd(2,i)==p_1(2)+r2*v_p1p9(2)];
        S = solve(eqns, [r1 r2]);
        r1=vpa(S.r1);
        r2=vpa(S.r2);
        v_p4pV(:,i)=r1*v_p4hd(:,i); % vector from point 4 to point V (volume)
        V_chamber_max(i)=(A_p491+A_p412+A_p423-0.5*norm(cross(v_p4p9,v_p4pV(:,i))))*B_WW_opt;

    elseif
((iota_487+iota_476+iota_491)<=psi(i))&&(psi(i)<(iota_487+iota_476+iota_491+iota_412))
        syms r1 r2 %point p_V as crossing
        eqns =
[p_4(1)+r1*v_p4hd(1,i)==p_1(1)+r2*v_p1p2(1),p_4(2)+r1*v_p4hd(2,i)==p_1(2)+r2*v_p1p2(2)];
```

```
        S = solve(eqns, [r1 r2]);
        r1=vpa(S.r1);
        r2=vpa(S.r2);
        v_p4pV(:,i)=r1*v_p4hd(:,i); % vector from point 4 to point V (volume)
        V_chamber_max(i)=(A_p412+A_p423-0.5*norm(cross(v_p4p1,v_p4pV(:,i))))*B_WW_opt;

    elseif
((iota_487+iota_476+iota_491+iota_412)<=psi(i))&&(psi(i)<(iota_487+iota_476+iota_491+iota_412*
iota_423))
        syms r1 r2 %point p_V as crossing
        eqns =
[p_4(1)+r1*v_p4hd(1,i)==p_2(1)+r2*v_p2p3(1),p_4(2)+r1*v_p4hd(2,i)==p_2(2)+r2*v_p2p3(2)];
        S = solve(eqns, [r1 r2]);
        r1=vpa(S.r1);
        r2=vpa(S.r2);
        v_p4pV(:,i)=r1*v_p4hd(:,i); % vector from point 4 to point V (volume)
        V_chamber_max(i)=(A_p423-0.5*norm(cross(v_p4p2,v_p4pV(:,i))))*B_WW_opt;
    else
        V_chamber_max(i)=0;
    end
end
```

Calculation of the limit of number of revolutions

```
nGrenz=(l*60*Q)/(V_chamber_max(1)*2*pi*R_active_out_opt); %i/min
%               limit of number of revolutions --> the first water
%               interacting cell is fully filled
nGrenz=double(nGrenz);
```

Temporary behaviour of the power of the impulsive force

The calculation of the impulsive force bases on the principal of linear momentum. It serves to determine torque caused by the momentum.

```
F=0;
for j=1:1:nMax
    if (v_t-j*2*pi*R_active_out_opt/60)>=0
        F(j)=(v_t-j*2*pi*R_active_out_opt/60)^2*rhow*Q/v_t;
    else
        F(j)=-(v_t-j*2*pi*R_active_out_opt/60)^2*rhow*Q/v_t;
    end
end
```

Radius of emphasis according to Nuernbergk

The radius of emphasis is calculated depending from filling level of the cells

```
Rs=0;
for j=1:1:nMax
    if j<=nGrenz
        Rs(j)=(((Q*60)/(2*pi*nGrenz*B_WW_opt)+(R_active_out_opt-a_real)^2)^(0.5));
    else
        Rs(j)=(((Q*60)/(2*pi*j*B_WW_opt)+(R_active_out_opt-a_real)^2)^(0.5));
```

```
        end
end
```

Temporary behaviour of the gravitational torque

Torque that is caused by the weight of the water in the cells. The radius of emphasis as well as the inertia caused by the rotation are included.

```
M=0;
for i=1:1:Y
    for j=1:1:nMax
        if Q*60/j*(1/k_opt-d/(2*pi*R_active_out_opt)) < V_chamber_max(i)
            M(j,i)=Rs(j)*rhow*Q*60/j*(1/k_opt-d/(2*pi*R_active_out_opt))*(((g-
4*pi^2*(j^2)/(60^2)*Rs(j)*cos(alpha_0+asin(s/R_active_out_opt)+i*alpha))*sin(alpha_0+asin(s/R_
active_out_opt)+i*alpha))+((2*pi*j/60)^2*Rs(j)^2*sin(alpha_0+asin(s/R_active_out_opt)+i*alpha)
*cos(alpha_0+asin(s/R_active_out_opt)+i*alpha)));
                % for all cells that are not filled to the possible maximum
        else
            M(j,i)=Rs(j)*rhow*V_chamber_max(i)*(((g-
4*pi^2*(j^2)/(60^2)*Rs(j)*cos(alpha_0+asin(s/R_active_out_opt)+i*alpha))*sin(alpha_0+asin(s/R_
active_out_opt)+i*alpha))+((2*pi*j/60)^2*Rs(j)^2*sin(alpha_0+asin(s/R_active_out_opt)+i*alpha)
*cos(alpha_0+asin(s/R_active_out_opt)+i*alpha)));
                % for all cells that are filled to the possible maximum
        end
    end
end


M=sum(M')'; % Sum of the lines of matrix M(j,i) to sum all cells
```

Temporary behaviour of total torque and idling speed

Sum of the torques caused by gravity and impulsive forces. By locating the intersection of the behaviour of the total torque with the horizontal axis the cut out speed nCutOut is identified.

```
M=M+F'*(R_active_out_opt-0.5*a_real); %Nm % Sum of the torques caused by
%                                            gravity and impulsive forces

% determination of the cut out speed
w=find(M<=0);
nCutOut=w(1,1); %1/min % rotational speed for which the power output
%                       gets <0 for the first time
n1= 1:1:nCutOut; %i/min % control varaible for the rotational speed
```
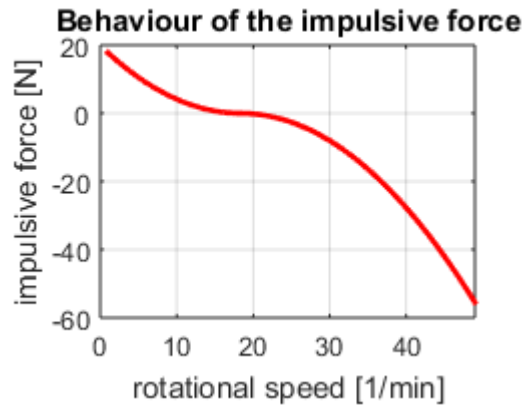
Behaviour of impulsive force with respect to nCutOut

```
F=0;
for j=1:1:nCutOut
    if (v_t-j*2*pi*R_active_out_opt/60)>=0
        F(j)=(v_t-j*2*pi*R_active_out_opt/60)^2*rhow*Q/v_t;
    else
        F(j)=-(v_t-j*2*pi*R_active_out_opt/60)^2*rhow*Q/v_t;
    end
end
```

```matlab
% Plot of the behaviour of the impulsive force
figure()
subplot(2,2,1)
plot(n1,F,'r','LineWidth',2)
grid on
title('Behaviour of the impulsive force')
xlabel('rotational speed [1/min]')
ylabel('impulsive force [N]')
xlim([0 nCutOut])
hold on
```


Behaviour of the impulsive force

Behaviour of the gravitational force with respect to nCutOut

```matlab
M=0;
for i=1:1:Y
    for j=1:1:nCutOut
        if Q*60/j*(1/k_opt-d/(2*pi*R_active_out_opt)) < V_chamber_max(i)
            M(j,i)=Rs(j)*rhoW*Q*60/j*(1/k_opt-d/(2*pi*R_active_out_opt))*(((g-
4*pi^2*(j^2)/(60^2)*Rs(j)*cos(alpha_0+asin(s/R_active_out_opt)+i*alpha))*sin(alpha_0+asin(s/R_
active_out_opt)+i*alpha))+((2*pi*j/60)^2*Rs(j)^2*sin(alpha_0+asin(s/R_active_out_opt)+i*alpha)
*cos(alpha_0+asin(s/R_active_out_opt)+i*alpha)));
            % for all cells that are not filled to the possible maximum
        else
            M(j,i)=Rs(j)*rhoW*V_chamber_max(i)*(((g-
4*pi^2*(j^2)/(60^2)*Rs(j)*cos(alpha_0+asin(s/R_active_out_opt)+i*alpha))*sin(alpha_0+asin(s/R_
active_out_opt)+i*alpha))+((2*pi*j/60)^2*Rs(j)^2*sin(alpha_0+asin(s/R_active_out_opt)+i*alpha)
*cos(alpha_0+asin(s/R_active_out_opt)+i*alpha)));
            % for all cells that are filled to the possible maximum
        end
    end
end
```

```matlab
end

M=sum(M')'; % Sum of the lines of matrix M(j,i) to sum all cells
AM1=M; % preparation for export of the behaviour the gravitational torque
%       to Excel

% Plot of the behaviour of the gravitational torque
subplot(2,2,2)
plot(n1,M,'r','LineWidth',2)
grid on
title('Behaviour of the gravitational torque')
xlabel('rotational speed [1/min]')
ylabel('torque [Nm]')
xlim([0 nCutOut])
hold on
```
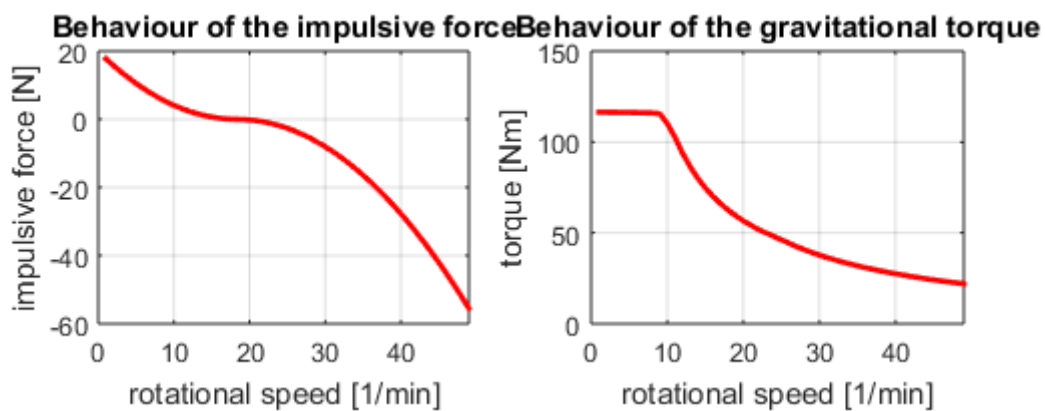

Final calculation of the behaviour of the total torque

Sum of the torques caused by gravity and impulsive forces.

```matlab
M=M+F'*(R_active_out_opt-0.5*a_real); %Nm %  Sum of the torques caused by
%                                             gravity and impulsive forces.

% Preparation of export to Excel
AM=M; % transposed M for export to Excel
M=M'; % M transposed
AF=F'*(R_active_out_opt-0.5*a_real); % transposed F for export to Excel

% Determination of the maximum total torque
Mmax=max(M);
```

```matlab
% Plot of the behaviour of the total torque
subplot(2,2,3)
plot(n1,M,'r','LineWidth',2)
grid on
title('Behaviour of total torque')
xlabel('rotational speed [1/min]')
ylabel('torqze [Nm]')
xlim([0 nCutOut])
ylim([0 Mmax+0.2*Mmax])
hold on

% Plot of the peak of the total torque
% rounding of the peak to the second decimal place
z1=round(Mmax*10)/10;

nMmax=find(M==Mmax);
var1=nMmax;
var11=var1(1,1);

% Plot of the peak of the total torque
plot(var11,z1,'o')
strc = cellstr(num2str(z1'));
text(var11+0.02*nCutOut,z1+0.1*Mmax,strc,'horizontalalignment','left')

var12=round(var11*10)/10;
plot(var11,0,'o')
strc2 = cellstr(num2str(var12'));
text(var11+0.02*nCutOut,0.1*Mmax,strc2,'horizontalalignment','left')
```
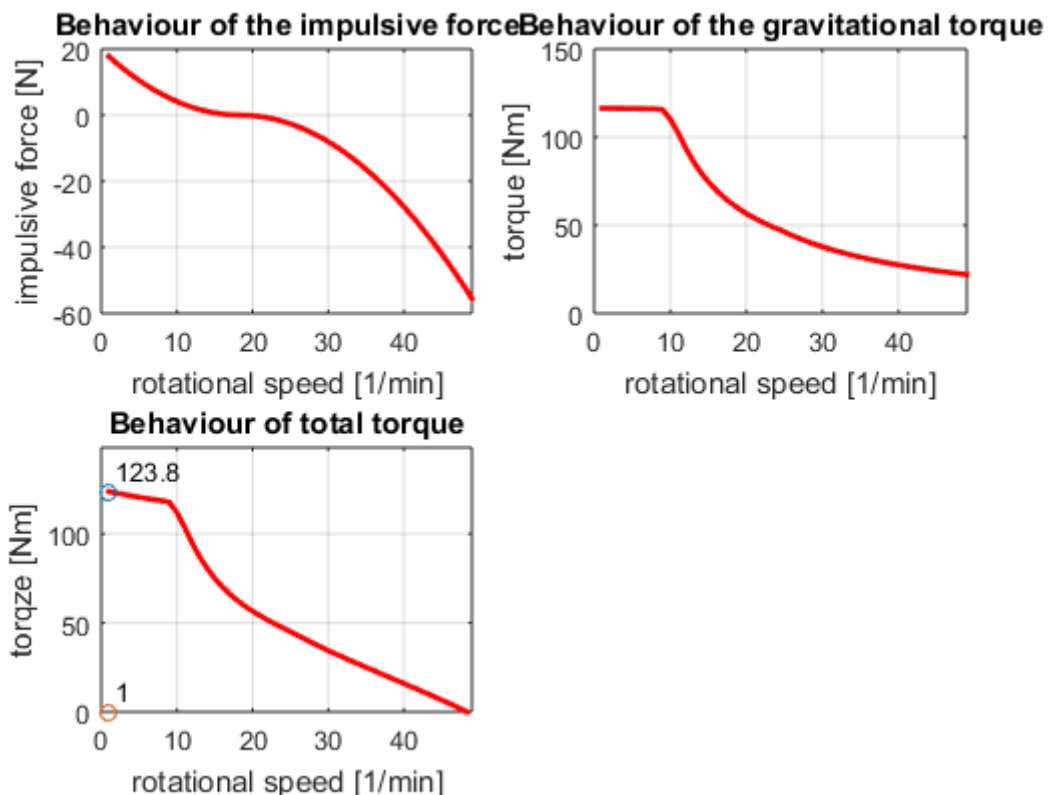
Calculation of the behaviour of the power

The power depends on the total torque and the rotational speed

```matlab
P=2*pi/60.*M.*n1;

% Preparation for the export to Excel
AP=P';

% Determiantion of the peak power
Pmax=max(P);
nPmax=find(P==Pmax);

% Determination of the total torque at peak power
M_Pmax=M(nPmax);

% Plot of the behaviour of the power
subplot(2,2,4)
plot(n1,P,'b','LineWidth',2)
grid on
title('Behaviour of the power')
xlabel('rotational speed [1/min]')
ylabel('power [W]')
xlim([0 nCutOut])
ylim([0 Pmax+0.2*Pmax])
hold on

% Plot of the peak power
z2=round(Pmax*10)/10;

var2=nPmax;
var21=var2(1,1);

plot(var21,z2,'o')
strc = cellstr(num2str(z2'));
text(var21+0.02*nCutOut,z2+0.1*Pmax,strc,'horizontalalignment','left')

var22=round(var21*10)/10;
plot(var21,0,'o')
strc2 = cellstr(num2str(var22'));
text(var21+0.02*nCutOut,0.1*Pmax,strc2,'horizontalalignment','left')


% Determination of the rotational speed at PDim
nDim=find(P>=PDim);
nDim=nDim(1,length(nDim));
PDim=P(nDim);
M_PDim=M(nDim);

% Plot of the dimensioning point
z3=round(PDim*10)/10;

var3=nDim;
var31=var3(1,1);

plot(var31,z3,'o')
strc = cellstr(num2str(z3'));
text(var31+0.02*nCutOut,z3+0.1*Pmax,strc,'horizontalalignment','left')
```
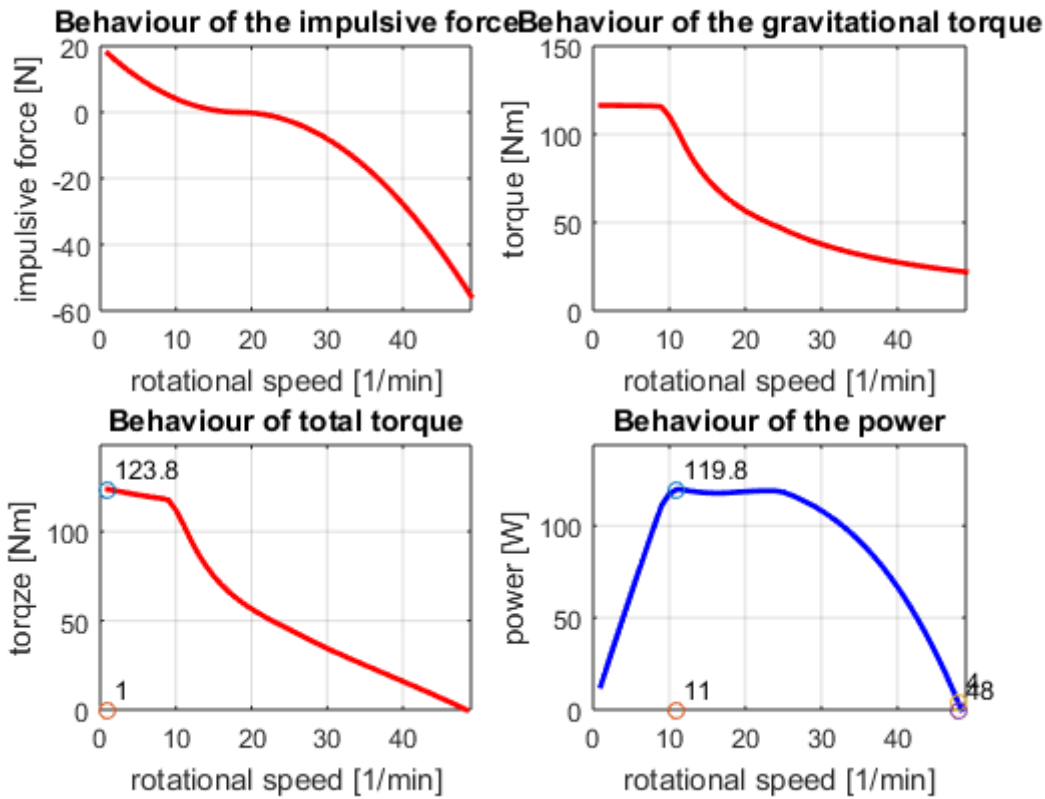
```
var32=round(var31*10)/10;
plot(var31,0,'o')
strc2 = cellstr(num2str(var32'));
text(var31+0.02*nCutOut,0.1*Pmax,strc2,'horizontalalignment','left')
```


Calculation of the efficiency

The efficiency is determined using the reference power calculated at the beginning and the maximum power. A total efficiency and an efficiency only referring to the water wheel is calculated.

```
Eta_tot=Pmax/Pref_tot; %- % total efficiency
Eta_WW=Pmax/Pref_WW; %- % efficiency only according to water wheel diameter
```

Output of calculated values - part 2

```
str4 = sprintf('Calculated values:\n\nReference Power:\nPref [W]\t\t\t%.2f\n\nMaximum:\nPmax
[W]\t\t\t%.2f\nnPmax [1/min]\t\t%.2f\nM_Pmax [Nm]\t\t\t%.2f\n\nall cells entirely
filled:\n\nMin [1/min]\t\t%.2f\n\ncut out rotational speed:\n\nCutOut
[1/min]\t\t\t%.2f\n\ndimensioning point:\nPDim [W]\t\t\t%.2f\n\nDim [1/min]\t\t\t%.2f\nM_PDim
[Nm]\t\t\t%.2f\n\n efficiency:\neta_tot [-]\t\t%.2f\neta_WW [-
]\t%.2f',Pref_tot,Pmax,nPmax,M_Pmax,nGrenz,nCutOut,PDim,nDim,M_PDim,Eta_tot,Eta_WW);
figure,
uicontrol('Style','edit','min',1,'max',10,...
        'String',[str4],...
        'Enable','inactive',...
        'Units','Normalized','Position',[.2,.1,.65,0.8])
```

```
Calculated values:

Reference Power:
Pref [W]        264.92

Maximum:
Pmax [W]        119.85
nPmax [1/min]     11.00
M_Pmax [Nm]      104.04

all cells entirely filled:
nMin [1/min]      8.95

cut out rotational speed:
nCutOut [1/min]    49.00

dimensioning point:
PDim [W]          4.00
nDim [1/min]      48.00
M_PDim [Nm]        0.80

efficiency:
eta_tot [-]   0.45
eta_WW [-]   0.56
```

Preparation for output to Excel - part 2

```
excel_2=[Y;Pref_tot;nGrenz;nCutOut;Pmax;nPmax;M_Pmax;Mmax;PDim;nDim;M_PDim;Eta_tot;Eta_WW];
```

Export to Excel

```
%{
% DEACTIVATION OF EXPORT TO EXCEL
% Export of input variaples, parameters and calculatec values to Excel
xlswrite('Output.xlsx',excel_1,N_sheet,['I8'])
xlswrite('Output.xlsx',excel_2,N_sheet,['I26'])

% Export of the gravitational torque to Excel
xlswrite('Output.xlsx',AM1,N_sheet,['C4'])

% Export of the total torque to Excel
xlswrite('Output.xlsx',AM,N_sheet,['D4'])

% Export of the impulive torque to Excel
xlswrite('Output.xlsx',AF,N_sheet,['B4'])

% Export of the power to Excel
xlswrite('Output.xlsx',AP,N_sheet,['E4'])
%}
```

Final textbox at the end of the calculation

```
box4=msgbox('Operation successfully completed','Sucess');
```
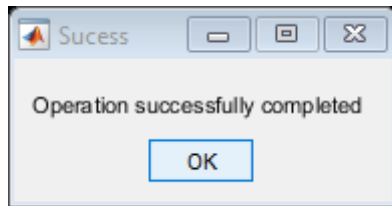

Published with MATLAB® R2015a

D)   Technical drawings for the prototype modules

Wall element:

Front view
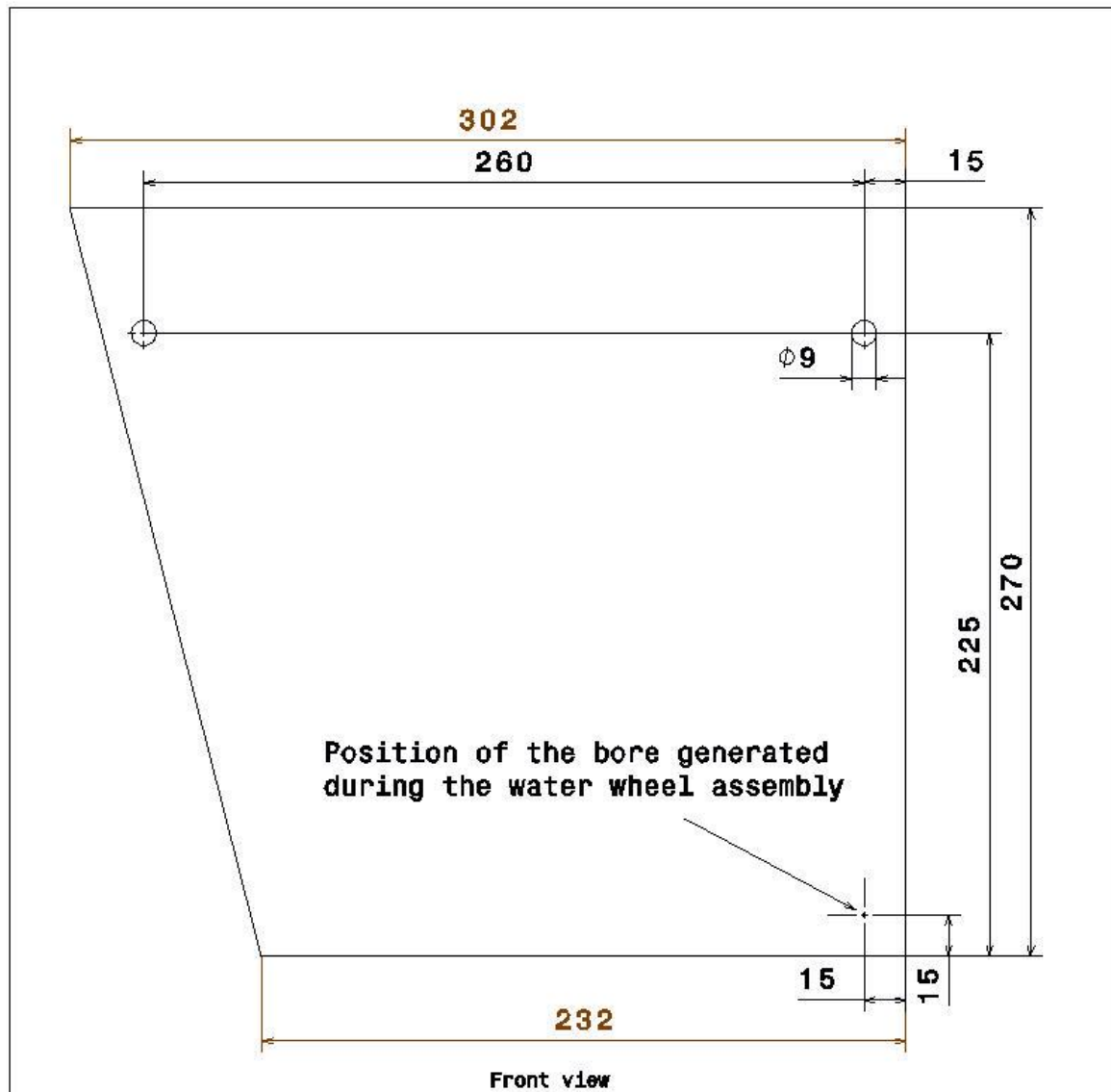
thickness of the sheet metal: 0.5 to 1.0 mm

Modular water wheel design	permisible allowance gerneral tolerances ISO 2768-mk	surface	scale 1:1	X,X g
			material 1.0116	
	date	name		
proc.	07/2017	Geß	Wall element	
che.				
norm				
			Part number: P1	sheet 1 / 1 sh.
				format: A4 ISO

Paddle element

Detail A
Scale: 1:1

The flap at the
top end has to be
created manually as
final process step
(e.g. with a hammer)

Folded view

15°

-62°

all thin dotted lines represent
finger brake bends

Unfolded view

360
300
45°
30
R1.5
114
R1.5
45° 90°
351
440
452
R1.5
45° 90°
R3
6 ⌀
38
15

all bending radii are 1 mm

all side flaps are bent to 90°

Thickness of the sheet metal: 0.5 to 1.0 mm

		surface		Scale 1:2	X,X g
permissible allowance general tolerances ISO 2788-mk			name	material 1.0116	
	date	07/2017	ga5		
proc.				Paddle element	
che.					
norm					

Modular water wheel design

Part number: P2

sheet 1
1 sh.

format: A3 ISO

Bottom element

Folded view

30°

233
175
90°
45°
120°
R1.5
30
R1.5

300
360

all thin dotted lines
represent finger
brake bends

all bending radii are 1 mm

all side flaps are bent to 90°

tickness of the sheet metal:
0.5 to 1.0 mm

Unfolded view

Modular water wheel design	permissible allowance	surface	scale: 1:2	X,X g
	general tolerances ISO 2768-mk		material	1.0116
		name		
	Datum		Bottom element	
	proc. 07/2017	Geß		
	chc.			
	norm		Part number: P3	
				sheet 1
				1 sh
			format: A4 ISO	

E)   Bill of the used sheet metal plates

makerspace

Seite 1 / 1

UnternehmerTUM MakerSpace GmbH

Lichtenbergstr. 6
D-85748 Garching

Tel. +49 89-18 94 69-270
Fax +49 89-18 94 69-270

invoice@maker-space.de
www.maker-space.de

UnternehmerTUM MakerSpace GmbH | Lichtenbergstr. 6 | D-85748 Garching
Lukas Geß
Mathildenstraße 1B
80336 München

Kundennummer	211927
Auftragsnummer	0007549
Rechnungsnummer	17-5-02266
Rechnungsdatum	29.05.2017

Rechnung

Pos.	Anz	ME	Bezeichnung	E-Preis	G-Preis	Ust.
1	3	Stk.	Stahlblech verzinkt 0,75 x 1000 x 2000 mm	29,87 €	89,61 €	1

Summe (Netto):	89,61 €

Netto Ust. 1	Ust. 19%	Netto Ust. 2	Ust. 7%	Netto Ust. 0	Ust. 0%	Rechnungsbetrag
89,61 €	17,03 €	0,00 €	0,00 €	0,00 €	0,00 €	106,64 €

Bitte geben Sie als Verwendungszweck bei der Überweisung Ihren Namen und die von uns angegebene Rechnungsnummer an.

Wurde kein Leistungszeitpunkt angegeben entspricht das Rechnungsdatum dem Leistungszeitpunkt.

Der Rechnungsbetrag ist innerhalb von 7 Werktagen nach Erhalt der Rechnung auf das untenstehende Bankkonto ohne Abzüge zu überweisen.

Wir bedanken uns für Ihren Auftrag.

Mit freundlichen Grüßen

MakerSpace

UnternehmerTUM MakerSpace GmbH
Lichtenbergstr. 6, 85748 Garching
Geschäftsführer:
Dr. Helmut Schönenberger, Philip Handy

Bankverbindung:
Deutsche Bank München
IBAN: DE59 7007 0010 0013 7000 00
BIC: DEUTDEMMXXX

Registergericht München: 215361
St.Nr. 143/189/10333
Ust-ID-Nr. DE297588569